8-2018

Cholinergic Control of Cortical Circuit Activity

Rajan Dasgupta

CHOLINERGIC CONTROL OF CORTICAL CIRCUIT ACTIVITY

by

Rajan Dasgupta, M.Sc.

APPROVED:

_____
Michael Beierlein, Ph.D.
Advisory Professor

_____
Kevin A. Morano, Ph.D.

_____
Shin Nagayama, Ph.D.

_____
Harel Z. Shouval, Ph.D.

_____
M. Neal Waxham, Ph.D.

APPROVED:

_____
Dean, The University of Texas
MD Anderson Cancer Center UTHealth Graduate School of Biomedical Sciences

CHOLINERGIC CONTROL OF CORTICAL CIRCUIT ACTIVITY

A

DISSERTATION

Presented to the Faculty of

The University of Texas

MD Anderson Cancer Center UTHealth

Graduate School of Biomedical Sciences

in Partial Fulfillment

of the Requirements

for the Degree of

DOCTOR OF PHILOSOPHY

by

Rajan Dasgupta, M.Sc.

Houston, Texas

August, 2018

To my family

Acknowledgements

First, I must express my sincere gratitude to Michael, for his unwavering support and direction throughout my time in grad school, and, more importantly, for teaching me how to think like an electrophysiologist. I am deeply indebted also to my lab-mates: Frederik for his advice and contributions to my project, Juan for teaching me how to patch cells (a rather important lesson, as it turned out) and JJ for his assistance and friendship, both within and outside the lab.

I have been particularly fortunate to receive guidance from a fantastic and supportive advisory committee, and so would like to take this opportunity to thank all of its members. I should add here a special note of thanks to Dr Tong for kindly agreeing, on very short notice, to serve on my committee during my defense. Thanks are due also to all members of the staff both at GSBS and Neurobiology and Anatomy. In particular, I wish to thank Amanda, Lourdes, Sharon and Brenda for often stepping beyond their usual duties in order to make my ride through grad school a bit smoother.

Support outside the lab is often as important (if not more) as that within it, and I am happy to report that I received both in abundance. This work would not have been possible without the constant support and encouragement from my parents, who are the kindest people I know. Also, words cannot express my gratitude towards Bhavya, who has kept me focused and grounded, and continues to remind me of what is most important in life. And finally, to all my friends of various stripes and dispositions, I give my heartfelt thanks for both the insufferable moments and cherished memories alike; but mostly for the memories.

CHOLINERGIC CONTROL OF CORTICAL CIRCUIT ACTIVITY

Rajan Dasgupta, M.Sc.

Advisory Professor: Michael Beierlein, Ph.D.

Cholinergic neurons of the basal forebrain send extensive projections to all regions of the neocortex and are critically involved in a diverse array of cognitive functions, including sensation, attention and learning. Cholinergic signaling also plays a crucial role in the moment-to-moment control of ongoing cortical state transitions that occur during periods of wakefulness. Yet, the underlying circuit mechanisms of synaptic cholinergic function in the neocortex remain unclear. Moreover, acetylcholine continues to be widely viewed as a slow and diffuse neuromodulator, despite the preponderance of *in vivo* evidence demonstrating rapid cholinergic function. In this study, we used a combination of optogenetics and *in vitro* electrophysiology to examine spatiotemporally precise control of cortical network activity by endogenous acetylcholine. We show that even brief activation of cholinergic afferents could powerfully suppress evoked cortical recurrent activity for several seconds. This suppression was reliant on the engagement of both nicotinic and muscarinic acetylcholine receptors. Nicotinic receptors mediated transient suppression by acting in the superficial cortical layers, while muscarinic receptors mediated prolonged suppression in layer 4. In agreement, we found nicotinic-mediated excitation of inhibitory neurons in the supragranular layers, and muscarinic-mediated hyperpolarization of excitatory cells in layer 4. Together, these findings present novel circuit mechanisms for fast and robust cholinergic signaling in neocortex.

Table of contents

List of illustrations

List of tables

Chapter 1: Introduction

The brain is a highly dynamic organ. To keep up with the demands of a constantly changing external environment, the computational rules underlying brain function must also be continually and swiftly updated. The behavioral state, or the set of rules defining neuronal activity in the brain, is thus in constant flux. Although behavioral state is reflected in the activity of the entire mammalian brain, the effects of state transitions are most pronounced in the cerebral cortex, the so-called "seat of consciousness". During cortical states characterized by sleepiness or low arousal, circuits in the cerebral cortex spontaneously generate slow internal rhythms that are rapidly abolished when the animal shifts to a more aroused state. These cortical network dynamics can often have as large an influence on neuronal activity as the sensory stimulus itself, and must therefore be precisely regulated by several neuromodulatory inputs, chief among which is the cholinergic projection system to the cortex.

Cholinergic neurons in the mammalian forebrain send extensive axonal afferents throughout the cortical regions and have long been known to be crucial for several cognitive functions, including attention, sensory discrimination and learning. Defects in cholinergic signaling underlie pathologies like Alzheimer's disease and schizophrenia. More recently, cholinergic activity in the cerebral cortex has been shown to precisely regulate cortical state transitions. Thus, elucidating the neurophysiological mechanisms of cholinergic control of cortical network activity is of critical importance. In this chapter, we will summarize wiring principles in cortical circuits, neuromodulation of cortical activity as a function of brain states, and the known structure and circuit functions of cholinergic afferentation in the cortex.

1.1 Neocortical circuits

The cerebral cortex, the most recently evolved structure in the mammalian brain, is an exquisitely complex formation. Found to be disproportionately large in humans, this sheet of neurons occupying the anterodorsal extremity of the central nervous system is considered to be the basis of consciousness. Coordinated activity within and between networks of densely interconnected networks of dozens of different types of neurons in the cortex underlies cognition and all higher brain functions, including thought, motivated behaviors and complex planning. What rules dictate cortical structure and function are some of the most fundamental questions of neuroscience.

Organization of the rodent somatosensory cortex

Neurons in the mammalian cerebral cortex are found to be arranged in several distinct layers (Ramon y Cajal, 1899). The neocortex, which forms the largest part of the cerebral cortex and mediates most cognitive functions, comprises six layers. These layers are numbered 1-6 (from superficial to deep), with layers 2 and 3 often referred to together as layer 2/3. Each layer is distinct in terms of the density and types of prevalent neurons (Meyer et al., 2010), rules of wiring, and the cortical subnetworks they form part of (Feldmeyer, 2012). In the primary sensory cortices, including the somatosensory cortex, layer 4 is the primary recipient of sensory input from the thalamus (specifically the ventrobasal, or VB nucleus of the thalamus, in the case of somatosensory input). From layer 4, this sensory input is then relayed to layers 2/3 and 5, where it is amplified, transformed and communicated horizontally to neighboring

cortical areas (Li et al., 2013, Lien and Scanziani, 2013, Sarid et al., 2015). There is also evidence for some direct thalamocortical communication to layers 5 and 6 (Constantinople and Bruno, 2013). The neocortex also shows functional organization horizontally, and its circuits are arranged into distinct iterative units called columns (Mountcastle, 1997). Cortical interactions, both vertically (between cortical layers) and horizontally (between cortical columns) are dynamically regulated as a function of cortical state.

In rodents, the primary somatosensory cortex (S1) is dominated by the so-called "barrel field", a region where layer 4 is segregated into easily discernible and cytoarchitectonically distinct subregions called "barrels" (Figure 1.1) (Feldmeyer, 2012). Layer 4 barrels process input from the animal's whiskers and form a topographic representation of the mystacial vibrissae, such that neurons in a given barrel receive sensory input only from a single whisker (Simons and Carvell, 1989, Petersen, 2007). This specificity is possible in part because the dendrites of small spiny stellate cells (excitatory cells that serve as the main recipients of thalamocortical input) are spatially restricted to within the barrel boundaries.

Excitatory cells in the sensory cortices form distinct subnetworks

The vast majority (~85%) of neocortical neurons are excitatory glutamatergic cells in all layers (with the exception of layer 1, where the small numbers of neurons are exclusively GABAergic). Excitatory cells show great diversity in their axonal and dendritic morphologies, which leads to interesting distinctions in their functional organization within cortical microcircuits. For instance, although stellate cells in layer 4 have dendritic trees that are

confined within the barrel, other layer 4 glutamatergic cell types, such as pyramidal and star pyramidal cells, possess prominent apical dendrites that extend into layer 2/3, allowing them to sample horizontal inputs (Staiger et al., 2004), and suggesting that they may have a role in integrating corticocortical signals from wider areas. This notion is supported by their axonal morphologies as well; whereas axonal projections from stellate cells into layer 2/3 remain largely restricted to the same cortical column, layer 4 pyramidal cells have wide axonal arbors, often reaching several columns across. Excitatory cells in layer 2/3 tend to show pyramidal morphologies, with apical dendrites that sample horizontal signals in layers 1 and 2, and layer 4 input in layer 2/3. In addition to sending extensive lateral "recurrent" projections to neighboring cells, layer 2/3 pyramidal cells also project to layer 5. In layer 5, the dominant cell type are pyramidal cells with large somata and thick apical dendrites that reach up to layer 1, allowing them to integrate a wide variety of long-range and local cortical inputs (Shai et al., 2015). Finally, excitatory cells in layer 6 provide feedback projections onto thalamic relay cells (Guillery, 1967, Jones and Powell, 1968, Crandall et al., 2017). Thus, axonal and dendritic morphologies of excitatory cells are well-adapted to enable layer-specific functions.

Electrophysiologically, cortical excitatory cells generally have so-called regular-spiking (**RS**) phenotypes, characterized by wide (~1 millisecond half-width) action potentials, relatively low firing rates, slow monophasic after-hyperpolarizations (AHPs) and initial spike doublets upon current injection (Connors and Gutnick, 1990, Beierlein et al., 2003), thus allowing them to be distinguished from local inhibitory cells. Also, cortical excitatory neurons share extensive recurrent connections with one another, allowing them to amplify sensory input and to generate self-sustaining activity (Beierlein et al., 2002, Shu et al., 2003).

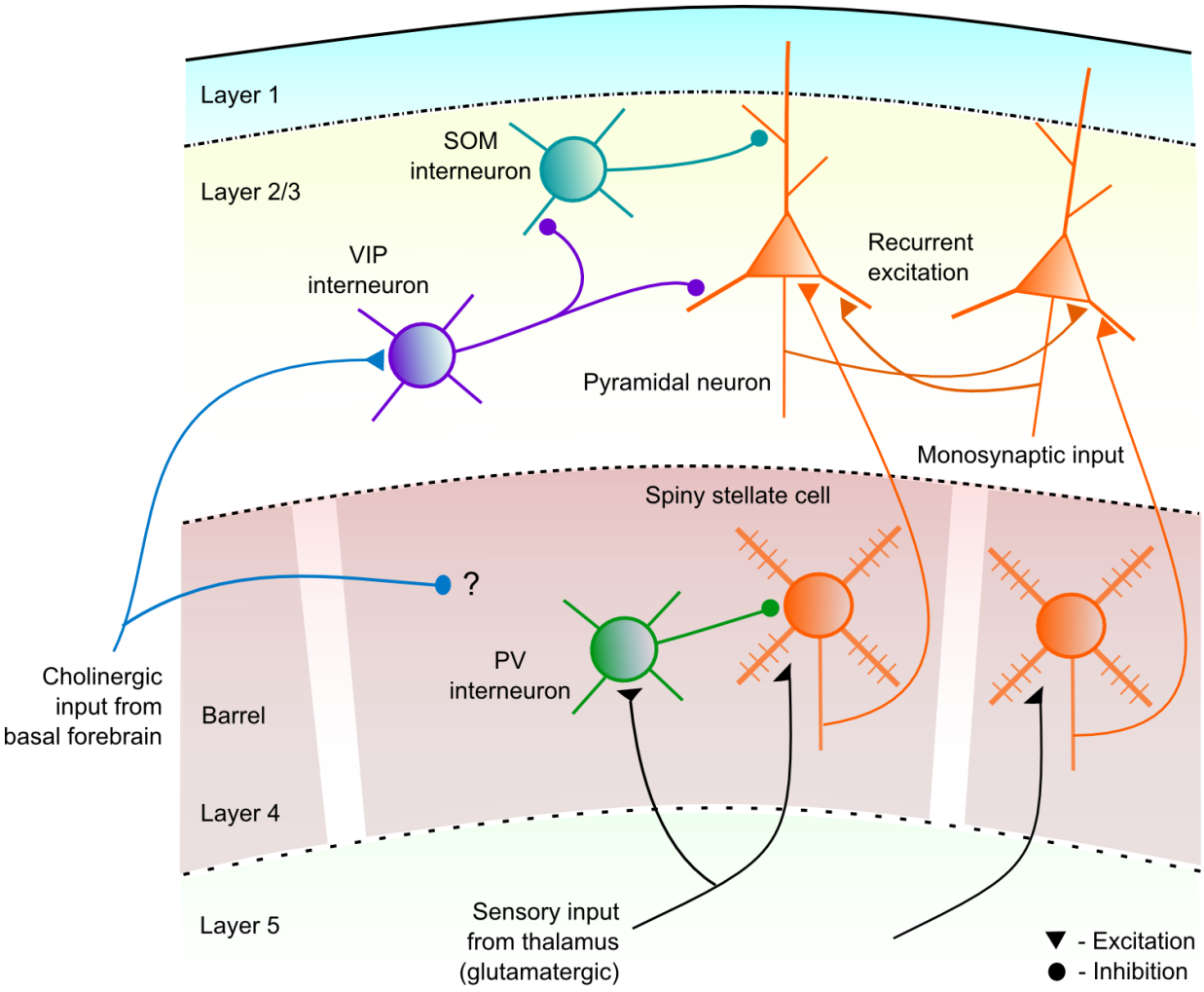

Figure 1.1: Schematic of rodent primary somatosensory "barrel" cortex. Spiny stellate cells in layer 4 are the primary recipients of thalamocortical input. They in turn provide excitatory drive to layer 2/3 pyramidal cells that also share extensive "recurrent" connections with one another. All cortical layers contain several different classes of GABAergic interneurons. PV cells form feed-forward inhibitory circuits and target proximal dendritic and somatic regions of excitatory cells, while SOM cells target distal dendrites. VIP cells inhibit both SOM cells and excitatory neurons, thus mediating either disinhibition or inhibition. How these various cell types are modulated by fast cholinergic signaling is not entirely clear.

Neocortical inhibitory cell types form stereotypical circuit motifs

Although comprising only ~15% of cortical neurons, inhibitory GABAergic cells are crucial players in cortical circuit functions, critical not only for the maintenance of stable excitation/inhibition ratios (Xue et al., 2014), but also the mediation of complex cognitive functions like sensory processing (Hubel and Wiesel, 1962), decision-making (Guo et al., 2014) and learning (Letzkus et al., 2011). Cortical inhibitory interneurons show even greater diversity than excitatory cells in their morphologies, genetic identities, electrophysiological properties and circuit functions (Ramon y Cajal, 1899, Fishell and Heintz, 2013). Significant disagreements persist in the field regarding the most appropriate method to classify interneuron subtypes (Jiang et al., 2015, Barth et al., 2016). Most classification schemes rely on a combination of parameters (such as morphology and electrical properties), but none are devoid of problematic inconsistencies, overlapping groups and exceptions. One of the more commonly used schemes divides interneuron subtypes into three broad clusters based on their expression patterns of distinct molecular markers:

1. **PV** interneurons express the Ca^{2+}-binding protein parvalbumin. About 40% of all cortical inhibitory neurons are PV expressing.
2. **SOM** interneurons express the neuropeptide somatostatin and comprise about 30% of cortical interneurons.
3. **5HT3aR** interneurons that express an ionotropic serotonin receptor make up most of the remaining 30% of GABAergic cells (Lee et al., 2010). This group can be subdivided further into two groups: **VIP** cells express vasoactive intestinal peptide,

while non-VIP cells are characterized by their expression of the protein reelin (Wamsley and Fishell, 2017).

The principal advantages of using this classification scheme are twofold. First, these three groups together encompass ~99% of cortical interneurons, with very little overlap between the groups (with some exceptions, such as reelin- or parvalbumin-expressing SOM cells). Second, basing classification on genetic markers enables the manipulation of specific subgroups using available transgenic mouse lines (such as PV-Cre or SOM-Cre mice), thereby also allowing for experimental consistency across research groups (Taniguchi et al., 2011). It should be noted, however, that each of these groups contains several subtypes within them that feature important differences in morphologies, layers of preponderance and circuit functions.

PV cells, the best characterized interneuron group, typically show fast-spiking (**FS**) phenotypes, with high firing rates (often >200 Hz), low input resistances, large rheobase values and fast (~0.3 millisecond half-width) action potentials. They form powerful feed-forward inhibitory circuits that accompany every major excitatory cortical pathway (Feldmeyer et al., 2013), including the VB inputs to layer 4 stellate cells, and layer 4 inputs to layer 2/3 (Helmstaedter et al., 2008). Layer 4 FS cells are rapidly recruited by sensory input (Cruikshank et al., 2007), leading to disynaptic inhibition of stellate cells (Beierlein et al., 2003) and thereby creating a short temporal window for thalamocortical excitation/integration in layer 4 (Gabernet et al., 2005, Bruno and Sakmann, 2006). Feedforward inhibition also precludes recurrent excitatory activity for weak stimuli (Pinto et al., 2003). Moreover, PV cell axons target proximal dendrites, somata and axon initial segments of pyramidal cells, affording them robust control of excitatory spike output (Kawaguchi and Kubota, 1997). In

fact, certain forms of cortical-dependent learning are contingent upon brief alleviation of PV-mediated inhibition by disinhibitory pathways (Letzkus et al., 2011, Letzkus et al., 2015). PV neurons also inhibit one another (Pfeffer et al., 2013), at times leading to paradoxical increases in network inhibition when they are experimentally suppressed (Kato et al., 2017).

SOM cells show a variety of non-fast spiking (**non-FS**) firing properties, featuring depolarized resting potentials, adapting action potentials with half-widths around 0.6 milliseconds, biphasic AHPs, and often prominent I_H-mediated sag conductances (Ma et al., 2006) with hyperpolarizing current injections. SOM cells derive most of their excitatory drive from local or long-range cortical excitatory cells, forming feedback inhibitory circuits (Wamsley and Fishell, 2017). Unlike PV cells, SOM neurons largely avoid inhibiting one another (Pfeffer et al., 2013). They do, however, strongly inhibit all other cortical excitatory and inhibitory cell types, leading to SOM-mediated suppression of local recurrent activity evoked by sensory input (Kato et al., 2015, Adesnik, 2017, Kato et al., 2017). Also unlike PV cells, SOM cells target distal regions of pyramidal cell dendrites (Kawaguchi and Kubota, 1997) and are involved in control of dendritic computation. In layer 4, SOM cell axonal arbors are restricted within barrel boundaries (Muñoz et al., 2017).

5HT3aR cells are the most diverse group of the three and thus somewhat difficult to define. They also show non-FS phenotypes with adapting, irregular or late-spiking properties. 5HT3aR cells are most prevalent in the superficial layers 1 and 2/3, where they make up ~95% and ~50% of all inhibitory neurons, respectively (Rudy et al., 2011). VIP cells are the best-characterized subgroup. Several recent studies have identified a stereotypical disinhibitory

circuit from VIP to SOM cells in layer 2/3 (Pfeffer et al., 2013, Fu et al., 2014). However, VIP cells also directly inhibit pyramidal cells (Peters, 1990, Alitto and Dan, 2012), and there likely exists a balance between VIP-mediated inhibition and disinhibition of cortical networks *in vivo* (Garcia-Junco-Clemente et al., 2017, Kuchibhotla et al., 2017). Layer 1 interneurons have also been shown to engage disinhibitory mechanisms via their inhibition of PV cells (Letzkus et al., 2011). Thus, cortical inhibitory interneurons comprise several distinct subgroups that form stereotypical circuit motifs, the dynamic interactions amongst which are still the subject of intense research.

1.2 Cortical states

Cortical circuits are signal aggregators. In stark contrast to most peripheral sensory neurons that faithfully transduce stimuli to action potentials with little variability (Yang et al., 2016), cortical neuronal responses, even in primary sensory areas, are highly variable from trial to trial when presented with identical stimuli. What causes this variability? While the underlying circuit principles and stimulus-independent information contained in this variability are only beginning to be elucidated, it is becoming clear that cortical circuits integrate bottom up sensory inputs with numerous top down inputs signaling internal state, expectation and motivation, among other things (Kuchibhotla et al., 2017). In effect, this means that cortical neuronal outputs are determined by the interplay between at least three distinct predictable factors:

(i) sensory input from thalamus,

(ii) stable network features (cellular physiology, wiring principles, synaptic dynamics) and

(iii) dynamic contextual signals (neuromodulatory inputs, long-range corticocortical inputs),

along with one unpredictable factor, noise. The previous section provided a brief overview of stable network organization in rodent barrel cortex. In this section, we will introduce cortical state dynamics, which are a part of the contextual signals being aggregated by sensory cortices and a principal determinant of cortical circuit activity.

The external environment an animal typically finds itself in is in constant flux, requiring it to continually adapt its behavioral state to the changing environmental conditions. For example, the presence of a predator would require arousal and vigilance to external cues,

whereas the absence of one would indicate to the animal that it is safe to rest or sleep. While changes accompanying behavioral state transitions are comprehensive, they are perhaps most pronounced in the nature of cortical network activity. To keep up with a changing environment, the rules that determine global cortical network activity *in vivo* are also highly dynamic and transitory. The cortical state, put simply, is the set of rules defining spatial and temporal network dynamics in large cortical circuits (Harris and Thiele, 2011).

Cortical states are defined using a few dynamic network properties

The most well recognized and best-studied transitions in cortical state are those that occur between sleep and wakefulness. The nature of cortical activity is strikingly different between awake periods and periods of what is known as slow-wave sleep, or SWS (Hobson, 2005, Lee and Dan, 2012). Because cortical states are reflected in the activity patterns of large networks of neurons, they are best detected *in vivo* by techniques that sample synaptic dynamics from large populations of cells. Recordings using the electroencephalogram (EEG) were the first to reveal that in human subjects, cortical activity during sleep was dominated by slow, large amplitude voltage oscillations, suggesting it was highly "synchronized" (Berger, 1969). But when the subject was awake, cortical activity was marked by fast low amplitude patterns, indicating "desynchronization". Another common method to detect global cortical state transitions involves monitoring the local field potential (LFP) of cortical circuits, which is generated by the summation of extracellular voltages produced by dendritic currents in several neurons spread over large volumes of cortical tissue (Kajikawa and Schroeder, 2011, Herreras, 2016). Paralleling findings in EEG, SWS in rodents is accompanied by a drastic increase in

low frequency power (1-4 Hz, signatures of synchronized oscillatory activity) in cortical LFP recordings (Gervasoni et al., 2004). Cortical state dynamics can be sampled intracellularly as well. Sleep-related cortical states are reflected in current-clamp recordings by slow synchronized oscillations between periods of depolarization and quiescence (Steriade et al., 1993, Steriade et al., 2001), a behavior that can be mimicked in acute slice preparations under special conditions to generate alternating "Up" and "Down-states" (Neske et al., 2015), while awake state recordings generally lack synchronous activity (Constantinople and Bruno, 2011).

Thus, transitions between sleep and awake states are characterized by pronounced shifts in the synchronicity of cortical activity. This has led to a simple rule-of-thumb distinction between synchronized SWS and desynchronized awake cortical states. However, recent evidence indicates that treating the awake state as a single monolithic desynchronized state is an oversimplification (McGinley et al., 2015b). Awake periods are a continuum of constantly and rapidly shifting sub-states themselves (Poulet and Petersen, 2008, Reimer et al., 2014, McGinley et al., 2015a, Vinck et al., 2015, Reimer et al., 2016), with each sub-state possessing distinct neurophysiological and network properties. In fact, shifts in awake cortical states can produce dramatic changes in neuronal coding of sensory input, which are often as large as those produced by changes in the stimulus itself (Niell and Stryker, 2010, Lee et al., 2013, Fu et al., 2014).

In broad terms, sub-states of wakefulness can be classified as either low arousal states - "quiet wakefulness" - or high arousal states called "active waking" (Figure 1.2). Analogous to awake and sleep states, the degree of cortical synchrony is the main feature that sets apart low

from high arousal states - low arousal is characterized by slow synchronized fluctuations in cortical membrane potentials that resemble SWS (Poulet and Petersen, 2008), whereas shifts to arousal are signified by rapid suppression of this activity (Gentet et al., 2010, Eggermann et al., 2014, Reimer et al., 2014, Vinck et al., 2015). High arousal states often carry the additional feature of membrane depolarization (Polack et al., 2013, Reimer et al., 2014, Schneider et al., 2014), which is caused at least in part by increased drive from thalamocortical inputs (McCormick, 1992, Eggermann et al., 2014). As a result of decreased membrane potential synchrony, cortical neuronal firing also becomes decorrelated during arousal, leading to reduced signal and noise correlations (Goard and Dan, 2009, Pinto et al., 2013, Reimer et al., 2014). States of arousal are also accompanied by reduced long-range corticocortical synchrony, resulting in sharp contractions in the cortical area activated by sensory input (Kimura et al., 1999, Roberts et al., 2005, Ferezou et al., 2006, Petersen and Crochet, 2013). Additionally, cortical state dynamics during wakefulness are expressed externally by such features as pupil diameter and muscle tone. Pupil diameter especially is highly correlated with arousal levels (Reimer et al., 2014, McGinley et al., 2015a, Reimer et al., 2016, Shimaoka et al., 2018) and is fast becoming widely adopted as an easily accessible yet reliable and sensitive measure of behavioral state. Finally, shifts to high arousal states are often accompanied by exploratory behavior like whisking or locomotion (Eggermann et al., 2014, Fu et al., 2014, Reimer et al., 2014, Schneider et al., 2014), although locomotion is not necessary for arousal (Vinck et al., 2015). Thus, the waking state offers a rich plethora of behavioral sub-states with a diverse set of psychophysical properties. It is important to note, however, that while a comparison of high and low arousal states offers useful distinguishing features, they are but end-points in a much larger spectrum of waking sub-states (McGinley et al., 2015a).

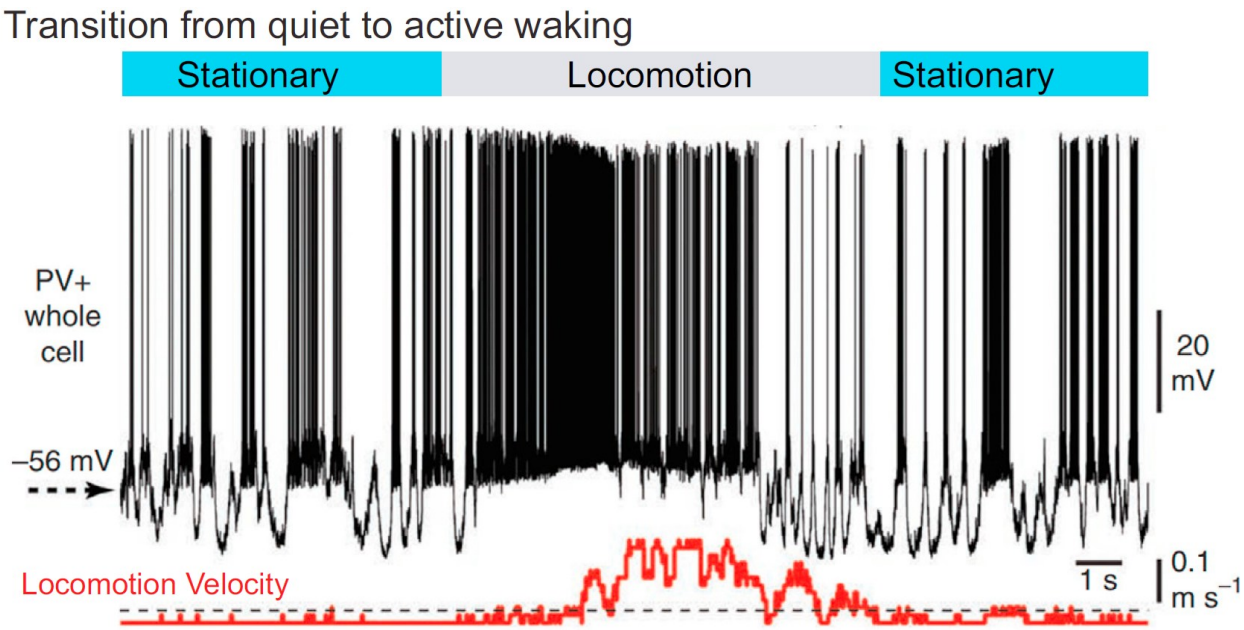

Figure 1.2: Transitions to high arousal states are marked by suppression of slow synchronous cortical activity. The top trace shows an *in vivo* whole cell current-clamp recording from a layer 2/3 PV interneuron in the mouse visual cortex. The mouse was head-fixed but allowed to freely move on a spherical treadmill. The motion in the treadmill is quantified in the bottom red trace; times during which the treadmill velocity was above threshold (dashed line) were considered periods of locomotion, an indicator of active waking or a high arousal state. During periods of quiet wakefulness, the PV cell showed slow spontaneous oscillatory activity that was rapidly abolished when the animal shifted to a more aroused state. (Figure from Polack et al., 2013, as adapted in McGinley MJ, Vinck M, Reimer J, Batista-Brito R, Zagha E, Cadwell CR, Tolias AS, Cardin JA, McCormick DA (2015b) Waking state: rapid variations modulate neural and behavioral responses. Neuron 87:1143-1161, used with permission)

High arousal cortical states are optimized for stimulus-driven behaviors

Awake cortical state has a profound influence on the animal's behavioral performance. As a general rule, arousal-related changes tend to optimize cortical activity for sensory processing, thereby improving discrimination performance. During high arousal states, signal to noise ratio of sensory coding by cortical circuits is markedly improved (Vinck et al., 2015); the component of neuronal spike output determined by sensory input (signal) is increased, while that determined by cortically generated activity (noise) is suppressed (Bennett et al., 2013). This is achieved by engaging two parallel mechanisms: (i) by suppressing spontaneous rhythmic cortical activity (Gervasoni et al., 2004, Eggermann et al., 2014) and reducing noise correlations (Kimura and Baughman, 1997, Goard and Dan, 2009, Reimer et al., 2014), while concurrently (ii) improving the ability of sensory input to drive spiking in individual excitatory neurons: thalamocortical sensory inputs are enhanced (McCormick, 1992, Halassa et al., 2014) and subsets of excitatory neurons are disinhibited (Letzkus et al., 2011, Lee et al., 2013, Fu et al., 2014, Kuchibhotla et al., 2017). The net effects are a prominent arousal-mediated sharpening of sensory responses (Fu et al., 2014, Reimer et al., 2014), increased gain in sensory-evoked spiking (Niell and Stryker, 2010, Bennett et al., 2013) and greater reliability of sensory responses from trial to trial (Goard and Dan, 2009, Marguet and Harris, 2011). Behaviorally, this underlies improved sensory coding - animals can perceive more details in the stimulus and similar stimuli can be better discriminated (Pinto et al., 2013, Engel et al., 2016). Furthermore, attentional performance during aroused states is greatly improved, as demonstrated by faster reaction times in attention-demanding behavioral tasks (Lovett-Barron et al., 2017). However, very high levels of arousal can be stressful, leading to detrimental

effects on task performance (Yerkes and Dodson, 1908, McGinley et al., 2015a). Thus, transitions from low to high arousal states generally underlie a shift towards processing external cues.

Cortical states are under precise control of neuromodulatory and other systems

Given their capacity to influence behavior, cortical states are tightly regulated by a host of overlapping systems. For the purposes of simplification, these systems may be segregated anatomically into two distinct but related groups:

(i) thalamocortical and corticocortical glutamatergic pathways, and

(ii) subcortical neuromodulatory pathways

Long-range glutamatergic inputs to cortical circuits play important roles in the regulation of cortical states (Chen et al., 2013, Zagha and McCormick, 2014). Although somatosensory cortical responses are generally suppressed during high arousal states (Ferezou et al., 2006, Shimaoka et al., 2018), sensory-evoked responses are enhanced by arousal in the primary visual and auditory cortices (Reimer et al., 2014, Kato et al., 2015). One underlying cause for this enhancement is increased firing in thalamic relay neurons due both to direct depolarization (McCormick, 1992) and disinhibition of sensory thalamic nuclei (Halassa et al., 2014). In addition, long-range corticocortical inputs may enhance sensory responses by engaging local disinhibitory circuits (Lee et al., 2013), although such inputs have also been shown to increase local inhibition (Schneider et al., 2014).

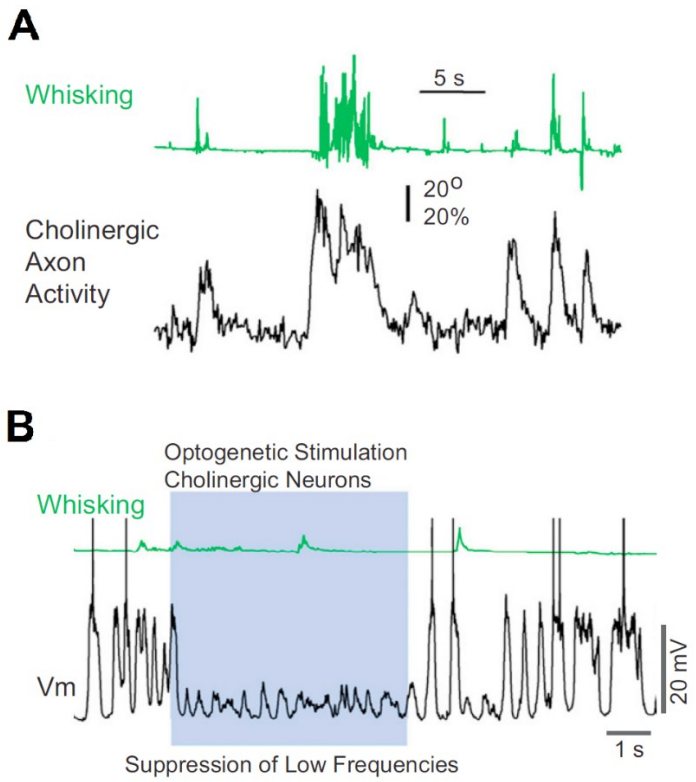

Figure 1.3: Cholinergic signaling is correlated with state transitions and suppresses slow cortical activity. (A) The axons of cholinergic projections neurons expressing the calcium indicator GCaMP6s were imaged in the primary somatosensory cortex of an awake head-fixed mouse, while its whisker movements were monitored. Periods of whisking were highly correlated with activity in cholinergic afferents. **(B)** Cholinergic signaling blocks slow cortical activity. Black trace shows a current-clamp recording from a layer 2/3 neuron showing spontaneous low frequency activity that is powerfully suppressed when cholinergic afferents are optogenetically activated. (Figures from Eggermann et al., 2014, as adapted in McGinley MJ, Vinck M, Reimer J, Batista-Brito R, Zagha E, Cadwell CR, Tolias AS, Cardin JA, McCormick DA (2015b) Waking state: rapid variations modulate neural and behavioral responses. Neuron 87:1143-1161, used with permission)

Cortical state dynamics are also under powerful control of multiple parallelly and/or synergistically acting neuromodulatory systems. In particular, the cholinergic and noradrenergic cortical projection systems have long established and crucial roles in the control of sleep/wake cycles, arousal and attentional modulation (Aston-Jones et al., 1999, Jones, 2004, Aston-Jones and Cohen, 2005, Xu et al., 2015), and are known to powerfully promote wakefulness, arousal and selective attention. To cite but a few examples, suppressing noradrenergic discharges in the cortex promotes slow-wave EEG activity (Berridge et al., 1993, Berridge et al., 2012), activating cortical cholinergic afferents suppresses slow membrane potential fluctuations (Metherate et al., 1992), cortically projecting cholinergic neurons show elevated activity *in vivo* during periods of cortical desynchronization (Duque et al., 2000), blocking cholinergic signaling mitigates the effects of attentional modulation (Herrero et al., 2008) and optogenetic activation of cholinergic afferents promotes immediate transitions to wakefulness (Han et al., 2014). In a recent study, Eggermann et al. found that the arousal-related suppression of slow cortical activity observed *in vivo* was almost entirely mediated by cholinergic signaling (Eggermann et al., 2014) (Figure 1.3). Although the cholinergic and noradrenergic projection systems to the cortex arise from anatomically distinct subcortical nuclei and are largely independent, they nevertheless likely act in conjunction to produce the cortical state dynamics observed *in vivo* (Polack et al., 2013, Reimer et al., 2016). Another recent multispecies study found that some of the cholinergic and noradrenergic nuclei controlling cortical states in mice were evolutionarily conserved in fish (Lovett-Barron et al., 2017), cementing the roles of acetylcholine and noradrenaline as critical determinants of global behavioral state. Intriguingly, the frontal cortex sends extensive glutamatergic inputs to the noradrenergic projection nuclei in the brainstem, raising the possibility of indirect feedback

modulation of cortical state dynamics. It is now beginning to emerge that this control is mediated over several distinct timescales, each with its own cellular and synaptic mechanisms, and unique consequences for behavior.

Thanks to recent advances in *in vivo* imaging and recording techniques, the elegant temporal precision with which acetylcholine controls cortical state dynamics is beginning to be revealed. In the same study cited above, Eggermann et al. used the calcium-reporting protein GCaMP6s to monitor cholinergic activity in the primary somatosensory cortex simultaneously with the animal's whisking behavior (an exploratory behavior that served as a marker for arousal, Figure 1.3). They found that sharp increases in cholinergic afferent activity invariably preceded bouts of whisking by a few hundred milliseconds, suggesting tight coupling of cholinergic signaling with transitions to high arousal states (Eggermann et al., 2014). Their results were corroborated in a later study by Reimer et al. that found that cortical cholinergic signaling was highly correlated with other behavioral indicators of arousal like pupil diameter and locomotion (Reimer et al., 2016). Furthermore, phasic fluctuations in cholinergic afferent activity can lead to transient changes in cortical acetylcholine levels (Parikh et al., 2007). In another study, optogenetic activation of cholinergic afferents in V1 led to rapid transitions to desynchronized cortical dynamics within 150 milliseconds (Pinto et al., 2013). Reliable cortical state modulation is a crucial component of moment-to-moment adjustment of brain function depending on behavioral demands. Because it is critical that state transitions during wakefulness be achieved in rapid timescales, their regulatory mechanisms must be capable of fast yet spatiotemporally precise signaling. Thus, fast synaptic signaling by neuromodulatory systems is increasingly gaining prominence in mediating rapid state transitions during waking.

1.3 The cholinergic projection system in the neocortex

The cholinergic projection system constitutes one of the major neuromodulatory systems of the vertebrate brain. In the forebrain, these projections arise largely from two sources: (i) the peduncolupontine and laterodorsal tegmental nuclei of the brainstem that project primarily to the thalamus (Ballinger et al., 2016), and (ii) a heterogeneous group of nuclei located rostro-ventral to the thalamus, known as the basal forebrain (BF). BF cholinergic afferents reach all regions of the neocortex (Woolf and Butcher, 2011), can be found in all cortical layers and the majority of cortical cell types express cholinergic receptors (Muñoz and Rudy, 2014). Functionally, they are a principal determinant of firing rates and cortical states, even in primary sensory areas (Harris and Thiele, 2011). The central role played by these projections in myriad cognitive and behavioral phenomena has been a matter of established dogma for decades (Shiromani et al., 1987, Hasselmo, 2006).

Deficits in cortical cholinergic signaling underlie numerous debilitating disorders. Neurodegeneration of cholinergic neurons is an early step leading to dementia in Alzheimer's disease (Mufson et al., 2008). Moreover, expression patterns of cholinergic receptors are altered in various forms of schizophrenia (Terry, 2008): schizophrenic brains show postmortem deficits in expression of both metabotropic (Zavitsanou et al., 2004), and ionotropic cholinergic receptors (Guan et al., 1999). Notably, increases in cholinergic tone also lead to severe cognitive deficits (Kolisnyk et al., 2013), indicating that precise bidirectional regulation of cholinergic signaling from the BF is critical for normal cognitive function. The

following section will review some of the structure and functions of the BF cholinergic projection system to the neocortex.

BF cholinergic projections relay behavioral signals in a temporally precise manner

Cholinergic neurons in the BF are found interspersed with glutamatergic and GABAergic neurons within a number of morphologically distinct nuclei, including the vertical and horizontal limbs of the diagonal bands of Broca and the nucleus basalis magnocellularis (NB, in humans known as the nucleus basalis of Meynert) (Ballinger et al., 2016). In both rodent and primate brains, these regions show heavy histochemical and/or immunohistochemical labeling for acetylcholinesterase (Andrä et al., 1988) and choline acetyltransferase (Satoh et al., 1983, Mesulam et al., 1984, Pinto et al., 2013, Herman et al., 2016), indicating a concentrated presence of local cholinergic neurons. Although they are also involved in local cholinergic signaling, most BF cholinergic cells are distal projection neurons that send extensive, long-range and effusively branched but stereotypical axonal afferents to most parts of the mammalian forebrain. In addition to the neocortex, BF cholinergic cells also send projections to the hippocampus, amygdala, the olfactory bulb and some hypothalamic nuclei (Lucas-Meunier et al., 2003, Müller and Remy, 2017). Thus, BF nuclei are a principal source of cholinergic afferentation in the forebrain, and thereby serve central roles in the control of behavioral states.

The long-range cholinergic input to the neocortex stems almost exclusively from the NB, along with some inputs from the substantia innominata (Nelson and Mooney, 2016).

Much of what is known about rodent NB afferent and efferent anatomy is derived from studies carried out in rats. In the BF, cholinergic cells are a small minority (5% in rats) (Gritti et al., 2006), but this proportion has been reported to be much higher in primates (80-90%) (Mesulam et al., 1983, Raghanti et al., 2011). In spite of their small relative proportion amongst total cell bodies, long-range projections from the NB are composed predominantly of cholinergic cell axons (80-90% for neocortical projections) (Rye et al., 1984). Moreover, non-cholinergic cells in the NB often fail to show the temporally locked increases in firing rate with arousal seen in cholinergic neurons (Duque et al., 2000, Xu et al., 2015), even though local GABAergic cells can be activated by NB cholinergic cells (Yang et al., 2014). Taken together, it is likely that most of the functionally relevant information carried by long-range NB projections is cholinergic in nature. However, it should also be noted that some BF cholinergic cells may have dual identities; optogenetic activation of cholinergic cells has been reported to induce co-release of GABA in neocortical layer 1 (Saunders et al., 2015), and activation of BF cholinergic afferents in the entorhinal cortex can produce GABAergic responses in inhibitory cells (Desikan et al., 2018).

NB neurons sample a diverse array of behaviorally relevant inputs. NB receives input from several major subcortical limbic areas like the amygdala, medial hypothalamus (Jones and Cuello, 1989) and nucleus accumbens-ventral tegmental area (Haring and Wang, 1986). Perhaps as a consequence, NB cholinergic neurons are strongly and rapidly activated during stimuli that carry behavioral valence, such as rewards or punishments (Hangya et al., 2015). This allows the NB cholinergic projection system to broadcast behavioral contextual information in a temporally precise manner, thereby mediating multiple forms of learning

(Letzkus et al., 2011), including learning to accurately predict timing of reward (Chubykin et al., 2013). In rats, presentation of reward-predicting cues leads to brief and precise cholinergic transients in the frontal cortex within 2 seconds (Parikh et al., 2007), alongside slower forms of cholinergic signaling lasting minutes. In addition, NB cholinergic neurons serve to signal arousal levels: their firing rates show precisely time-locked increases during transitions to wakefulness or aroused states (Duque et al., 2000, Xu et al., 2015). In summary, the NB, and more specifically the cholinergic subpopulation within it, comprise a densely interconnected node that receives behaviorally important information and relays it to large parts of the forebrain, including all of the neocortex. This puts it in a favorable location anatomically to powerfully control cortical states according to changing behavioral needs.

Structure of cholinergic afferentation in neocortex

Although arousal represents a global change in the dynamic properties encompassing the whole brain, other forms cortical state modulation, such as directed attention, are more focal, affecting specific cortical regions or modalities (Harris and Thiele, 2011). It would seem that such precise region-specific cortical state control would require spatially specific and topographically defined cholinergic projections from the NB. However, the topographic organization of cholinergic cells within the NB is still a matter of debate (Coppola and Disney, 2018), partly because classical immunohistochemical methods have produced ambiguous results. Recent studies using viral injections and deep-brain stimulation have revealed a somewhat specific topographic arrangement of BF cholinergic cells that project to the frontal cortex (Bloem et al., 2014, Nagasaka et al., 2017). By carrying out focal virally-induced

expression of yellow fluorescent protein in BF cholinergic cells, Bloem et al. showed that cholinergic cells that were more rostrally located in BF tended to project to more rostral cortical regions, while caudally located BF cells projected more caudally (Bloem et al., 2014). It is unclear, however, how much functional specificity is conferred by this rough topography, since afferents from a single BF cholinergic cell can arborize over a wide cortical area, likely leading to significant overlapping afferentation from multiple cells in the same cortical region (Wu et al., 2014). Although region-specific acetylcholine release has been reported in the sensory cortices (Fournier et al., 2004), topographic specificity among sensory-projecting BF cells is not clear either: limited sensory cortical regions receive input from multiple BF cells spread over large areas (Nelson and Mooney, 2016).

In the vertical plane, there is even less specificity of cholinergic afferentation, as individual BF projection neurons form extremely long axons and arbors that reach across all layers (Wu et al., 2014), although in barrel cortex, cholinergic afferentation appears somewhat denser in layers 1 and 4. An additional complication is that a subset of interneurons in layer 2/3 show some of the genetic signatures of cholinergic neurons (von Engelhardt et al., 2007), although acetylcholine release from cortical neurons has not been definitively reported. In short, cholinergic afferentation in the cortex is very widespread in nature, and this has prompted speculation that cortical cholinergic signaling is spatially non-specific (Lucas-Meunier et al., 2003). However, spatial specificity of cortical cholinergic signaling may be achieved through other means, such as the ultrastructural features of acetylcholine release sites, or differences in expression patterns of cholinergic receptors among cortical neurons and how readily those receptors are engaged under various forms of cholinergic signaling (Muñoz

and Rudy, 2014). Indeed, mounting functional evidence *in vivo* suggests that cholinergic signaling in the cortex is in fact highly region-specific (Herrero et al., 2008, Guillem et al., 2011, Kalmbach and Waters, 2014). Thus, elucidating the structural and functional mechanisms of cholinergic signaling in neocortical circuits will be critical to gaining a mechanistic description of spatiotemporally specific cortical state control by acetylcholine.

1.4 Mechanisms of cholinergic signaling in neocortical circuits

Every major cognitive behavior is under the influence of cortical acetylcholine. Cholinergic signaling is critical for mediating both global arousal (Metherate et al., 1992) and focal attention (Harris and Thiele, 2011). It is involved in both the transient processing of sensory inputs (Metherate, 2004, Thiele, 2013) and in the establishment long-term learning and memories (Hasselmo, 2006, Chubykin et al., 2013). It affects synaptic transmission between local neurons (Kimura and Baughman, 1997, Origlia et al., 2006, Amar et al., 2010) and long-range communication between distal cortical neurons (Muñoz and Rudy, 2014). Applying cholinergic antagonists on the cortical surface leads to deficits in attention and other cognitive functions (Leblond et al., 2002, Herrero et al., 2008), as does optogenetically silencing cholinergic afferents (Gritton et al., 2016). Transitions to high arousal states are closely correlated temporally with increased activity in cholinergic afferents (Eggermann et al., 2014, Reimer et al., 2016), and activation of cholinergic signaling causes rapid switches to desynchronized/decorrelated cortical states (Pinto et al., 2013, Kalmbach and Waters, 2014, Chen et al., 2015) that feature reduced corticocortical synchrony and restricted receptive field sizes (Roberts et al., 2005, Silver et al., 2008).

Clearly, the functions of acetylcholine in the neocortex are myriad and complex. However, the mechanistic underpinnings of spatiotemporally precise cholinergic control of cortical activity remain largely unknown. A significant hurdle is the absence of a large body of information about cholinergic modulation at the circuit level that could bridge phenomena at the cellular and systems levels. Therefore, it is essential to understand how cholinergic

signaling modulates activity in well-defined canonical microcircuits, which form the most essential unit of information processing in the neocortex (Mountcastle, 1997, Feldmeyer et al., 2013, Hirabayashi and Miyashita, 2014). This section will briefly review the known cellular and receptor sub-types engaged by cortical acetylcholine, the specific circumstances under which they are likely engaged, and their various circuit-level consequences. In addition, it will highlight critical gaps in our understanding of cholinergic signaling in the neocortex, in particular the spatiotemporal dynamics of cholinergic-mediated control of cortical network activity.

Cholinergic signaling in neocortex may involve both volume and classical synaptic transmission

The spatiotemporal dynamics of signaling by any neurotransmitter depend critically on two factors:

(i) the structural properties of its synapses that determine how rapidly and specifically receptors are engaged, and

(ii) postsynaptic kinetics of signaling that determine the temporal properties of downstream effects mediated by the receptors once engaged.

The location of neuromodulatory receptors relative to sites of release is critical in determining the spatiotemporal dynamics of its function. In the neocortex, cholinergic signaling may occur via either classical or volume transmission (Zoli et al., 1999). Classical synaptic transmission typically features close apposition of presynaptic release sites and

postsynaptic receptors. This type of signaling preferentially recruits receptors that are clustered in the postsynaptic domain near sites of acetylcholine release. Thus, the defining feature of classical transmission is that single release events are sufficient to engage receptors with high probability, enabling efficient entrainment and temporally precise control of postsynaptic activity (Beierlein, 2014). As a result, classical synaptic transmission leads to fast one-to-one (i.e., spatiotemporally precise) synaptic communication (Zoli et al., 1999). In certain instances, fast and precise signaling can be achieved even in the absence of ultrastructurally defined synapses: although some studies have reported the lack of postsynaptic receptors close to acetylcholine release sites in the neocortex (Lendvai and Vizi, 2008), ionotropic cholinergic receptors are nevertheless capable of mediating spatiotemporally precise signaling (Bennett et al., 2012, Arroyo et al., 2014). Finally, classical synaptic transmission has customarily been thought to be dominated by ionotropic signaling, especially with regards to neuromodulatory transmitters like acetylcholine.

Volume transmission, on the other hand, requires multiple release events and slow diffusion and/or spillover of transmitter through extracellular space in order to engage receptors, leading to temporally imprecise signaling. This typically occurs when receptors are located far from the release site, for instance, in the case of extrasynaptic metabotropic receptors that are located outside the postsynaptic density (Descarries and Mechawar, 2000). Owing to their nonoptimal location, they can typically only be engaged under special forms of high-frequency cholinergic input that cause spillover of acetylcholine outside the immediate confines of the synaptic cleft. Another example of volume transmission is mediated by presynaptically located metabotropic or ionotropic receptors, that influence synaptic release probability (Kimura and

Baughman, 1997, Amar et al., 2010) and short-term dynamics (Urban-Ciecko et al., 2018). Presynaptic receptors may be present on synapses releasing a different (heterosynaptic signaling) or the same transmitter (autosynaptic signaling). In the latter case, presynaptic signaling can mediate powerful auto-regulation of release (Sun et al., 2013). Importantly, volume transmission can allow transmitter released from a single axonal afferent to potentially engage receptors on multiple postsynaptic neurons (Zoli et al., 1999). Thus, this form of signaling is also spatially imprecise. Because neuromodulatory actions are conventionally considered to also be generally slow and diffuse, metabotropic cholinergic signaling has long been thought to function almost exclusively via volume transmission (Lucas-Meunier et al., 2003).

It is still unclear which form of transmission, volume or classical, cortical cholinergic signaling is predominantly reliant upon (Muñoz and Rudy, 2014). In the neocortex, evidence for classical cholinergic synapses (with thickened varicosities close to postsynaptic densities) has been sparse (Descarries et al., 1997, Descarries and Mechawar, 2000). However, cholinergic afferents do form synaptic specializations (Smiley et al., 1997) that are located adjacent to cortical neuronal dendrites (Turrini et al., 2001). An emerging picture of cholinergic signaling suggests that both modes of transmission are prominent and act in conjunction with one another (Parikh et al., 2007, Sarter and Kim, 2015). Multiple spatiotemporally distinct signaling modes may even be a general feature of cortical neuromodulation (Sarter and Kim, 2015).

Ionotropic and metabotropic cholinergic signaling

In addition to modes of transmission, the kinetics of the postsynaptic mechanisms that are activated following ligand binding to the receptor are also critical factors in the spatiotemporal dynamics of cholinergic signaling. Cortical acetylcholine can act via the engagement of both ionotropic nicotinic (nAChRs) or metabotropic muscarinic receptors (mAChRs), expressed pre- or postsynaptically in various cortical neuronal cell types. The pentameric cation channel nAChRs display relatively fast kinetics (Bennett et al., 2012, Arroyo et al., 2014), mediating excitatory postsynaptic currents (EPSCs) that subside within 500 ms. In the neocortex, nAChRs are typically either homomeric α7 or heteromeric α4β2 subtypes, which differ in their Ca^{2+} permeability (the former subtype is permeable, the latter, not), kinetics (decay time constants for α7 EPSCs are ~5 ms, while those for α4β2 EPSCs can be >200 ms) (Arroyo et al., 2012) and expression patterns.

Muscarinic receptors are metabotropic receptors that may be coupled to either $G_{q/11}$ (in the case of "M1-type" mAChRs) or $G_{i/o}$ ("M2-type" mAChRs) proteins in the postsynaptic membrane (Muñoz and Rudy, 2014), leading to highly diverse downstream effects, including activation/deactivation of K^+-channels (Carr and Surmeier, 2007, Eggermann and Feldmeyer, 2009), Ca^{2+} release from intracellular stores (Gulledge and Stuart, 2005, Gulledge et al., 2007), activation of Protein Kinase C (Cantrell et al., 1996), and so on. Unlike nAChR-mediated signaling, the temporal profiles of mAChR-mediated effects are determined chiefly by the kinetics of their downstream biochemical pathways (Jensen et al., 2009). Resultantly, mAChR-mediated signaling is typically prolonged, lasting on the order of several seconds.

Besides differences in their kinetics, there also exist important distinctions between nAChRs and mAChRs in their presumed modes of engagement: whereas most cortical nAChRs are thought to be engaged rapidly via classical synaptic transmission, mAChRs are considered to be almost entirely reliant on volume transmission (Lucas-Meunier et al., 2003). This notion has persisted despite evidence for the rapid synaptic recruitment of mAChRs in subcortical structures like the TRN (Sun et al., 2013).

Nicotinic receptor expression and function

Nicotinic receptors are expressed in a cell-type specific manner by both glutamatergic and GABAergic neurons in the neocortex (Poorthuis et al., 2013). Their expression and function are best characterized on the dendrites of cortical inhibitory interneurons, where they primarily mediate direct postsynaptic depolarization. Dendrites of layer 1 inhibitory interneurons are the most common site of expression for α7 nAChRs (Letzkus et al., 2015, Poorthuis et al., 2018), where they generate fast EPSCs and dendritic Ca^{2+} transients. Layer 1 cells inhibit local PV interneurons, their nAChR-mediated activation can cause disinhibition of layer 2/3 pyramidal cells (Letzkus et al., 2011). A number of recent studies have also reported the α4β2 nAChR-mediated recruitment of inhibitory cells by endogenously released acetylcholine but have nonetheless failed to arrive at a definitive answer regarding their resultant network effects. EPSCs mediated by α4β2 nAChRs are prominent in a large proportion of superficial layer GABAergic neurons (Arroyo et al., 2012, Arroyo et al., 2014, Poorthuis et al., 2014). In particular, the non-FS VIP cell subpopulation is strongly activated by cholinergic input *in vivo* (Alitto and Dan, 2012, Pi et al., 2013, Kuchibhotla et al., 2017). Because VIP cells strongly

inhibit local SOM and PV cell populations (Lee et al., 2013, Pfeffer et al., 2013, Fu et al., 2014), their recruitment leads to powerful disinhibition of subsets of pyramidal cells, a function critical for certain forms of learning (Pi et al., 2013). However, VIP cells also directly inhibit pyramidal cells, and *in vitro* studies have produced contradictory results – optogenetic activation of cholinergic afferents can cause disynaptic inhibition of pyramidal cells (Arroyo et al., 2012). *In vivo*, there likely exists a balance between general nAChR-mediated inhibition and selective disinhibition of smaller subpopulations of pyramidal cells (Garcia-Junco-Clemente et al., 2017, Kuchibhotla et al., 2017), thereby leading to the sparse firing properties of layer 2/3 cells (Petersen and Crochet, 2013).

Nicotinic receptor-mediated signaling on cortical excitatory cells has not been widely demonstrated. Deep layer pyramidal neurons are activated by nAChRs in multiple species (Verhoog et al., 2016, Obermayer et al., 2017), although the use of exogenous agonist application in these studies methods makes interpretation of their functional relevance difficult. Layer 5 and 6 glutamatergic cells can also be activated by nAChRs engaged via synaptic mechanisms (Hedrick and Waters, 2015, Hay et al., 2016, Nelson and Mooney, 2016). Nicotinic receptors are expressed presynaptically at some cortical glutamatergic synapses, such as the thalamocortical terminals in layer 4 of primary visual cortex (Disney et al., 2007) and glutamatergic synapses onto SOM cells (Urban-Ciecko et al., 2018), where they increase release probability. However, it remains unclear under what conditions these receptors are engaged *in vivo*.

Muscarinic receptor expression and function

Muscarinic receptors are broadly expressed in all regions of the neocortex (Volpicelli and Levey, 2004, Thiele, 2013) in a variety of cell types. M1-type (M1, M3 and M5) mAChRs, when expressed postsynaptically, act primarily by inhibiting tonically active K^+ channels, such as K^+ leak channels (Madison et al., 1987), leading to membrane depolarization. M2-type (M2 and M4) mAChRs, on the other hand, activate inwardly rectifying K^+ (GIRK) channels, leading to postsynaptic hyperpolarization (Eggermann and Feldmeyer, 2009, Sun et al., 2013). Because mAChR signaling has traditionally been considered to be purely a neuromodulatory influence, postsynaptic actions of both mAChR subtypes have been interpreted largely in the context of their indirect effects via glutamatergic and GABAergic signaling (Lucas-Meunier et al., 2003, Lucas-Meunier et al., 2009), such as changes in the excitability of GABAergic cells (Kawaguchi, 1997) or the mediation of dendritic shunting inhibition. Presynaptically, mAChRs expressed at glutamatergic synapses between excitatory cells reduce probability of glutamate release (Kimura and Baughman, 1997, Amar et al., 2010), thereby decreasing the efficacy of corticocortical communication. This, coupled with nAChR-mediated enhancement of the efficacy of thalamocortical excitation (Disney et al., 2007) is thought to underlie cholinergic-mediated improvements in signal-to-noise ratio of sensory encoding in cortical circuits during high arousal states (Thiele, 2013). In some cases, mAChRs can also control the nature of nAChR-signaling in an activity-dependent manner (Brombas et al., 2014). Finally, cortical muscarinic signaling also mediates long-term synaptic plasticity: M2- and M1-type mAChRs facilitate long-term potentiation and depression in layer 2/3 glutamatergic synapses, respectively (Origlia et al., 2006). Lasting muscarinic-mediated increases in the efficacy of

glutamatergic synapses are thought to underlie several forms of learning, such as reward timing in the primary sensory cortices (Gavornik et al., 2009, Chubykin et al., 2013).

Studies examining direct mAChR-mediated effects on cortical neuronal outputs have identified a plethora of postsynaptic effects. In barrel cortex, layer 4 stellate cells are persistently hyperpolarized in an mAChR-dependent manner by the puff application of acetylcholine (Eggermann and Feldmeyer, 2009), but whether endogenous acetylcholine produces similar effects is not known. Pyramidal cells in layer 5 exhibit biphasic mAChR-mediated responses: acetylcholine puffs produce initial hyperpolarizations (mediated by Ca^{2+}-activated K^+ (SK) channels), followed by slower depolarization (Gulledge and Stuart, 2005, Gulledge et al., 2007, Gulledge et al., 2009). Studies employing synaptic mechanisms to activate mAChRs *in vitro* are extremely rare: Hedrick and Waters have shown both mAChR-mediated hyperpolarization and depolarization of pyramidal neurons resulting from optogenetic activation of cholinergic afferents (Hedrick and Waters, 2015). With regards to GABAergic cells, SOM interneurons in layers 2/3 and 4 are powerfully activated by mAChRs (Fanselow et al., 2008), an effect that is thought to contribute to cortical desynchronization associated with arousal (Chen et al., 2015). A recent study found *in vivo* evidence for the rapid mAChR-mediated activation of layer 4 SOM interneurons, coincident with shifts to aroused states (Muñoz et al., 2017). However, it is difficult to deduce which of these responses are relevant in rapid forms of cholinergic signaling (since exogenous application does not reveal the underlying spatiotemporal dynamics) or to combine these myriad effects into a unified model of mAChR-mediated control of cortical network activity.

Spatiotemporally precise cholinergic control of cortical circuits remains largely unexplored

While the literature for cholinergic signaling in the cortex is long and extensive, much of the existing work has taken broad-based approaches, making it difficult to identify some of the nuances of cholinergic function. For instance, numerous studies have investigated cell-type specific expression patterns of cholinergic receptors in the neocortex (Volpicelli and Levey, 2004, Arroyo et al., 2014, Poorthuis et al., 2014, Groleau et al., 2015), without sufficiently examining their relative spatial distributions on the dendrites or their distances from presynaptic varicosities, thus precluding inferences about the underlying kinetics or the conditions under which they are engaged. Studies examining the function of cholinergic afferentation have similar shortcomings: the overwhelming majority have employed exogenous application of acetylcholine or its agonists, which, besides generating non-physiological concentrations of ligands in the extracellular milieu, do not discriminate between receptors that are engaged by volume or synaptic transmission *in vivo* (Unal et al., 2015). Thus, in order to better understand the spatiotemporal dynamics of cortical cholinergic function, it is imperative to investigate the action of acetylcholine released under physiologically-relevant conditions by employing modern tools like optogenetics.

The lack of mechanistic evidence for precise cortical signaling is particularly true for mAChRs. The arguments for spatiotemporally imprecise mAChR signaling are two-fold: their supposed reliance on volume transmission, and the onset latencies for the second messenger systems they activate. The notion of volume transmission has been bolstered by the paucity of

mAChRs close to acetylcholine release sites (Yamasaki et al., 2010). However, neocortical cholinergic synapses may not always show the signatures of conventional synapses (Muñoz and Rudy, 2014), and postsynaptic mAChRs are often localized with and functionally coupled to channels in a membrane-delimited fashion, allowing for fast PSC latencies. For instance, stimulating cholinergic afferents in the TRN leads to the activation mAChR-mediated K^+ currents with short and reliable latencies (Sun et al., 2013). Most importantly, the view of mAChRs purely as slow neuromodulators is difficult to reconcile with recent *in vivo* evidence of rapid and powerful mAChR-mediated control of cortical states and arousal-related behaviors; particularly the observation that mAChR activation leads to decorrelation of cortical activity on very fast timescales (Goard and Dan, 2009, Pinto et al., 2013, Muñoz et al., 2017).

In summary, there is very little *in vitro* evidence for the rapid engagement of mAChRs, with clear and direct consequences for cortical network activity. Despite the known contribution of mAChRs to cognitive control on fast timescales, knowledge of a circuit-level mechanism for rapid cell-type specific mAChR signaling in neocortex is conspicuously lacking. As evidence for fast mAChR-mediated control of cortical state dynamics continues to grow, this gap is becoming ever more glaring.

Chapter 2: Materials and Methods

Reproduced from Dasgupta R, Seibt F, Beierlein M (2018) Synaptic release of acetylcholine rapidly suppresses cortical activity by recruiting muscarinic receptors in layer 4. J Neurosci 38:5338-5350.

2.1 Animals

We used bacterial artificial chromosome (BAC)-transgenic mice of either sex expressing ChR2 under the control of the choline acetyltransferase (ChAT) promoter (ChAT–ChR2–EYFP) (Zhao et al., 2011). Animals were purchased from Jackson Labs (https://www.jax.org/strain/014546) and maintained as hemizygous. This mouse line carries additional copies of the vesicular acetylcholine transporter (VAChT) gene, potentially leading to enhanced release of acetylcholine (Kolisnyk et al., 2013). Therefore, additional experiments were carried out using ChAT-Cre/Ai32(ChR2-YFP) mice, generated by crossing ChAT-Cre animals (https://www.jax.org/strain/006410) with Cre-dependent reporter Ai32(ChR2-YFP) mice (https://www.jax.org/strain/012569), as described previously (Hedrick et al., 2016). Some experiments were performed using C57BL/6 wild-type mice. All animals used in this study were treated following procedures in accordance with National Institutes of Health guidelines and approved by the University of Texas Health Science Center at Houston (UTHealth) animal welfare committee.

2.2 Slice preparation

Animals aged P12-16 were anesthetized using isoflurane and then decapitated. The brains were rapidly removed and placed in ice cold cutting solution saturated with 95% O_2–5% CO_2, that consisted of the following (in mM): 212 sucrose, 2.5 KCl, 1.25 NaH_2PO_4, 10 $MgSO_4$, 0.5 $CaCl_2$, 26 $NaHCO_3$, and 11 glucose. Thalamocortical slices (Agmon and Connors, 1991) (400 μm) were cut using a vibratome (VT1200 S, Leica Biosystems) and immediately transferred to artificial cerebrospinal fluid (ACSF, saturated with 95% O_2–5% CO_2), maintained at 35°C and consisting of the following (in mM): 126 NaCl, 2.5 KCl, 1.25 NaH_2PO_4, 2 $MgCl_2$, 2 $CaCl_2$, 26 $NaHCO_3$ and 10 glucose. Slices were incubated at 35°C for 20 minutes and then stored at room temperature until used for experiments.

2.3 Electrophysiology

Electrophysiological recordings were performed in a recording chamber (RC-26GLP, Warner Instruments) perfused with ACSF saturated with 95% O_2–5% CO_2 and warmed to 31-34°C using an in-line heater connected to a temperature controller (TC-324B, Warner Instruments). Cells were visualized via infrared differential interference contrast (IR-DIC) using a fixed stage microscope (BX51WI, Olympus) equipped with an infrared camera (IR-1000, Dage-MTI). Recordings were acquired using an amplifier (Multiclamp 700B, Molecular Devices), filtered at 3–10 kHz, and digitized at 20 kHz with a 16-bit analog-to-digital converter (Digidata 1440A; Molecular Devices). For voltage-clamp recordings of glutamatergic or GABAergic activity in the absence of mAChR-dependent postsynaptic responses, glass

pipettes (3-5 MΩ) were filled with a cesium-based internal solution consisting of (in mM): 120 $CsMeSO_3$, 1 $MgCl_2$, 1 $CaCl_2$, 10 CsCl, 10 HEPES, 3 QX-314, 11 EGTA, 2 Mg-ATP, and 0.3 Na-GTP (adjusted to 295 mOsm and pH 7.3). For current-clamp recordings, and voltage-clamp recordings of cholinergic postsynaptic responses, we used a potassium-based internal solution consisting of (in mM): 133 K-Gluconate, 1 KCl, 2 $MgCl_2$, 0.16 $CaCl_2$, 10 HEPES, 0.5 EGTA, 2 Mg-ATP, and 0.4 Na-GTP (adjusted to 290 mOsm and pH 7.3). Where indicated, 5 mM BAPTA was included to block increases in intracellular calcium concentration.

Cortical activity was evoked using extracellular electrical stimuli (1-20 μA). Stimuli were generated using an isolated pulse stimulator (Model 2100, A-M Systems) and delivered via a glass electrode filled with ACSF. For some experiments exogenous cholinergic agonists were applied using a Picospritzer (Parker Automation).

NBQX, DHβE, AF-DX 116, picrotoxin, CGP 55845, D-APV, and MLA were obtained from R&D Systems. All other chemicals were obtained from Sigma-Aldrich.

2.4 Optogenetics

Cholinergic afferents were activated using 5 millisecond (ms) pulses of blue light using an LED light source (UHP-T-450-EP, Prizmatix) delivered through a 60X, 0.9NA water-immersion objective (Olympus) with an effective illumination diameter of <250 μm. Light intensity was adjusted to ~60 mW at the back aperture of the objective and kept constant throughout all experiments. During recordings the objective was centered over the soma of the

recorded neuron. For dual recordings of cells located in distinct cortical layers, postsynaptic responses for each cell were recorded sequentially.

2.5 Experimental design and statistical analyses

In order minimize response variability due to differences of ChR2 expression between animals, we first quantified cholinergic synaptic responses onto neurons in the thalamic reticular neurons (TRN) for each animal (Sun et al., 2013). Neurons were recorded in voltage-clamp and cholinergic afferents were activated locally with individual pulses (0.5 ms) of constant intensity, as described above. If nicotinic EPSCs had amplitudes less than 50 pA, ChR2 expression was considered too low and slices were not used for experiments. A fraction of ChAT-Cre/Ai32(ChR2-YFP) animals show ChR2 expression in glutamatergic neurons (Hedrick et al., 2016). For TRN recordings, such ectopic expression resulted in light-evoked fast EPSCs and slices were not further considered for experiments.

Data were analyzed using custom macros written in IGOR Pro (Wavemetrics). Statistical tests were performed in Prism 5 (Graphpad). Evoked recurrent activity recorded in voltage-clamp was quantified as charge transferred to the recorded cell, by calculating the area under the PSC trace in a time window starting 90 ± 3 ms after the first electrical pulse and ending when evoked activity returned to baseline. For a given cell, the same time window was used for paired and unpaired trials. To account for changes in response magnitudes in unpaired trials over the course of pharmacological experiments, responses recorded in paired trials in a given drug condition were normalized to responses recorded in unpaired trials in the same drug

condition and time period. Decay time constants of postsynaptic cholinergic currents were determined by fitting single exponential functions to responses averaged over >10 trials. Unpaired comparisons were performed using the two-tailed unpaired t test. Paired comparisons were made using the Wilcoxon signed rank test or paired Student's t test. Differences were considered significant when $p \leq 0.05$. Data are shown as mean ± SEM.

Chapter 3: Results

Reproduced in part from Dasgupta R, Seibt F, Beierlein M (2018) Synaptic release of acetylcholine rapidly suppresses cortical activity by recruiting muscarinic receptors in layer 4. J Neurosci 38:5338-5350.

Cholinergic projections from the BF to the neocortex are extensive (Woolf and Butcher, 2011) and play crucial roles in varied cognitive processes such as attention (Herrero et al., 2008) and fear conditioning (Letzkus et al., 2011). Acetylcholine has a profound effect on cortical state, and recently, cortical cholinergic signaling has been implicated in the rapid transitions from idleness to arousal that occur *within* periods of waking (Goard and Dan, 2009, McGinley et al., 2015b, Reimer et al., 2016), predicting a high degree of specificity and precision in the underlying signaling mechanisms (Muñoz and Rudy, 2014).

Cholinergic fibers are prevalent in all cortical layers (Bloem et al., 2014, Wu et al., 2014). Although fast cholinergic signaling has traditionally been thought to rely on nAChRs (Letzkus et al., 2011, Arroyo et al., 2012), recent *in vivo* evidence indicates that rapid cholinergic-mediated changes in cortical activity have mAChR-mediated mechanisms (Goard and Dan, 2009, Eggermann et al., 2014, Muñoz et al., 2017). However, the circuit mechanisms of fast cortical modulation by the synaptic engagement of mAChRs remain unclear.

Here, we sought to determine how the synaptic release of acetylcholine rapidly alters cortical network activity by employing *in vitro* electrophysiology.

3.1 Synaptic release of acetylcholine suppresses evoked cortical activity

We investigated the role of cholinergic synaptic signaling in regulating cortical activity by employing optogenetic techniques in somatosensory (barrel) cortical slices of ChAT-ChR2-EYFP mice expressing ChR2 in cholinergic neurons (Zhao et al., 2011). Where indicated, experiments were carried out in slices derived from ChAT-Cre/Ai32(ChR2-YFP) mice (Hedrick et al., 2016). Cortical activity was evoked by applying brief stimulus bursts (4 stimuli, 40 Hz) delivered through extracellular glass electrodes placed in layer 4. To monitor activity, we targeted layer 2/3 pyramidal cells in the same cortical column and performed voltage-clamp recordings using a Cs^+-based internal solution (Figure 3.1A). Stimulus bursts generated postsynaptic responses consisting of short-latency monosynaptic EPSCs with little latency jitter, as well as long-latency polysynaptic activity (onset: 45.7 ± 6 ms, duration: 678.9 ± 50.9 ms, n = 19 cells) which displayed considerable jitter from trial-to-trial (Figure 3.1B). Stimulus intensity was adjusted to reliably evoke polysynaptic activity for the majority of trials (90.3 ± 3%, n = 19 cells) in a given recording. As polysynaptic responses are thought to be mediated by recurrent excitatory connections in local cortical networks (Beierlein et al., 2002), we will refer to these responses as recurrent activity. To examine fast cholinergic modulation of recurrent activity, we paired extracellular stimulation in layer 4 with single light pulses (5 ms duration), to mimic the phasic discharge pattern of BF cholinergic neurons observed in vivo (Lee et al., 2005, Hangya et al., 2015). Light pulses were centered on the recorded neuron and applied 15 ms prior to the onset of stimulus bursts. This led to a reliable and repeatable suppression of recurrent activity (quantified as a change in EPSC charge transfer) compared to unpaired trials lacking cholinergic stimulation (unpaired: 105±15 pC, paired: 27.8±4 pC, 29.8

± 0% compared to unpaired trials, n = 19 cells, $p < 0.001$, Wilcoxon signed rank test; Figure 3.1B-E). Similar findings were obtained for ChAT-Cre/Ai32(ChR2-YFP) mice (17.7±0% compared to unpaired trials, n = 2 cells). In contrast, monosynaptic EPSCs evoked by the first two stimuli were unaltered by optical activation (unpaired: 197.5±35 pA, paired: 199.6±36 pA, 100.9 ± 2% compared to unpaired trials, n = 19, $p = 0.5$, two-tailed paired t-test; Figure 3.1F).

To examine the effect of cholinergic activation on the output of layer 2/3 pyramidal cells, we recorded in current-clamp to detect spikes. In unpaired trials, recurrent activity evoked few spikes in layer 2/3 neurons (unpaired: 1.18±0.4 spikes per trial; Figure 3.2B,D). Optical stimulation led to a reduction of spiking activity (paired: 0.38±0.2 spikes per trial, 36.4 ± 11% compared to unpaired trials, n = 6 cells, $p = 0.01$, Wilcoxon signed rank test; Figure 3.2).

We then asked whether cortical recurrent activity initiated by thalamocortical input to layer 4 could be similarly inhibited by cholinergic stimulation. Electrical stimulation in the TRN produced short latency (<3 ms) monosynaptic EPSCs in layer 4 neurons with stellate morphologies (Figure 3.3A,B), suggesting that they were produced by stimulation of thalamocortical afferents from the VB (Beierlein and Connors, 2002). Thalamocortically evoked recurrent activity was also robustly suppressed by cholinergic input (Figure 3.3C,D). Together, our data indicate that brief activation of cholinergic afferents reliably suppresses recurrent activity in cortical networks.

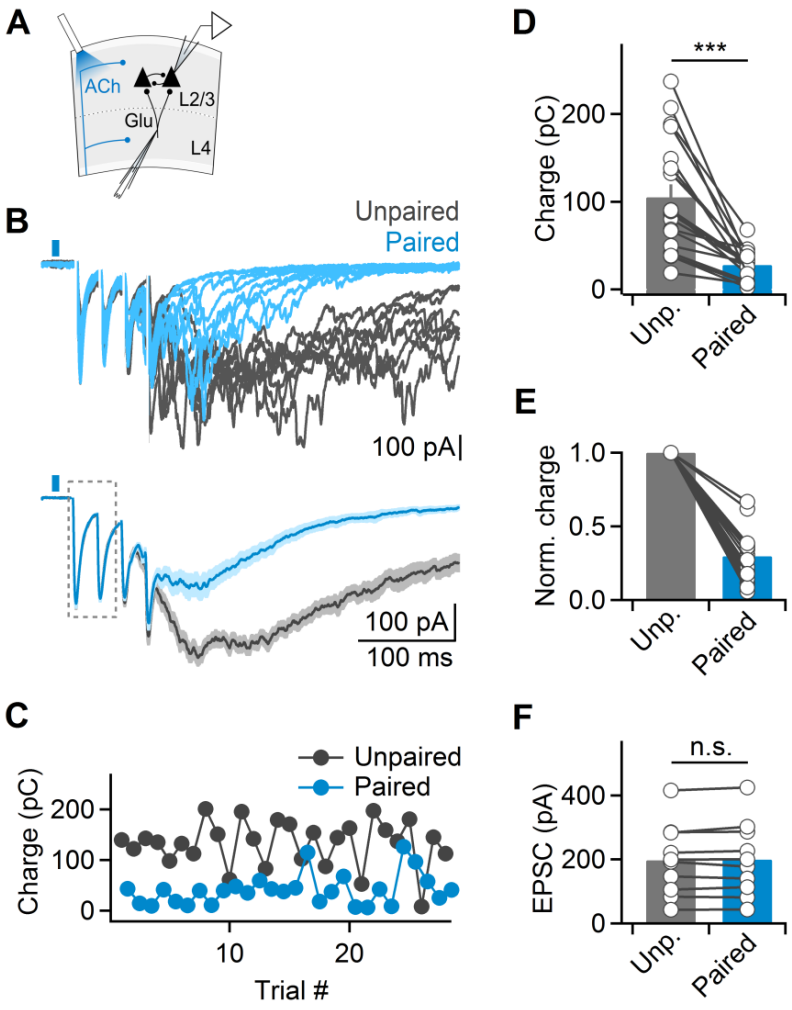

Figure 3.1: Acetylcholine release evoked by single light pulses suppresses evoked cortical recurrent activity. (A) Schematic of experimental setup. Cortical recurrent activity was evoked using brief bursts of extracellular stimuli applied in layer 4 (L4) and was recorded in voltage-clamp in layer 2/3 (L2/3). Cholinergic afferents (ACh) were activated using single light pulses (5 ms), 15 ms prior to electrical stimulation. **(B)** *Top:* Representative recording showing multiple trials of recurrent activity, in the absence (unpaired, black traces) or presence of optical stimulation (paired, blue traces). *Bottom:* EPSCs averaged across all unpaired and paired trials. Note lack of change in amplitude of monosynaptic EPSCs (outlined) **(C)** For the same cell shown in B, plot depicts recurrent activity (quantified as EPSC charge transfer), in

paired trials (blue) alternated with unpaired trials (black). **(D)** Summary data showing light-evoked suppression of recurrent activity in layer 2/3 neurons (n = 19 cells). **(E)** Same data as in (D), normalized to unpaired responses. **(F)** Summary data showing average amplitude of monosynaptic EPSC evoked by the first two stimuli (n = 10 cells), for unpaired and paired trials. Shaded areas and error bars denote SEM.

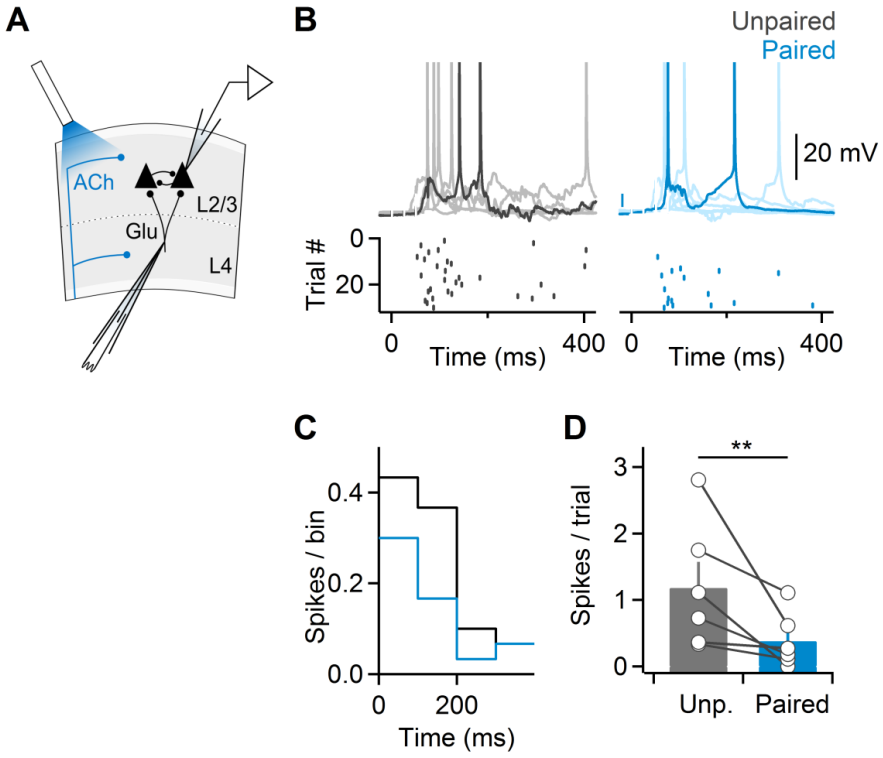

Figure 3.2: Acetylcholine release reduces action potential firing during recurrent activity. (A) Schematic of experimental setup. Cells were held in current-clamp with minimal current injection to keep the cell at ~-60 mV. Recurrent activity evoked via electrical stimulation in layer 4 was monitored in layer 2/3 neurons and paired with optical activation of cholinergic afferents. **(B)** Representative experiment showing consecutive trials of recurrent activity, under paired (black) or unpaired (blue) conditions. Raster plots indicate the timing of action potentials in individual trials. **(C)** Peristimulus time histogram for the same cell

showing total spikes per 100 ms bin across trials. (**D**) Summary data (n = 6 layer 2/3 neurons) showing acetylcholine-mediated decrease in neuronal activity. Error bars denote SEM.

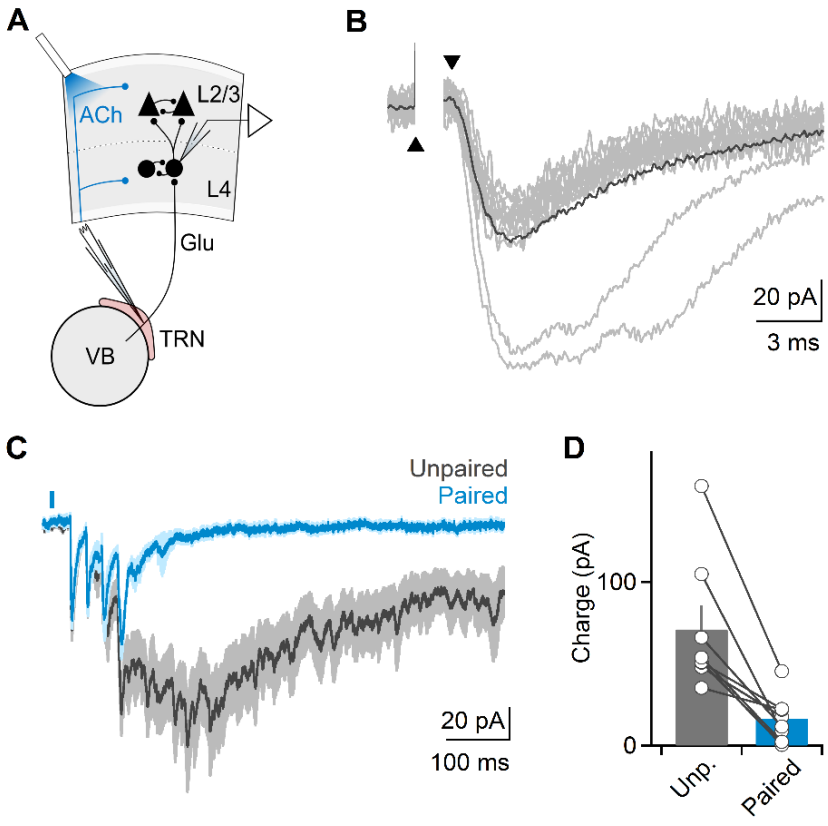

Figure 3.3: Acetylcholine release suppresses cortical recurrent activity evoked by stimulation of thalamocortical input. (A) Schematic of experimental setup. Thalamocortical afferents from the VB nucleus were stimulated electrically with brief bursts by means of a glass electrode placed within the adjoining TRN, and cortical recurrent activity was monitored by recording in layer 4. **(B)** Individual trials (gray) and average trace (black) from an example cell showing short latency between stimulus and EPSC onsets (black arrowheads). **(C)** Averaged EPSCs in paired and unpaired trials for the same cell, showing strong suppression of evoked cortical activity when paired with brief optical activation. **(D)** Summary data from 8 cells. Shaded areas and error bars denote SEM.

3.2 Cholinergic transmission does not affect the balance of excitation and inhibition in cortical networks

Next, we tested whether cholinergic signaling uniformly suppressed recurrent activity within the local network, by conducting simultaneous recordings from neighboring layer 2/3 neurons located within ~200 μm of one another (Figure 3.4A). This revealed strong covariation of cholinergic suppression of recurrent activity from trial to trial (Figure 3.4B,C), indicating that neurons that form part of the same local network are uniformly suppressed by cholinergic input.

The rapid suppression of recurrent activity with optical stimulation could be mediated by a selective cholinergic-mediated activation of local cortical inhibitory interneurons, leading to a decrease in the ratio between excitation and inhibition in the local network (Lucas-Meunier et al., 2009). To account for this possibility, we tested if cholinergic signaling equally reduced activity in local inhibitory neuronal networks by simultaneously recording EPSCs and inhibitory postsynaptic currents (IPSCs) in neighboring neurons, voltage-clamped at -70 and 0 mV, respectively (Figure 3.5A). Suppression of recurrent activity varied widely across cell pairs, ranging from 71.1% to 1.2% compared to unpaired trials. However, suppression of excitatory and inhibitory activity was virtually identical for a given cell pair ($R^2 = 0.98$; Figure 3.5B,C). Thus, cholinergic signaling did not modify the balance of synaptic excitation and inhibition in layer 2/3 during recurrent activity. Taken together, these results suggest that synaptically released acetylcholine uniformly suppresses recurrent activity without significantly altering the excitation/inhibition ratio of cortical networks.

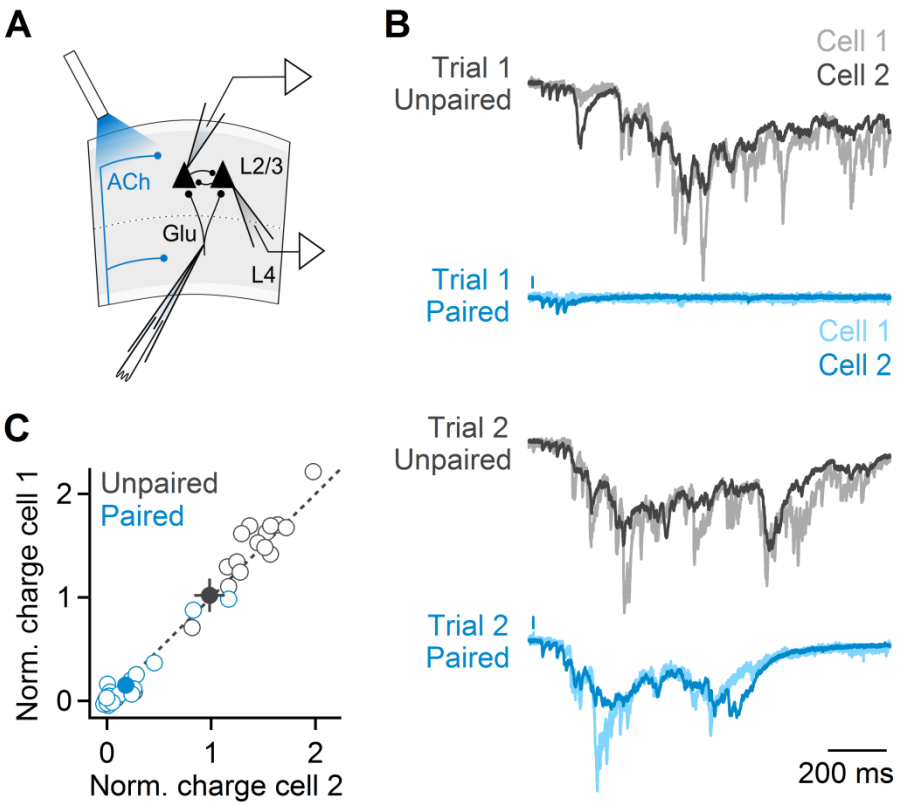

Figure 3.4: Magnitude and suppression of recurrent activity are tightly correlated within layer 2/3 local networks. (A) Recurrent activity evoked in layer 4 was recorded in voltage-clamp from two neighboring layer 2/3 neurons (held at -70 mV to isolate EPSCs), with (paired) or without (unpaired) prior activation of cholinergic afferents. **(B)** Representative experiment showing overlaid responses from both neurons for two paired (blue) and two unpaired (black) trials recorded consecutively. **(C)** Magnitude of recurrent activity (measured as EPSC charge transfer) in individual trials (n = 22 trials) for the two cells shown in (B). Responses for each cell are normalized to the respective average recurrent activity across all unpaired trials. Filled circles denote average responses. Error bars denote SEM.

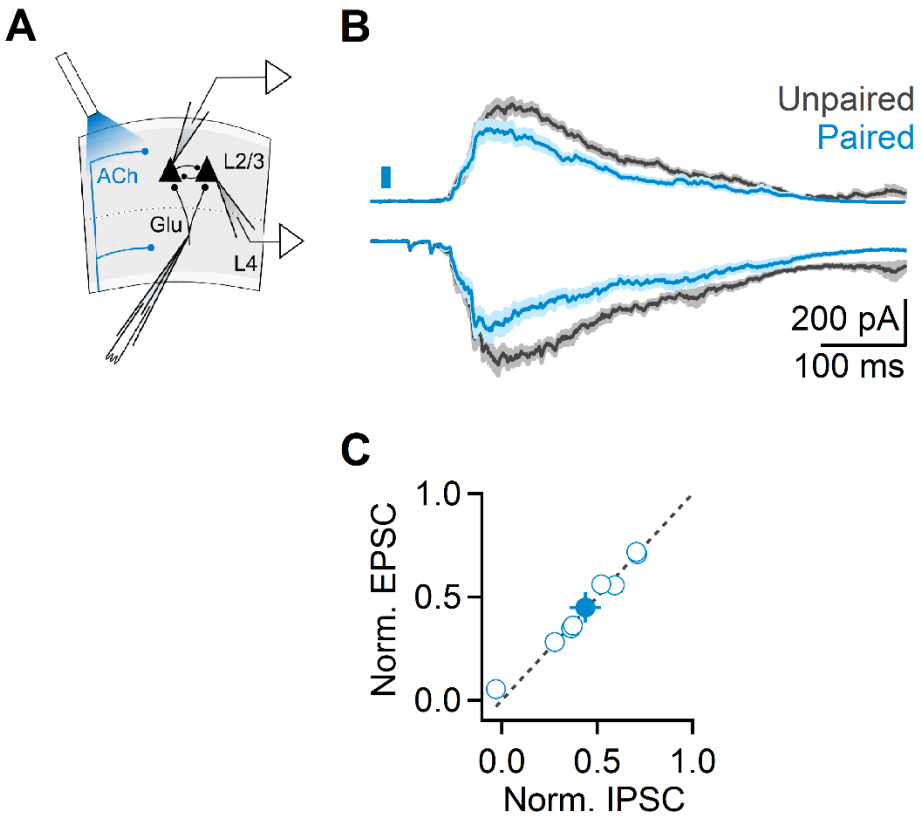

Figure 3.5: Acetylcholine release evoked by single light pulses does not alter excitation/inhibition balance in cortical networks. (A) Recurrent activity evoked in layer 4 was recorded in voltage-clamp from two neighboring layer 2/3 neurons, held at -70 mV and 0 mV to isolate EPSCs and IPSCs, respectively. **(B)** Recurrent activity recorded as EPSCs and IPSCs (black: unpaired, blue: paired) from pairs of neighboring layer 2/3 cells. **(C)** Summary data plotting normalized suppression of EPSCs and IPSCs, for all cell pairs (n = 8). Shaded areas and error bars denote SEM.

3.3 Cholinergic suppression is largely mediated by mAChRs

Both nAChRs and mAChRs are expressed in different types of neocortical neurons (Muñoz and Rudy, 2014), but how these receptors are activated by endogenous acetylcholine to mediate cholinergic control of cortical circuits is not well understood. We found that bath application of atropine to block mAChRs significantly reduced cholinergic suppression (paired: 36.7 ± 5% compared to unpaired trials, atropine: 77.9 ± 4%, $n = 10$, $p < 0.01$, Wilcoxon signed rank test; Figure 3.6A,B), indicating that acetylcholine increases evoked by single light pulses can rapidly recruit mAChRs.

Atropine application additionally led to a small increase in recurrent activity in unpaired trials (118.7 ± 9% compared to control, $n = 15$, $p = 0.03$, Wilcoxon signed rank test, Figure 3.7A), suggesting that cortical activity is also controlled via persistent activation of mAChRs. To determine whether this reduction was due to enhanced levels of ambient acetylcholine in our transgenic mouse model (Kolisnyk et al., 2013), we repeated these experiments in slices derived from wild-type animals. Bath application of atropine still led to an increase in recurrent activity, although this effect did not reach statistical significance (120 ± 11% compared to control, $n = 10$, $p = 0.07$, Wilcoxon signed rank test, Figure 3.7B). This suggests that persistent activation of mAChRs might not be limited to ChAT-ChR2-EYFP mice.

Compared to the effects of blocking mAChRs, washing in MLA and DHβE to block α7 and non-α7 nAChRs, respectively, led to a smaller but significant reduction of cholinergic

suppression (paired: 27.5 ± 7% compared to unpaired trials; MLA and DHβE: 42.5 ± 6%, n = 10, $p < 0.01$, Wilcoxon signed rank test; Figure 3.6C). Furthermore, MLA and DHβE application did not lead to an increase in recurrent activity in unpaired trials (96.4 ± 7% compared to control, n = 7, $p = 0.25$, Wilcoxon signed rank test) suggesting that tonic activation of nAChRs is not prominent.

Although both α7 and α4β2 nAChRs are expressed in the superficial layers, activation of cortical cells by α7 nAChRs has not been widely reported (Arroyo et al., 2012). In agreement, we found that washing in MLA alone to selectively block α7 receptors while leaving non-α7 nAChR signaling intact had no effect on cholinergic suppression of recurrent activity (paired: 38.1 ± 5% compared to unpaired trials; MLA: 37.3 ± 3%, n = 5, $p = 0.34$, Wilcoxon signed rank test; Figure 3.8).

In addition to evoking acetylcholine release, optical stimuli might lead to the liberation of GABA from BF afferents (Saunders et al., 2015) or from neocortical ChAT-positive GABAergic neurons (von Engelhardt et al., 2007) which express ChR2 in our transgenic mouse lines. However, we found that the combined application of both mAChR and nAChR antagonists completely eliminated suppression of recurrent activity (control: 30.4 ± 7% compared to unpaired trials; antagonists: 99.9 ± 8%, n = 8, $p < 0.01$, Wilcoxon signed rank test; Figure 3.6C), suggesting that light-evoked effects on recurrent activity were exclusively mediated by acetylcholine.

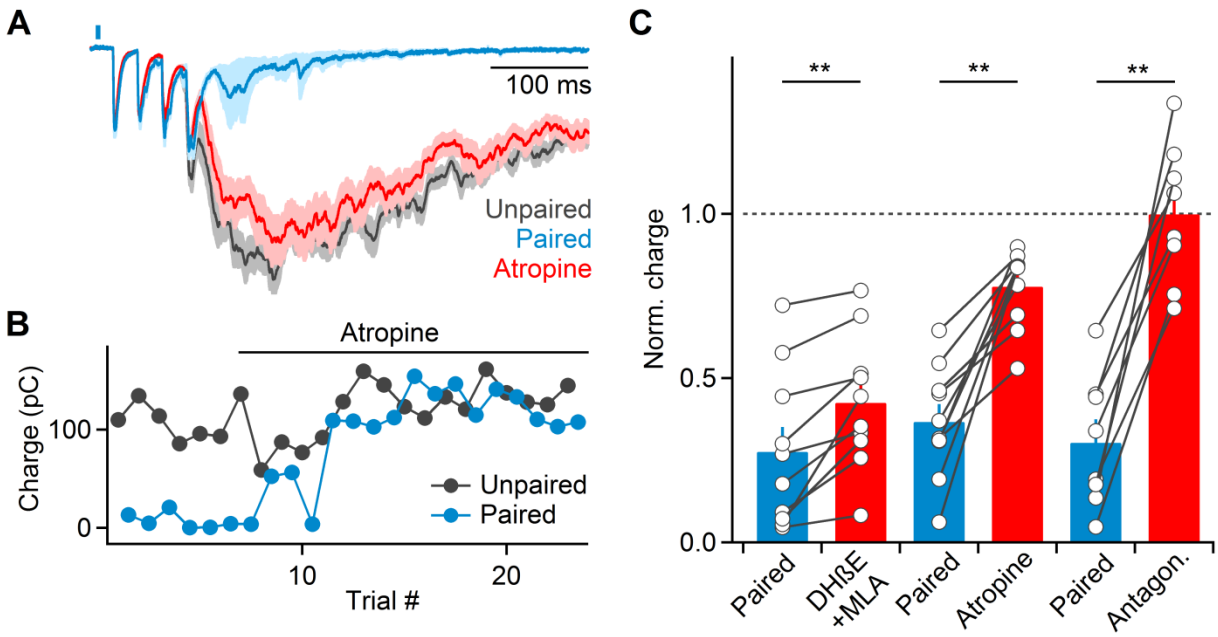

Figure 3.6: Cholinergic suppression of recurrent activity is mediated by both nAChRs and mAChRs. (A) Voltage-clamp recordings from a representative layer 2/3 cell showing that bath application of the mAChR antagonist atropine (10 μM) largely blocks cholinergic suppression of recurrent activity (blue: average EPSCs in paired control trials, red: average EPSCs in paired trials following atropine application, gray: average EPSCs in unpaired trials). Data were normalized to magnitude of recurrent activity in unpaired trials under the same conditions. **(B)** Magnitude of recurrent activity for the same cell across unpaired (black) and paired (blue) during atropine application. **(C)** Summary data of recurrent activity (normalized to activity in unpaired trials) prior to and after bath application of nAChR antagonists (500 nM DHβE + 5 nM MLA, n = 10 cells), atropine (10 μM Atr. n = 10 cells), or both (n = 8 cells). Shaded areas and error bars denote SEM.

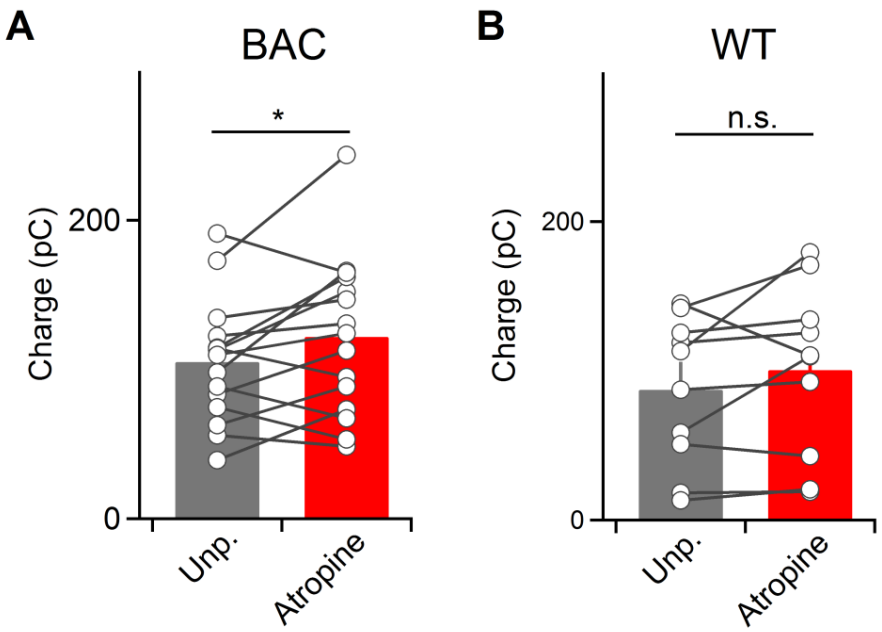

Figure 3.7: Persistently active mAChRs suppress cortical activity in the absence of evoked acetylcholine release. (A) Summary data from BAC transgenic ChAT-ChR2-EYFP (BAC) mice. Evoked cortical recurrent activity, when averaged across unpaired trials that lack optical stimulation, shows a slight increase in magnitude when mAChRs are blocked (n = 15 cells). **(B)** Summary data from wild-type (WT) mice shows a similar, albeit statistically insignificant, effect (n = 10). Error bars denote SEM.

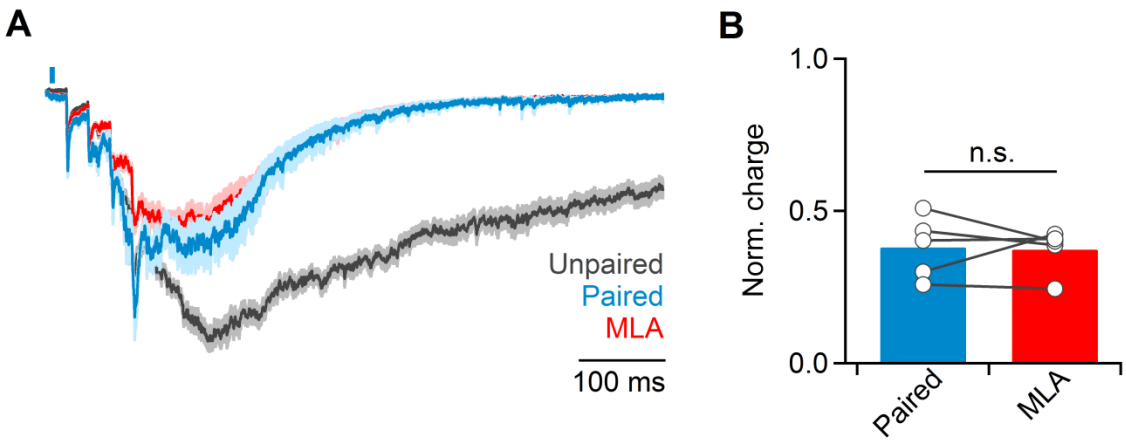

Figure 3.8: α7 nAChRs play no role in cholinergic-mediated suppression of recurrent activity. (A) Voltage-clamp recordings from an example layer 2/3 cell, showing no change in cholinergic suppression of recurrent activity following the pharmacological blockade of α7 nAChRs with 5 nM MLA (blue: average EPSCs in paired control trials, red: average EPSCs in paired trials following MLA application, gray: average EPSCs in unpaired trials). **(B)** Summary data of normalized recurrent activity from 5 cells. Shaded areas and error bars denote SEM.

3.4 Transient acetylcholine increases lead to prolonged suppression of recurrent activity

The crucial role of mAChRs in the suppression of recurrent activity predicts that BF-evoked suppression should be long-lasting. To examine this possibility, we progressively increased the delay between optical activation of cholinergic afferents and extracellular stimulation to evoke recurrent activity. Suppression of recurrent activity was maximal for delays of 1 and 2 seconds and remained prominent even at 5 second delays, with delays of 8 seconds no longer yielding significant reductions in activity (Figure 3.9A,B).

A strong reduction of recurrent activity several seconds after the release of acetylcholine does not appear to be compatible with a role for nAChRs. Indeed, for experiments with delays of 5 seconds between optical and electrical stimulation, bath application of atropine or the M2/M4 mAChR antagonist AF-DX 116 completely eliminated cholinergic suppression (control: 46.1 ± 8% suppression, atropine/AF: 99.2 ± 5% suppression, $n = 11$, $p < 0.01$, Wilcoxon signed rank test; Figure 3.10A,B). Thus, nAChRs and mAChRs mediate cholinergic suppression of recurrent activity on distinct timescales, with nAChRs mediating transient reduction and mAChRs being responsible for long-lasting reduction of cortical activity.

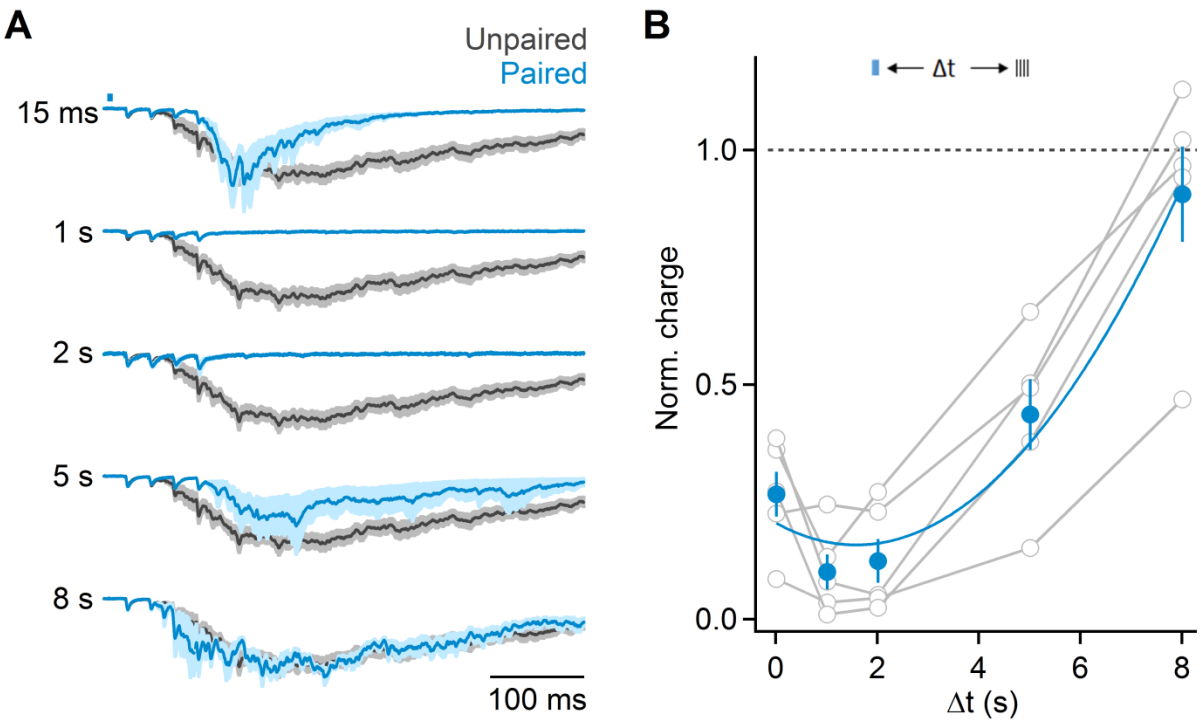

Figure 3.9: Cholinergic-mediated suppression of recurrent activity is long-lasting. (A) Representative recording showing average EPSCs during unpaired (black) and paired (blue) trials, for a range of temporal delays (15 - 8000 ms) between optical and electrical stimulation. Data were normalized to magnitude of recurrent activity in unpaired trials under the same conditions. **(B)** Summary data quantifying light-evoked suppression of recurrent activity (normalized to responses in unpaired trials) as a function of temporal delay between and electrical stimulation (n = 5 cells). Summary data were fit by a third order polynomial (χ^2=0.013). Shaded areas and error bars denote SEM.

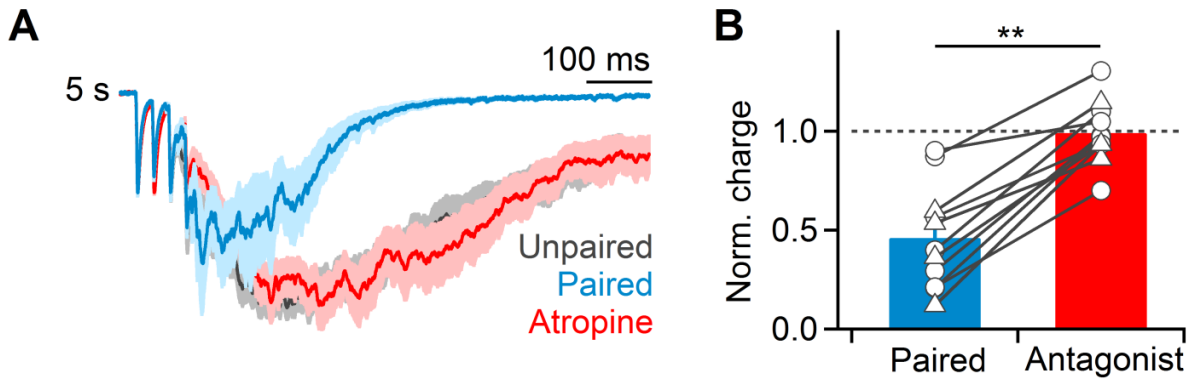

Figure 3.10: Sustained suppression of cortical recurrent activity is mediated entirely by mAChRs. (A) Representative recording showing that for 5 s delays between optical and electrical stimulation, suppression of recurrent activity (blue) was entirely reversed by bath application of atropine. **(B)** Summary data showing elimination of light-evoked suppression of recurrent activation following of bath application of either atropine or 10 µM AF-DX 116 (circles: atropine, n = 7 cells; triangles: AF-DX 116, n = 4 cells), for experiments as shown in (C). Shaded areas and error bars denote SEM.

3.5 Cholinergic suppression via mAChRs is prominent in layer 4

Next, we tested if the contributions of nAChRs and mAChRs to cholinergic suppression could be localized to distinct cortical layers. To address this question, we surgically removed layers 1-3 by performing cuts parallel to the pial surface just above layer 4, and carried out recordings from layer 4 neurons deemed excitatory (Figure 3.11A). Extracellular stimulation applied to the same barrel still led to recurrent activity, but with reduced magnitude (uncut slice: 105 ± 15 pC, n = 19, layer 4-6 slice: 54.9 ± 8 pC, n = 15). Furthermore, we still observed robust light-evoked suppression of recurrent activity (38.5 ± 5% compared to unpaired trials, n = 15, $p < 0.001$, Wilcoxon signed rank test; Figure 3.11B,C). However, in contrast to our findings in intact slices, atropine almost completely reversed cholinergic suppression (control: 35.4±7% compared to unpaired trials, atropine: 92.8 ± 4%, n = 6, p = 0.01, Wilcoxon signed rank test; Figure 3.11B,C), while application of MLA and DHβE to block nAChRs no longer reduced cholinergic suppression (control: 35.1 ± 6% compared to unpaired trials, MLA and DHβE: 30.2 ± 5%, n = 6, p = 0.23, Wilcoxon signed rank test; Figure 3.11D,E). Furthermore, increasing the delay between optical and extracellular stimuli to 5 seconds still led to atropine-sensitive suppression of recurrent activity (control: 46.4 ± 8% compared to unpaired trials, atropine: 124.6 ± 27%, n = 5, p = 0.02, Wilcoxon signed rank test; Figure 3.11F,G). These data indicate that cholinergic inputs to layers 4-6 can mediate robust and long-lasting mAChR-mediated suppression of cortical activity. Furthermore, they suggest that the nAChR-dependent suppression of network activity primarily occurs in more superficial layers. However, it is possible that severing dendrites and translaminar projections eliminated the contributions of nAChR activation in deeper cortical layers.

To further constrain the location of mAChR-mediated suppression, we performed recordings from layer 5 pyramidal neurons in slices with layers 1-4 surgically removed, and evoked recurrent activity using electrodes placed in the white matter (Figure 3.12A). The magnitude of recurrent activity was further reduced under these conditions (uncut slice: 105 ± 15 pC, n = 19, layer 5-6 slice: 12.8 ± 3 pC, n = 6). Importantly, optical stimulation no longer reduced recurrent activity (90.9 ± 8% compared to unpaired trials, n = 6, p = 0.12, Wilcoxon signed rank test; Figure 3.12B,C), suggesting that fast synaptic acetylcholine release in the infragranular layers is not involved in the control of cortical activity, at least under our experimental conditions.

Taken together, our findings show that the contributions of nAChRs and mAChRs to the suppression of network activity are not uniform across cortical layers. Instead, they indicate that nAChR-dependent suppression is primarily mediated by layers 1-3, while mAChR-dependent suppression is particularly prominent in layer 4.

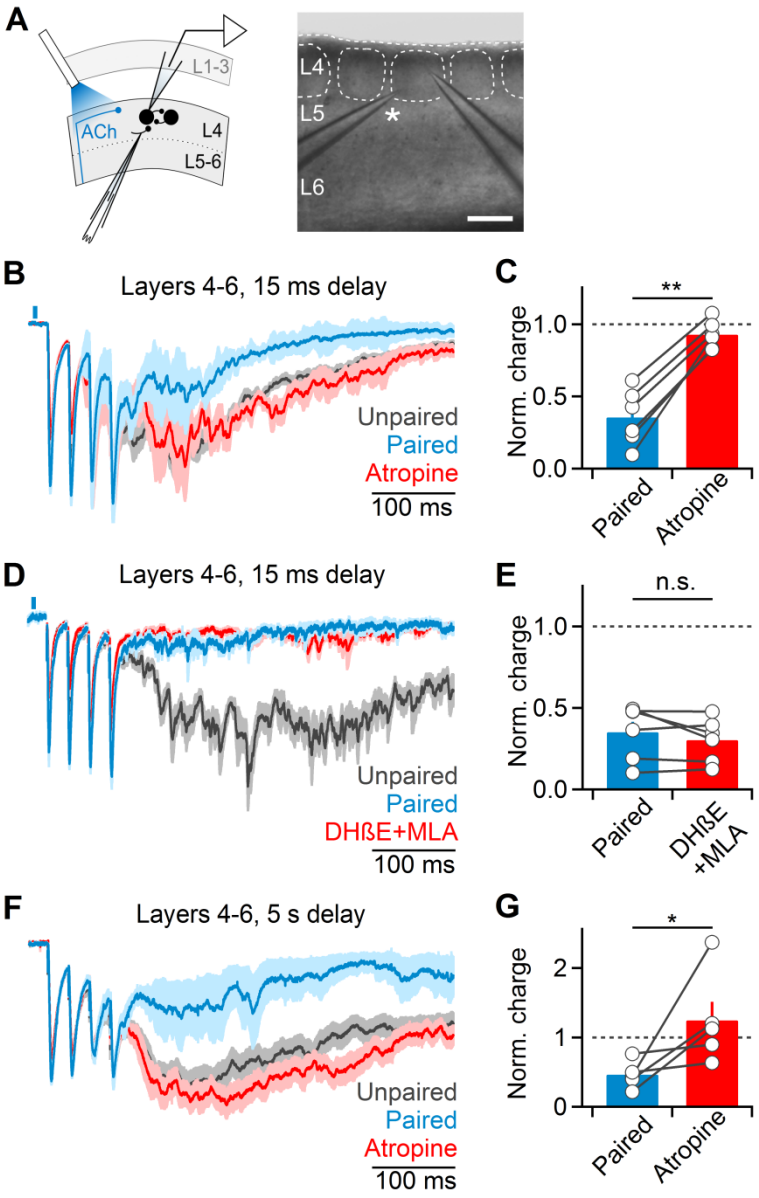

Figure 3.11: Cholinergic suppression of recurrent activity is layer-specific. (A-G) Recordings were carried out in slices following surgical removal of layers 1-3. **(A)** *Left*: Schematic indicating recording arrangement. *Right*: brightfield image of slice preparation, with layer 4 barrels outlined. Asterisk denotes stimulating electrode. Scale bar: 150 µm. **(B)** Representative recording of layer 4 neuron showing that cholinergic suppression of recurrent activity is entirely mAChR-mediated. **(C)** Summary data (n = 6 cells) showing complete

reversal of cholinergic suppression following atropine application. (**D**) Representative recording showing that nAChR antagonist application no longer reduces cholinergic suppression (n = 4 cells, DHβE alone: n = 2, DHβE+MLA: n = 2). **(E)** Summary data (n = 5 cells) for experiments as shown in (D). **(F)** Cholinergic suppression of recurrent activity is maintained for long delays (5 s) between optical and electrical stimuli and mediated my mAChRs. **(G)** Summary data (n = 5 cells) for experiments as shown in (F). Shaded areas and error bars denote SEM.

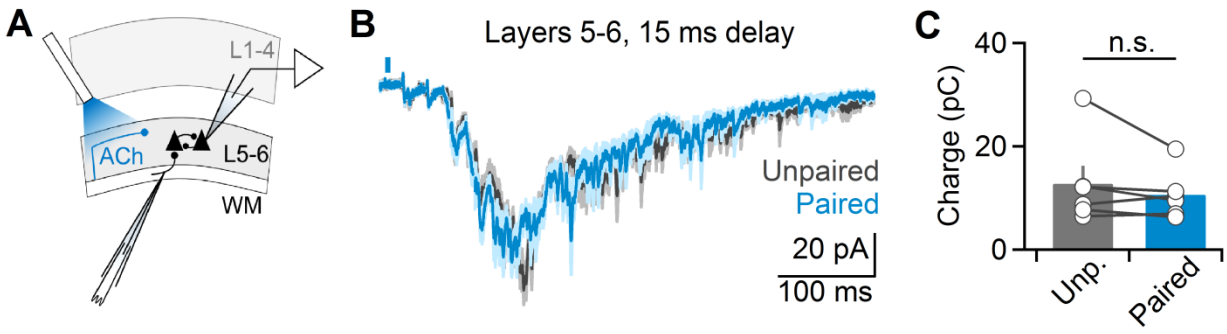

Figure 3.12: Surgical removal of layers 1-4 eliminates cholinergic suppression. (A) Layers 1-4 were surgically removed prior to recording. Recordings were carried out from layer 5 neurons and activity was evoked in the white matter below the same column. **(B)** Representative recording showing EPSCs averaged across paired and unpaired trials. **(C)** Summary data (n = 6 cells) for recordings as shown in (H). Shaded areas and error bars denote SEM.

3.6 Cholinergic postsynaptic responses are largely nAChR-mediated in the superficial layers

Our results described so far are consistent with the activation of nAChRs expressed in layer 2/3 GABAergic interneurons, leading to transient suppression of cortical activity. In addition, they suggest a prominent recruitment of mAChRs in layer 4, resulting in a long-lasting depolarization of GABAergic interneurons, a long-lasting inhibition of excitatory neurons, or both. Next, we carried out recordings from neurons in layers 1-4 using a K^+-based recording solution and determined the nature and frequency of light-evoked postsynaptic responses in different cell types. Neurons were classified as either regular-spiking (RS) cells considered excitatory, or as fast-spiking (FS) or non-fast-spiking (non-FS) cells considered inhibitory, based on their intrinsic firing properties (Beierlein et al., 2003) (Figure 3.13A, Table 3.1). In agreement with previous findings (Arroyo et al., 2012), neurons in layer 1 showed nAChR-mediated EPSCs (nEPSCs, 11/12 neurons) that were fully blocked by a combination of MLA and DHβE. In layer 2/3, a large percentage of inhibitory interneurons displayed nEPSCs that were blocked by DHβE (FS: 39%, non-FS: 77%; Figure 3.13B,C), while a minority of neurons displayed long-lasting mAChR-dependent currents (FS: 23%, non-FS: 5%; Figure 3.13B,C).

Table 3.1: Average values of intrinsic properties for different cell types in layers 2/3 (L2/3) and 4 (L4).

	L2/3 RS	L4 RS	L2/3 non-FS	L4 non-FS	L2/3 FS	L4 FS
Input resistance (MΩ)	162.2 ± 14	343.5 ± 22	313.7 ± 69	283.2 ± 134	125.9 ± 46	85.3 ± 14
Membrane τ (ms)	22.4 ± 2	28.3 ± 2	18.4 ± 2	14.2 ± 4	9.7 ± 1	8.1 ± 1
Spike half-width (µs)	931.0 ± 45	919.0 ± 53	600.7 ± 47	640.6 ± 66	383.7 ± 26	342.4 ± 28
Sag recovery (%)	9.1 ± 1	12.7 ± 1	17.8 ± 3	10.8 ± 2	18.1 ± 2	16.5 ± 2
n	10	10	10	5	11	8

Although optical activation mostly generated nEPSCs in layer 2/3 non-FS cells, they have been reported to express mAChRs (Chen et al., 2015). To confirm the existence of functional mAChRs in non-FS neurons as shown previously, we used a picospritzer to apply brief puffs of muscarine. For all neurons examined (n = 9) which showed a light-evoked nEPSP only, muscarine application led to a robust depolarization which was blocked by atropine (Figure 3.14). These data indicate that while mAChRs are prominently expressed in layer 2/3 non-FS neurons, they do not appear to be recruited by brief activation of cholinergic afferents.

While non-FS cells in the superficial layers can inhibit local pyramidal cells (Arroyo et al., 2012), their nAChR-mediated activation *in vivo* has been reported to cause disinhibition (Letzkus et al., 2011, Pi et al., 2013). To examine which paradigm was prevalent under our conditions, we recorded from layer 2/3 RS cells to detect GABAergic inputs in response to optical activation. In a small number of cells (n=2), cholinergic stimulation generated IPSCs with relatively long latencies and significant jitter from trial to trial, suggesting they were mediated by disynaptic mechanisms (Figure 3.15). Thus, non-FS interneurons engaged by cholinergic input were capable of driving inhibition of layer 2/3 excitatory cells.

In contrast to interneurons, most RS cells in layer 2/3 did not show light-evoked postsynaptic responses (75%; Figure 3.13B,C), with the remaining neurons displaying small-amplitude mAChR-dependent IPSCs (mIPSCs, 25%). Taken together, these findings indicate that the synaptic release of acetylcholine in superficial layers can suppress cortical activity via the recruitment of nAChRs in distinct types of interneurons.

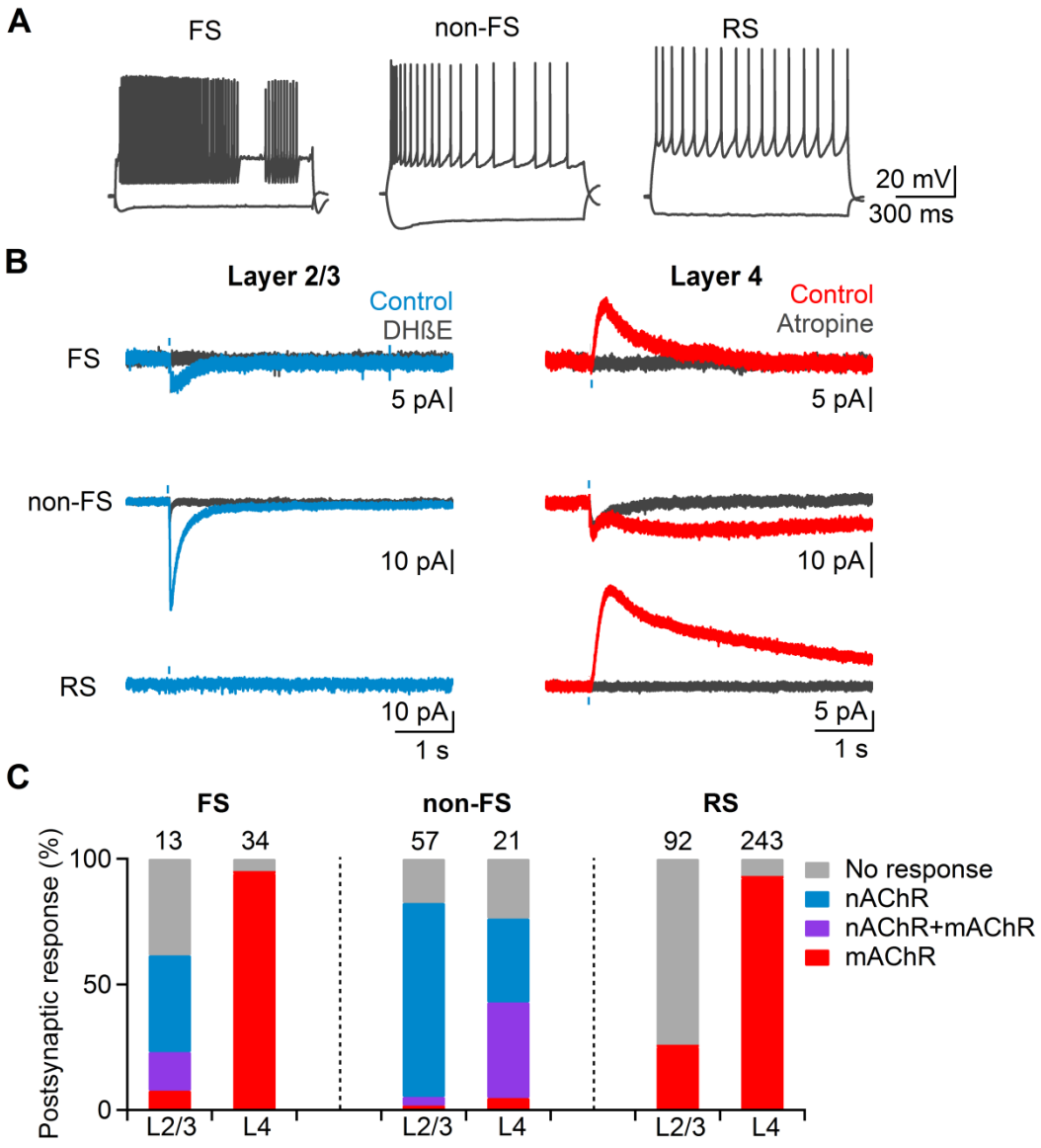

Figure 3.13: Cholinergic postsynaptic responses are layer-specific. (A) Cells in layer 2/3 and layer 4 were classified as either inhibitory FS, or non-FS cells or excitatory RS cells based on their intrinsic firing characteristics. **(B)** Example voltage-clamp recordings carried out in the presence of NBQX (10 µM), D-APV (25 µM), picrotoxin (50 µM) and CGP 55845 (5 µM) showing typical light-evoked responses. Most cells in layer 2/3 (left column) showed either no response or fast EPSCs (blue traces) blocked by DHβE (black traces). In layer 4 (right column)

the majority of neurons displayed slow postsynaptic responses (red traces) that were blocked by atropine (black traces). **(C)** Summary data showing likelihood of nAChRs and mAChR-mediated responses for each cell type. Numbers above bars indicate total number of cells recorded. Data generated in part by Frederik Seibt, used with permission.

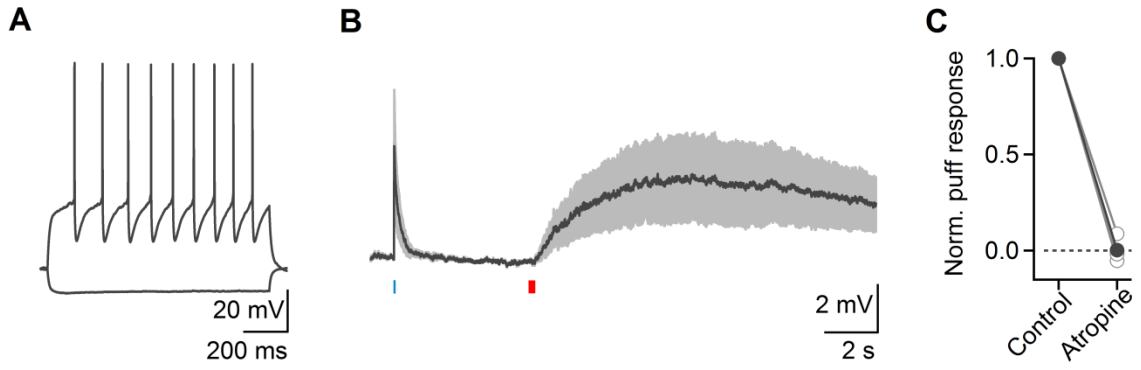

Figure 3.14: Synaptic release of acetylcholine primarily recruits nAChRs in layer 2/3 non-FS neurons. (A) Responses to hyperpolarizing and depolarizing current steps in an example layer 2/3 non-FS neuron. **(B)** Average response in current-clamp from layer 2/3 non-FS cells (n = 4) to 5 ms optical activation (blue bar) followed by a 200 ms puff of muscarine chloride (1 mM, red bar). **(C)** Summary data (n = 4 cells), showing that responses evoked by muscarine were completely blocked by atropine. Shaded areas and error bars denote SEM. Data generated in part by Frederik Seibt, used with permission.

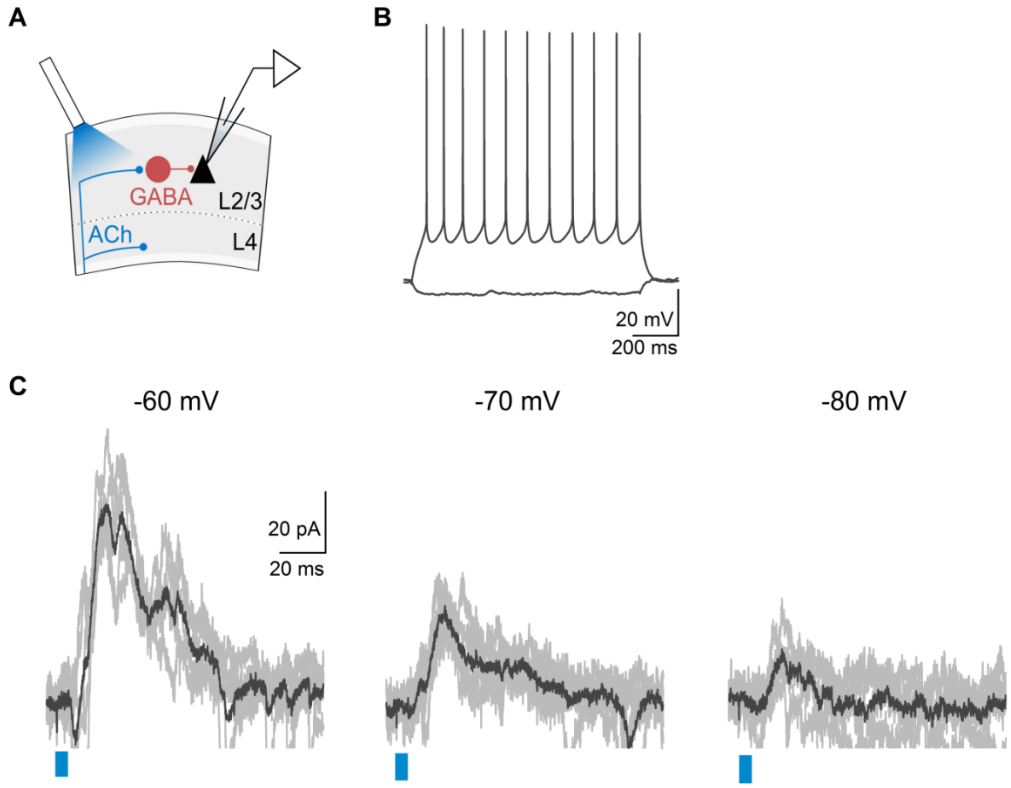

Figure 3.15: Brief optical activation leads to disynaptic inhibition of layer 2/3 excitatory neurons. (A) Recordings were made from identified layer 2/3 pyramidal cells using a K^+-based internal solution containing a low concentration of Cl^-, producing a Cl^- reversal potential of ~-82 mV. **(B)** Responses to depolarizing and hyperpolarizing current steps in a layer 2/3 cell, showing RS phenotype. **(C)** In the same cell, optical activation evoked long-latency GABAergic IPSCs with significant latency jitter. Shown here are individual trials in gray, and average trace in black.

3.7 Cholinergic postsynaptic responses are largely mAChR-mediated in layer 4

Recordings in layer 4 yielded dramatically different results. Almost all FS cells displayed atropine-sensitive mIPSCs (94%; Figure 3.13B,C), and never showed nAChR dependent responses. Non-FS interneurons responding to acetylcholine release displayed either isolated nEPSCs (33%), or biphasic responses consisting of nEPSCs and mAChR EPSCs (mEPSCs, 38%; Figure 3.13B,C). Furthermore, the large majority of RS cells showed mIPSCs (92%) that were blocked by atropine and AF-DX 116. mAChR-mediated responses were also detected in slices derived from ChAT-Cre/Ai32(ChR2-YFP) mice (FS: n = 2 cells, non-FS: n = 1 cell, RS: n = 29 cells). Postsynaptic mAChR-dependent responses displayed large cell type-specific differences in their kinetics (Figure 3.16). While mIPSCs in FS had relatively fast kinetics (rise time: 165.9 ± 10 ms, decay time constant: 844.2 ± 78 ms, n = 20), mIPSCs in RS cells were considerably slower (rise time: 328.3 ± 23 ms, decay time constant in voltage-clamp: 3281.7 ± 157 ms, n = 21, $p < 10^{-5}$, ANOVA). In non-FS cells, optical activation evoked mEPSCs that displayed extremely slow kinetics (rise time: 1248.3 ± 125 ms, decay time constant: 23.7 ± 5.4 s, n = 7, $p < 10^{-5}$, ANOVA; Figure 3.16), and caused increased spiking when paired with depolarizing current injections to induce action potentials (Figure 3.17). Taken together, these results suggest that brief cholinergic activation leads to the recruitment of mAChRs on most layer 4 neurons, leading, in turn, to postsynaptic activity in various cell types on dramatically different time scales.

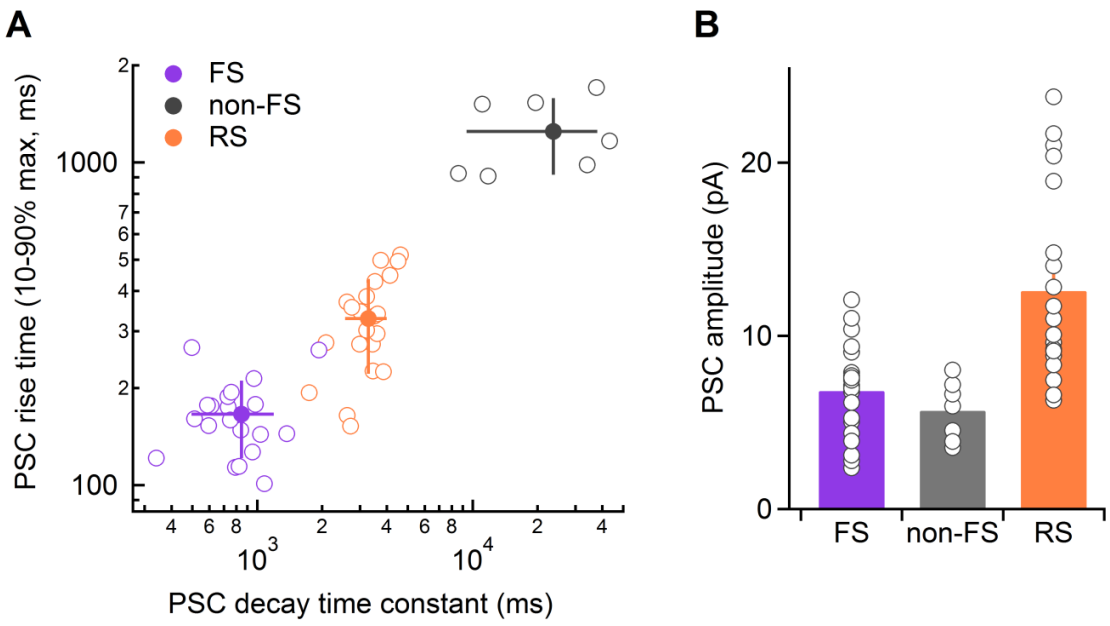

Figure 3.16: Postsynaptic mAChR-mediated responses in layer 4 have cell-type specific kinetics. (A) Rise times of mIPSCs plotted against their decay time constants from example layer 4 RS (n = 21) and FS (n = 20) cells, along with the same values for mEPSCs in layer 4 non-FS cells (n = 7). Note logarithmic scale on both axes. Error bars denote SD. **(B)** Summary of mAChR-mediated postsynaptic responses for the same cells as in (A). Error bars denote SEM.

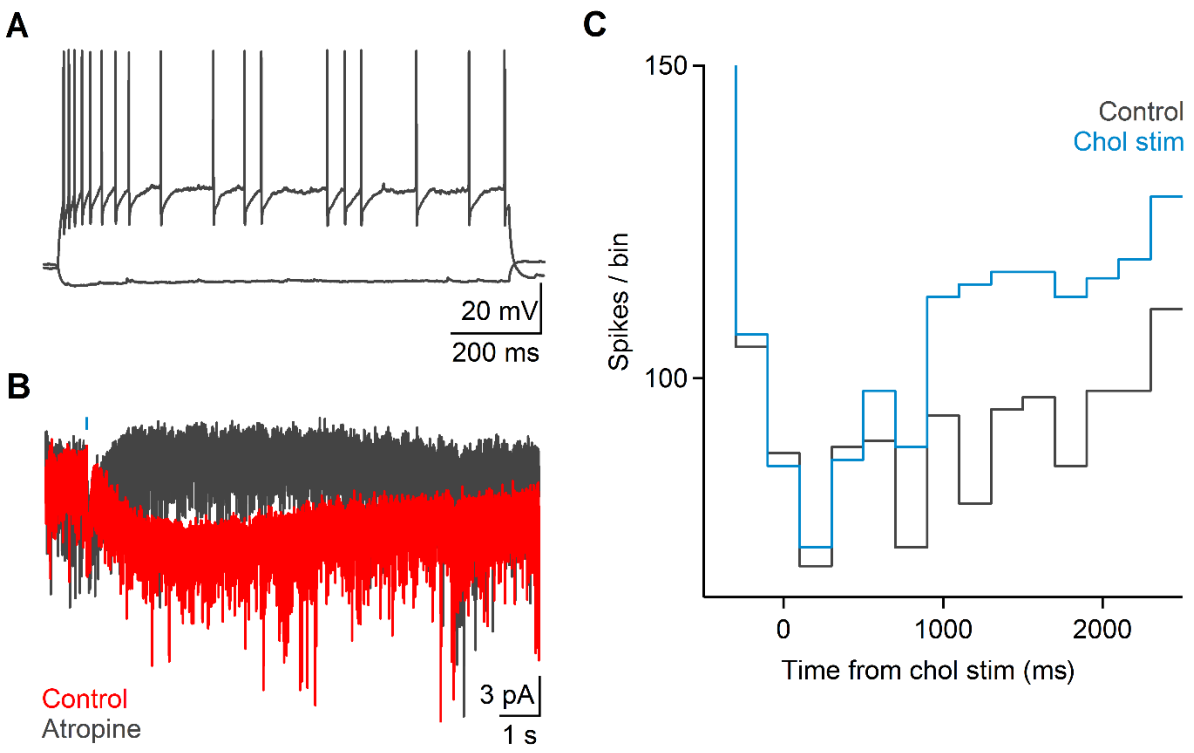

Figure 3.17: Brief cholinergic input excites layer 4 non-FS cells at long latencies. (A) Responses to depolarizing and hyperpolarizing current steps from an example layer 4 cell showing non-FS phenotype. **(B)** In the same cell, brief optical activation produced atropine-sensitive EPSCs with extremely slow rise and decay kinetics. **(C)** Peristimulus time histogram for the same cell showing spiking activity evoked by 3 s depolarizing current steps (black trace). Pairing this with cholinergic activation at a delay of 500 ms (blue trace) led to an increase in spike output, but with a latency of ~500 ms, presumably owing to the slow rise time kinetics of the underlying EPSCs.

3.8 mAChR-mediated IPSCs are most prominent in layer 4

Our data suggest that excitatory neurons in layer 4 are much more likely to receive cholinergic inputs compared to excitatory neurons in layer 2/3. Next, we compared the strength of cholinergic postsynaptic responses in excitatory neurons located in distinct layers. To account for postsynaptic response variability due to differences of ChR2 expression between slices and animals, we performed dual recordings from RS neurons in layer 4 and layer 2/3 or layer 4 and layer 5 in the same cortical column (Figure 3.18A). For almost all pairs examined, mIPSC amplitudes in layer 4 were larger compared to responses in either layer 2/3 or layer 5 (layer 2/3: 21.5 ± 10 % compared to layer 4, $n = 11$ pairs, $p < 0.001$; layer 5: 16.0 ± 5% compared to layer 4, $n = 14$ pairs, $p < 0.0001$, two-tailed paired t-test; Figure 3.18A,B). Finally, mIPSC amplitudes in layer 4 RS cells were indistinguishable between the two transgenic mouse lines (Cre/Ai32(ChR2-YFP): 9.0 ± 1.0 pA, $n = 8$ cells; ChAT-ChR2-EYFP: 11.0 ± 1.0 pA, $n = 23$ cells, $p = 0.38$, two-tailed unpaired t-test) suggesting that VAChT overexpression does not lead to a significant enhancement of response amplitudes. Thus, mAChR-mediated suppression of excitatory cells is a prominent feature of layer 4, the principal thalamorecipient layer of primary somatosensory cortex.

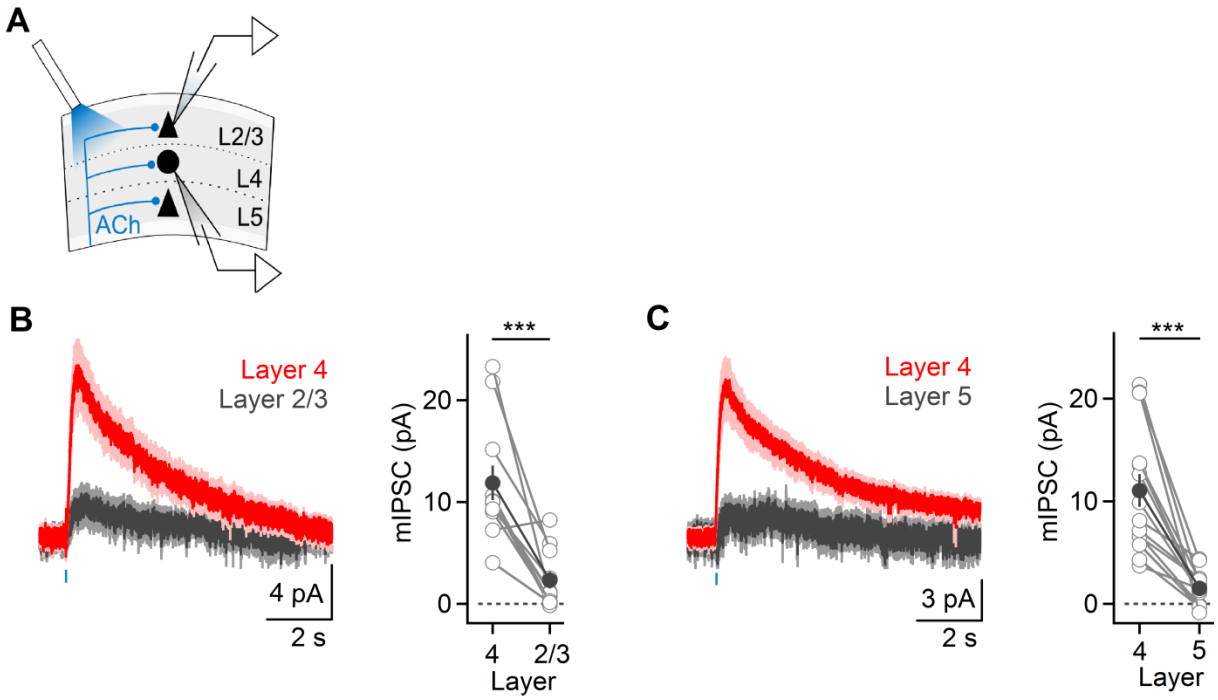

Figure 3.18: mIPSCs in RS cells are strongest in layer 4. Recordings were obtained in the presence of antagonists for GABAergic and glutamatergic synaptic transmission. **(A)** *Left:* Average IPSCs for simultaneously recorded pairs of layer 2/3 and layer 4 neurons (n = 11 pairs). *Right*: Summary data (11 layer 2/3 & 4 pairs). **(B)** *Left:* Average IPSCs for simultaneously recorded pairs of layer 4 and layer 5 neurons (n = 14 pairs). *Right*: Summary data (14 layer 4 & 5 pairs). All shaded areas and error bars denote SEM.

3.9 mAChR-mediated IPSCs in layer 4 RS cells are mediated by the activation of GIRK channels

Next, we probed the mechanisms mediating mIPSCs in layer 4 RS neurons. Synaptic currents had onset latencies of 30.6 ± 1 ms (n = 19 cells), reversed at ~-96 mV, displayed strong inward rectification and could be blocked by bath application of barium (15.11 ± 2% of control, n = 4 cells, p = 0.05, two-tailed paired t-test; Figure 3.19A,B), indicating the mIPSCs were mediated by GIRK conductances. By contrast, bath application of the small conductance calcium-activated potassium (SK) channel antagonist apamin had little effect on mIPSC amplitudes (93.0 ± 4% of control, n = 6 cells, p = 0.09, two-tailed paired t-test; Figure 3.19C,D) and recordings using an internal solution containing 5 mM BAPTA did not attenuate mIPSCs (n = 4 cells), suggesting that SK channel activation is not involved in mediating mIPSCs in layer 4 neurons.

Taken together, our data show that the synaptic release of acetylcholine in layer 4 leads to the recruitment of mAChRs in the large majority of RS cells, suggesting that the monosynaptic inhibition of excitatory neurons via the opening of K^+ conductances contributes to the prolonged suppression of recurrent activity.

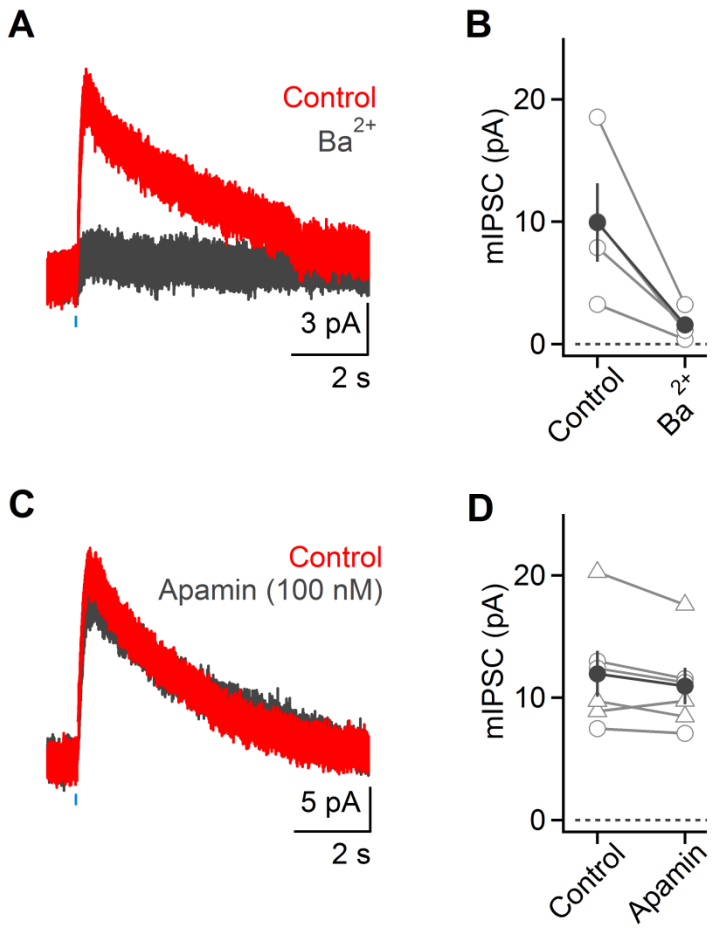

Figure 3.19: mIPSCs in layer 4 RS cells are mediated by GIRK conductances. (A) Light-evoked mIPSC in a layer 4 RS cell was blocked following Ba^{2+} (200 µM) application. **(B)** Summary data quantifying mIPSC reduction following Ba^{2+} application (n = 4 cells). **(C)** Application of the SK channel antagonist apamin (10 – 100 nM) has no effect on mIPSCs, as shown for layer 4 RS neuron. **(D)** Summary data quantifying mIPSC responses prior to and following apamin wash-in (circles: 10 nM, n = 3 cells; triangles: 100 nM, n = 3 cells). Error bars denote SEM.

3.10 Synaptic acetylcholine reduces neuronal firing in layer 4 RS cells

Next, we determined the impact of light-evoked mAChR IPSPs (mIPSPs) on postsynaptic action potential activity in RS cells, in the absence of recurrent activity. For RS neurons held at -70 mV, mIPSPs had amplitudes of 2.9 ± 0 mV and decay time constants of 5140.5 ± 427 ms (n = 25). When mIPSPs were paired with action potential firing evoked by depolarizing current steps, firing frequencies were rapidly (<100 ms) and persistently reduced compared to unpaired trials (n = 11, Figure 3.20A-C).

To examine cholinergic control under more physiological conditions, we paired optical stimulation with action potential activity (Δt = 1s) evoked by extracellular stimulation of glutamatergic afferents (4 stimuli at 40 Hz). For these experiments, we added the NMDAR antagonist APV (25 μM) to block recurrent activity and to isolate fast monosynaptic responses (Beierlein et al., 2002). Light-evoked mAChR IPSPs (mIPSPs) reduced synaptically-evoked action potential activity (57.9 ± 5% compared to unpaired trials, n = 10 cells, $p < 0.01$, Wilcoxon signed rank test; Figure 3.21A-C).

To test if these effects were mediated in part by a reduction of glutamate release, we paired glutamatergic and cholinergic inputs but performed voltage-clamp recordings using a Cs^+-based internal solution to block postsynaptic mIPSCs. Glutamatergic EPSCs were slightly but not significantly reduced (91.5 ± 2% compared to unpaired trails, n = 8 cells, $p = 0.13$, two-tailed paired t-test; Figure 3.22A), in an atropine-sensitive manner (atropine: 103.0 ± 2% compared to unpaired trails, n = 3 cells; Figure 3.22B). These data suggest that cholinergic

inputs trigger a rapid and long-lasting reduction of layer 4 RS cell activity by activating postsynaptic mAChRs.

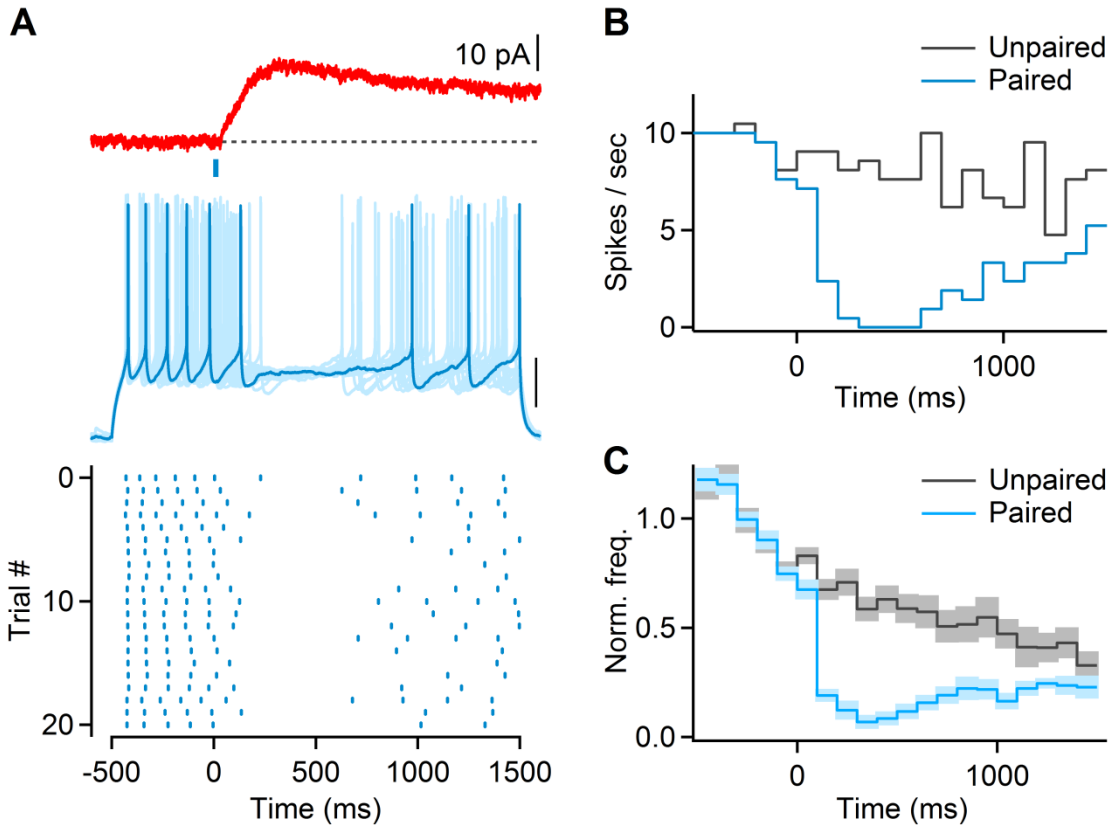

Figure 3.20: Cholinergic synaptic inputs to layer 4 reduce neuronal firing in RS cells. (A) *Top:* mIPSC in layer 4 RS cell. *Middle:* Multiple overlaid trials showing neuronal activity evoked by 2 s depolarizing current step paired with light stimulation applied with a 500 ms delay (indicated by blue bar). Scale bar: 20 mV. *Bottom:* Raster plot showing timing of action potentials over multiple trials, for the same neuron. **(B)** For the same cell as in (A), peristimulus time histogram (PSTH) for paired (blue) and unpaired (gray) current steps. **(C)** Average PSTH (n = 11 RS cells), normalized to average of first five 100 ms time bins for each cell. Shaded areas denote SEM.

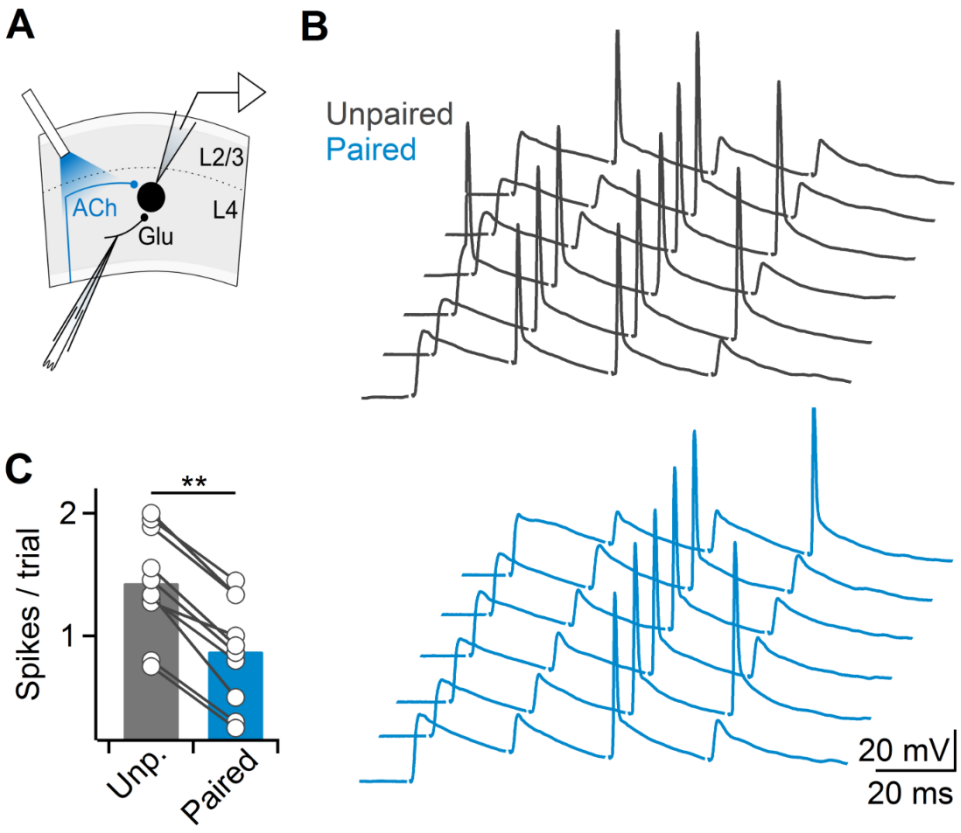

Figure 3.21: Cholinergic afferents to layer 4 RS cells suppress synaptically-evoked spiking. (A) Schematic of experimental setup. Glutamatergic EPSPs in layer 4 neuron were paired with single optical stimulus (5 ms), applied 1 s prior to electrical stimulation. **(B)** Glutamatergic-evoked spikes are significantly suppressed or delayed, as shown for several trials in control (black) or with paired optical stimulation (blue). **(C)** Summary data showing cholinergic-mediated suppression of spiking suppression (n = 10 cells).

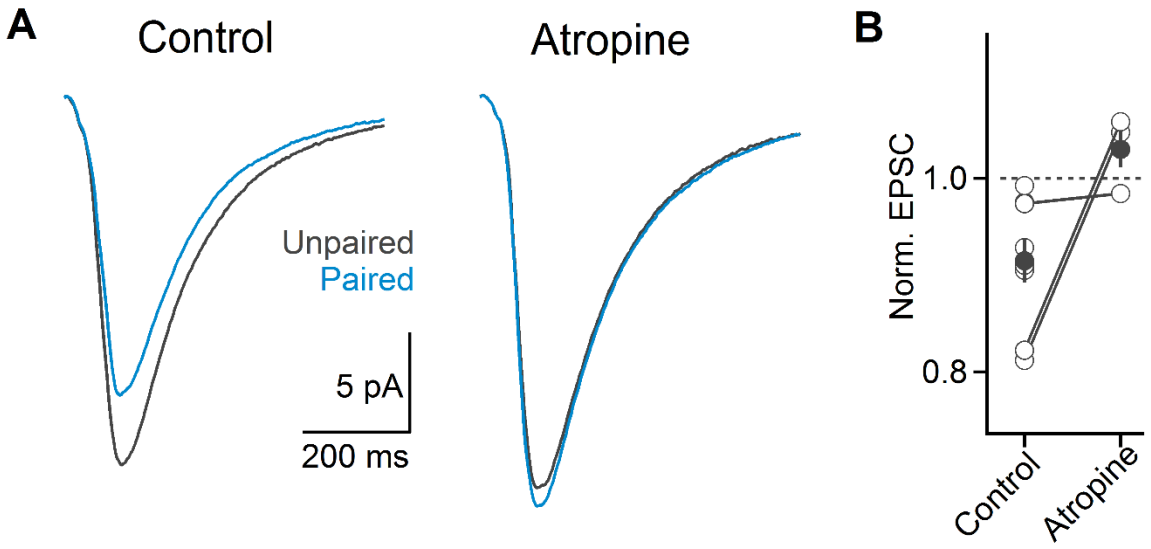

Figure 3.22: Cholinergic activation produces a small but insignificant mAChR-dependent reduction in glutamatergic EPSCs. (A) Electrically evoked glutamatergic EPSCs in an example layer 4 cell recorded using a Cs^{+}-based internal. EPSCs showed a slight reduction in amplitude when paired with brief cholinergic activation 1 s prior to electrical stimulation (*left*), that was blocked by the bath application of atropine (*right*). **(B)** Summary data of control-normalized EPSCs that were paired with optical activation, in the absence (n = 8 cells) or presence of atropine (n = 3 cells). Error bars denote SEM.

3.11 Synaptic acetylcholine suppresses layer 4 RS cells via hyperpolarizing inhibition

How does postsynaptic mAChR signaling influence the processing of subthreshold synaptic inputs? Activation of mAChRs and the opening of GIRK conductances will lead to a hyperpolarization of membrane potential and in addition, to an increase in membrane conductance generating a potential "shunt" (Eggermann and Feldmeyer, 2009). Shunting inhibition is thought to be a prominent mechanism underlying the spatiotemporal summation of excitatory and inhibitory synaptic inputs in neocortex and other brain areas (Koch, 1999). When probed with brief (300 ms) hyperpolarizing current steps, mIPSPs led to a significant reduction in input resistance of the postsynaptic RS cell (86.2 ± 3% compared to control, n = 14 cells, $p < 0.001$, Wilcoxon signed rank test; Figure 3.23A,B).

Next, we examined if subthreshold glutamatergic EPSPs are controlled by mAChR-mediated shunting inhibition, by activating glutamatergic afferents (4 stimuli at 40 Hz) during light-evoked mIPSPs (Δt = 1s; Figure 3.24A). Surprisingly, we found that both glutamatergic EPSP amplitude and area of the paired postsynaptic response were on average nearly identical to the linear sum of the EPSP and the mIPSP evoked separately (EPSP amplitude: 100.1 ± 2% compared to linear sum, n = 16, p = 0.16, EPSP area: 99.6 ± 2%, n = 16, p = 0.34, Wilcoxon signed rank test; Figure 3.24A,B). To test whether the lack of EPSP shunting was caused by biases in the sampling of cells, we paired evoked EPSPs and current steps with mIPSPs in the same cell. Although somatic current injections were consistently shunted across cells (89.6 ± 1% compared to control, n = 4 cells), paired EPSPs did not show any obvious trends (107.9 ±

9% compared to control, n = 4 cells; Figure 3.25). Together, our data suggest that cholinergic inputs to layer 4 RS cells reduce neuronal firing primarily via hyperpolarizing inhibition.

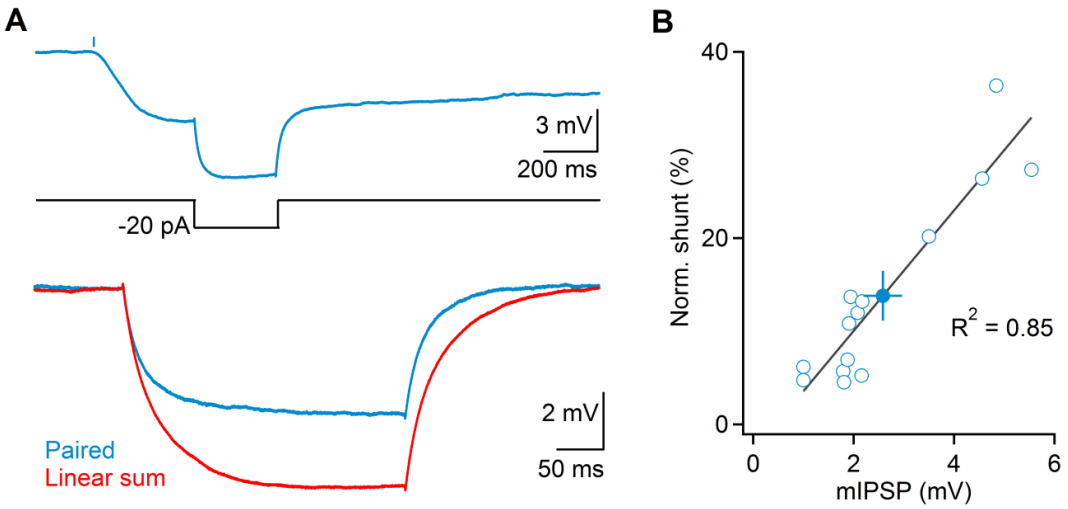

Figure 3.23: Voltage deflections evoked by somatic current steps are shunted by mIPSPs. **(A)** *Top*: Optically evoked mIPSP in a layer 4 RS cell was paired with a hyperpolarizing somatic current injection with a delay of 400 ms. *Bottom*: close-up of the hyperpolarizing step (blue trace) along with the linear sum of the mIPSP and somatic hyperpolarization generated separately (red trace), revealing significant shunting under paired conditions. **(B)** The magnitude of the shunt, quantified as the proportion of the control hyperpolarization that was lost when paired with mIPSP, shows a strong linear relationship when plotted as a function of the amplitude of the mIPSP (n = 14 cells). Error bars denote SEM.

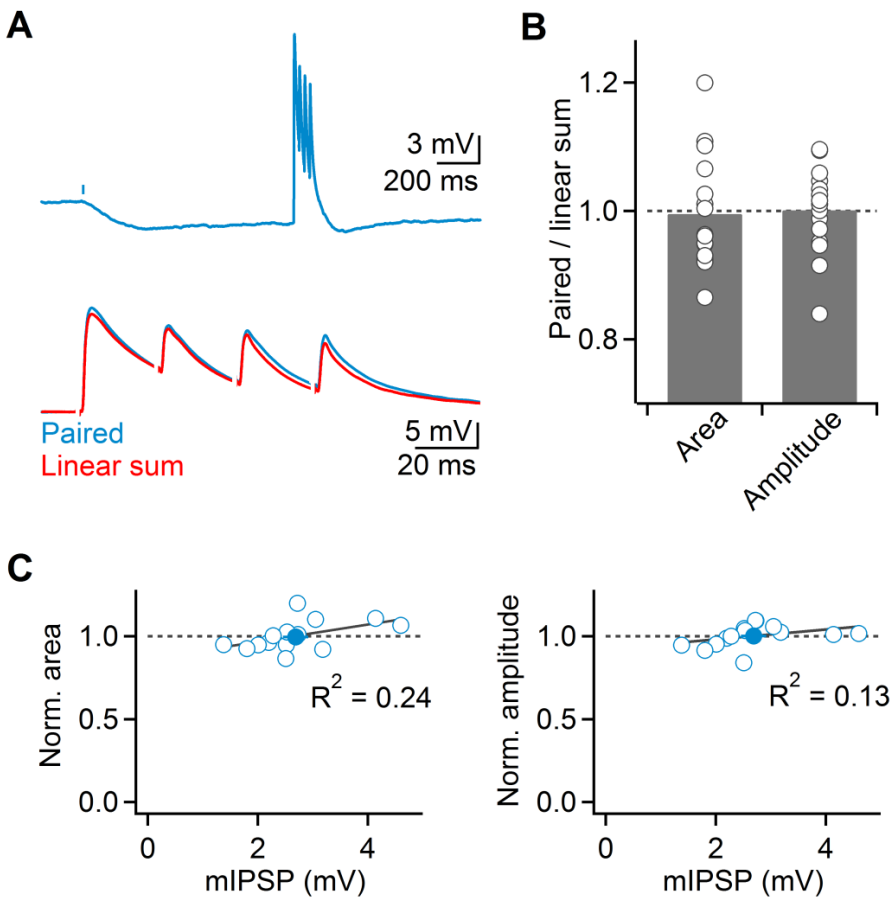

Figure 3.24: Cholinergic inputs to layer 4 RS cells mediate hyperpolarizing inhibition. **(A)** mIPSPs do not cause shunting of glutamatergic EPSPs. *Top*: light-evoked mIPSP was paired with a train (40 Hz) of electrically evoked glutamatergic EPSPs (delay: 1 s). Recordings were carried out in the presence of D-APV (25 µM) to prevent recurrent activity. *Bottom*, close-up of EPSPs in top trace showing that paired response (blue trace) is identical to linear sum of mIPSP and EPSPs evoked separately (red trace). **(B)** Summary data quantifying both area under the paired EPSPs and amplitude of the first paired EPSP, normalized to their respective unpaired controls (n = 16 cells). **(C)** Normalized EPSC area (*left*) and amplitude (*right*) data from (B) plotted as a function of mIPSP amplitude, showing no significant trend. Error bars denote SEM.

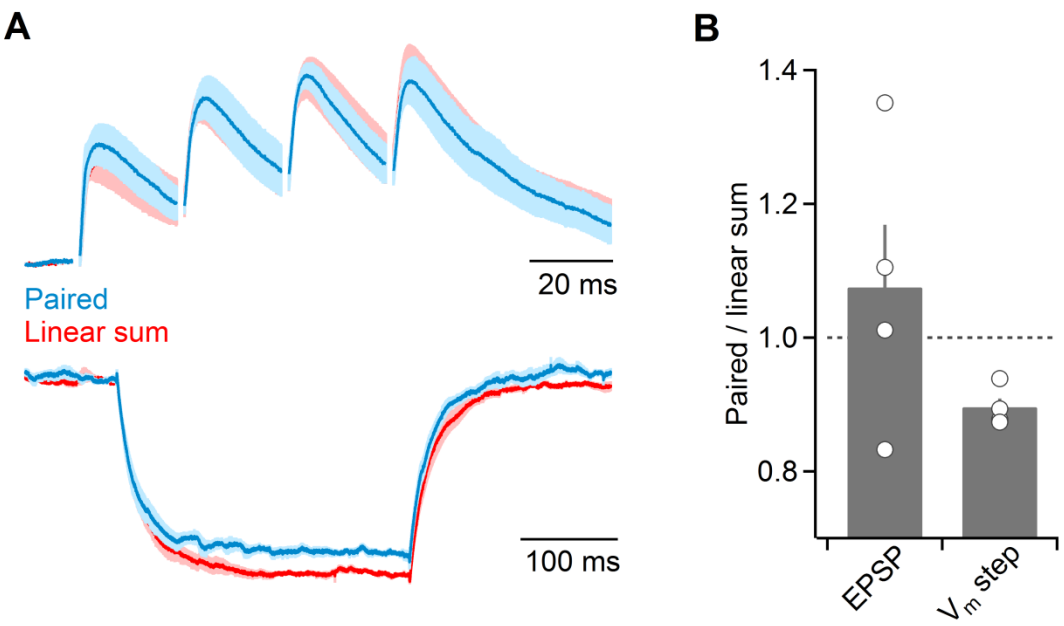

Figure 3.25: mIPSPs mediate shunting of somatic current injections but not EPSPs. (A) Although paired EPSPs show no change on average, paired current steps are consistently shunted. *Top*: EPSPs in layer 4 RS cells, paired with optically evoked mIPSPs at a delay of 1 s (blue trace), shown along with linear sum of EPSPs and mIPSPs evoked separately (red trace). Data were normalized and averaged across 4 cells. *Bottom*: For the same cells, normalized average traces of somatic hyperpolarizations, either paired with optical stimulation (blue trace) or linearly summed with an mIPSP evoked separately (red trace). **(B)** Summary data of EPSP and step amplitudes, revealing no clear trend for EPSPs but shunting of hyperpolarizing steps. Shaded areas and error bars denote SEM.

3.12 Summary

We investigated the mechanisms of cholinergic control of cortical activity *in vitro* by employing a combination of slice electrophysiology and optogenetics. By pairing electrically evoked recurrent activity with optical stimulation of cholinergic afferents, we demonstrated that brief cholinergic activation led to rapid and robust suppression of cortical activity. This suppression was achieved by the engagement of both nAChRs and mAChRs. In the supragranular layers, nAChR-mediated recruitment of inhibitory interneurons led to disynaptic inhibition of pyramidal cells and a transient suppression of activity. In layer 4, brief cholinergic stimulation reliably engaged postsynaptic mAChRs, leading to the activation of inhibitory cells and hyperpolarizing inhibition of excitatory neurons. This, in turn, mediated a prolonged suppression of recurrent activity, lasting several seconds. Taken together, these results show that even brief activation of cortical cholinergic afferents can cause rapid mAChR-mediated suppression of synchronous cortical activity, in contrast to the traditional view of mAChRs being slow and spatially imprecise neuromodulators.

Chapter 4: Discussion

Acetylcholine has a long and established literature as a potent regulator of cognitive function (McCormick, 1992, Hasselmo, 2006, Ballinger et al., 2016). Yet, the circuit mechanisms by which endogenous acetylcholine controls cortical function have been largely unexplored. Partly, this has been due to the persistent view of acetylcholine as a neuromodulator with signaling modes that are distinctly slower and less spatially precise than that achieved by classical neurotransmission (Lucas-Meunier et al., 2003). While tonic neuromodulatory effects of acetylcholine in the neocortex certainly exist (see, for instance, Figure 3.7), cholinergic signaling also mediates transient, temporally precise and cell-type specific effects. This is perhaps not surprising, given the critical role acetylcholine plays in such cognitive tasks as attention (Herrero et al., 2008) and learning of reward timing (Chubykin et al., 2013) which require extremely precise control over when and which cell types are activated or inhibited. Moreover, the activity patterns of BF cholinergic projection neurons are anything but tonic, showing highly correlated firing with behavioral states (Eggermann et al., 2014, Reimer et al., 2016), cortical rhythms (Lee et al., 2005) and behaviorally relevant stimuli (Hangya et al., 2015). Combined with recent evidence of fast cholinergic signaling *in vivo* (Pinto et al., 2013), there is an ongoing paradigm shift in the how cholinergic function in the neocortex is viewed.

Our results provide a mechanistic basis for fast and precise cholinergic control of cortical network activity *in vitro* (Dasgupta et al., 2018). To our knowledge, we provide the first evidence that even brief activation of cholinergic afferents can rapidly (within 100 ms) switch cortical circuits to a state that strongly disfavors synchronized Up-state-like activity

(Figure 3.1). Because attention-demanding tasks are associated with rapid fluctuations in acetylcholine levels in the neocortex (Parikh et al., 2007), there likely exist temporally precise cholinergic signaling mechanisms that can modulate cortical states at sub-second to seconds timescales. Our results provide evidence for such mechanisms. Interestingly, the rapid effects of synaptic acetylcholine were mediated largely by metabotropic receptors, suggesting that both nAChRs and mAChRs are capable of spatiotemporally precise signaling (Figure 4.1).

4.1 Brief cholinergic activation evokes long-lasting mAChR-mediated currents in layer 4

Rapid cholinergic suppression of cortical activity was largely mediated by the activation of mAChRs (Figure 3.6). Optogenetic stimulation evoked mAChR-mediated IPSCs in the vast majority of excitatory neurons of layer 4. These responses had fast onset latencies (30.6 ms) but were slow-decaying, with >5 s decay time constants in current-clamp recordings, suggesting that they are a principal mechanism of long-lasting cholinergic-mediated suppression of recurrent activity. The fast and reliable recruitment of postsynaptic mAChRs with brief cholinergic activation is similar to findings in the TRN (Sun et al., 2013), where cholinergic input produces a biphasic nAChR- and mAChR-mediated response. Furthermore, mIPSCs were sensitive to the M2/M4 specific antagonist AF DX-114. Subcellularly, M2/M4 mAChRs are coupled to $G_{i/o}$ proteins; upon receptor activation, the β/γ subunit of the G-protein is able to diffuse through the membrane and bind to various ion channels, activating or inhibiting them. M2/M4 mAChRs have previously been reported to activate GIRK K^+ channels with exogenous acetylcholine application (Eggermann and Feldmeyer, 2009). In agreement, mIPSCs in layer 4 RS cells showed strong inward rectification and could be

blocked by the application of $BaCl_2$ (Figure 3.19), suggesting a GIRK-mediated mechanism. They could not, however, be blocked by apamin or the inclusion of BAPTA in the internal solution, suggesting that Ca^{2+}-activated SK K^+ channels were not involved, contradicting previous reports (Gulledge and Stuart, 2005, Gulledge et al., 2007).

In addition to hyperpolarizing the membrane, the opening of additional K^+ channels should lead to a reduction in membrane resistance, thereby creating shunting inhibition of concurrent EPSPs (Koch, 1999). Shunting effects are particularly prominent for inhibitory synapses that are located between the glutamatergic synapses and the soma but diminish rapidly as the number of dendritic branch nodes between the synapses increase (Gidon and Segev, 2012). To test whether the opening of GIRK channels produced shunting inhibition in layer 4 RS cells, we paired optical activation of cholinergic input with glutamatergic EPSPs evoked via electrical stimulation within the same barrel. Because thalamocortical and corticocortical glutamatergic synapses are uniformly distributed over the entire lengths of RS cell dendrites (Schoonover et al., 2014), we expected to see a substantial reduction in the amplitude of the paired EPSPs resulting from shunting. Surprisingly, paired EPSPs were unaltered on average (Figure 3.24), although membrane conductance was clearly increased (Figure 3.23). It is possible that the electrical stimulation we used was biased towards recruiting more proximally located glutamatergic synapses, and/or brief optical activation preferentially recruited cholinergic synapses on distal dendritic regions, thereby precluding a significant shunt. Alternatively, mAChRs may have activated additional dendritic biochemical pathways that counteracted the effects of shunting. The dynamics of the dendritic currents resulting from mAChR activation in layer 4 RS cells remain elusive.

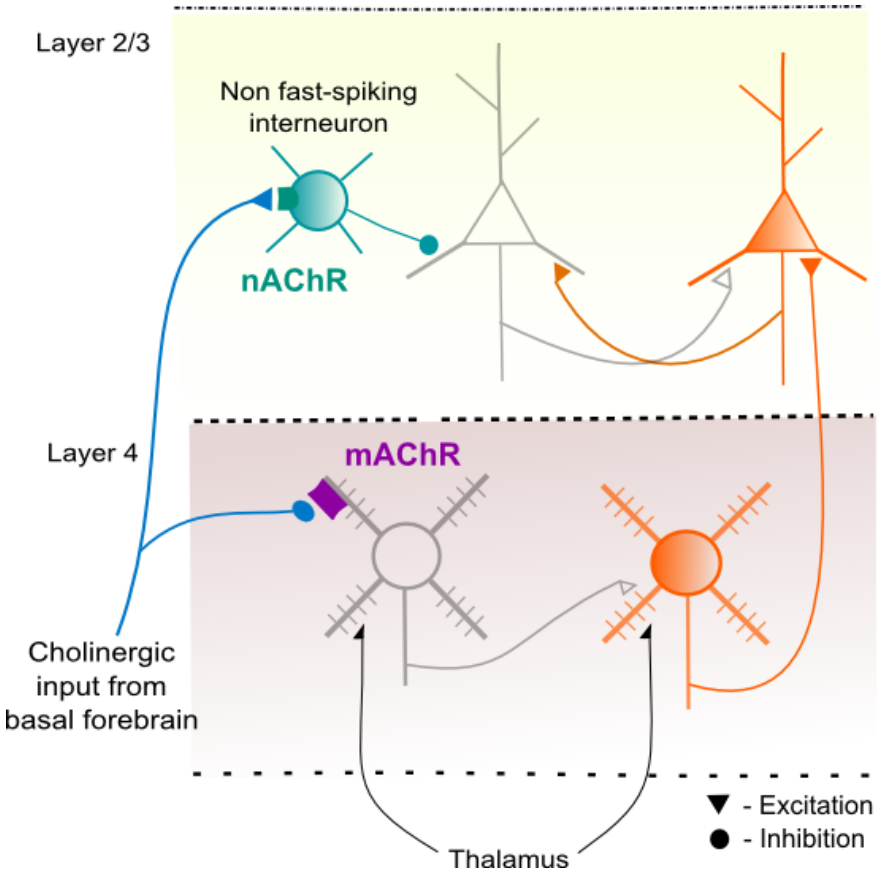

Figure 4.1: Synaptic acetylcholine suppresses recurrent activity by engaging both nAChRs and mAChRs. Our findings demonstrate that cholinergic receptor subtypes contribute to suppression of cortical activity in a layer-specific manner. In layer 2/3, cholinergic transmission engages nAChRs expressed on the majority of non-FS interneurons. This, in turn, leads to disynaptic inhibition of pyramidal cells, thus mediating transient suppression. In layer 4, most excitatory cells are directly inhibited by the rapid engagement of mAChRs, leading to a more prolonged form of suppression that lasts several seconds. Together, they serve as a circuit mechanism for the rapid cholinergic-mediated suppression of synchronous cortical activity observed during high arousal *in vivo*.

Besides mIPSCs on RS cells, a large proportion of non-FS cells in layer 4 also showed slow mAChR-mediated EPSCs (Figure 3.13). From our data, we cannot rule out that layer 4 non-FS interneurons contributed to cholinergic-mediated suppression. However, rise-times of mEPSCs in non-FS cells were exceptionally slow (Figure 3.16) and optical stimulation led to increased spike output only after a significant delay (Figure 3.17), making it unlikely that layer 4 non-FS interneurons contributed to suppression of recurrent activity at short delays. In a recent study, Muñoz et al. found that periods of whisking are associated with a strong mAChR-mediated activation of layer 4 SOM cells in S1 (Muñoz et al., 2017). Combined with reports of mEPSCs in SOM cells in other layers (Fanselow et al., 2008, Chen et al., 2015), it is tempting to speculate that the mAChR-activated non-FS cell group we identified were SOM-expressing. Regardless, layer 4 SOM cells in S1 tend to preferentially target other interneurons and their activation leads to *disinhibition* of cortical activity (Xu et al., 2013). Taken together, mAChR-mediated suppression of recurrent activity was likely mediated by the direct suppression of excitatory cells in layer 4.

4.2 nAChR-mediated activation of interneurons leads to inhibition of cortical activity

Rapid cholinergic-mediated suppression of recurrent activity was also dependent, to a lesser extent, on nAChR-signaling (Figure 3.6). In agreement, we observed prominent nAChR-mediated EPSCs in the majority of non-FS interneurons in the superficial layers (Figure 3.13), leading to inhibition of RS cells. There is, however, a significant body of *in vivo* work demonstrating that nAChR-mediated activation of inhibitory neurons leads to disinhibition of layer 2/3 excitatory cells (Letzkus et al., 2011, Pi et al., 2013, Fu et al., 2014). Although it

remains unclear how our data reconcile with those results, it is possible that different cortical areas are governed by completely distinct mechanisms of cholinergic action (Shimaoka et al., 2018). A likelier alternative is that both inhibition and disinhibition act concurrently. During high arousal states *in vivo*, layer 2/3 pyramidal cell responses to somatosensory input show long-tailed distributions, i.e., a small number of cells respond to whisker touch with high firing rates while the majority of neurons show sparse action potentials (O'Connor et al., 2010, Petersen and Crochet, 2013). This suggests that active waking is marked by sparse encoding of sensory input, engendered by the selective excitation/disinhibition of a small subset of neurons coupled with general inhibition of network activity (Kuchibhotla et al., 2017, Shimaoka et al., 2018). These phenomena may underlie the increase in signal to noise ratio of sensory encoding commonly associated with cholinergic neuromodulation (Reimer et al., 2014). Viewed in this context, our results serve to provide a circuit mechanism of cholinergic-mediated network suppression that may act in conjunction with disinhibition reported elsewhere.

Although cholinergic suppression of recurrent activity was no longer dependent on the contribution of nAChR-signaling in the isolated layers 4-6 (Figure 3.11), we nevertheless observed reliable nAChR-mediated EPSCs in a significant proportion of L4 non-FS interneurons (Figure 3.13). The cause for this apparent discrepancy remains unclear. It is possible that either: (i) nAChR-mediated responses in most layer 4 non-FS cells are not large enough to significantly affect their firing output, or (ii) most non-FS interneurons that are recruited by nAChR-signaling preferentially inhibit other interneurons and avoid inhibiting excitatory cells (Xu et al., 2013). Some of our observations appear to indicate that one or both of these possibilities may be true: optical stimulation could evoke disynaptic GABAergic

IPSCs in some layer 2/3 pyramidal cells (Figure 3.15), but similar PSCs were never observed in layer 4 RS cells. Future work will have to determine the exact circuit functions of nAChR-mediated excitation of layer 4 non-FS neurons.

4.3 Cholinergic signaling modes in the neocortex

Does cortical cholinergic signaling act primarily by means of classical or volume transmission? Decades of research has failed to arrive at a definitive answer. Structurally, very few studies have reported the presence of cholinergic receptors in close apposition to acetylcholine release sites (Descarries and Mechawar, 2000, Turrini et al., 2001), which is often considered to be a prerequisite for the fast point-to-point signaling typified by classical neurotransmission. This is particularly true for mAChRs, which do not appear to be expressed near sites of release (Yamasaki et al., 2010), and are thus thought to be reliant on volume transmission. Yet functionally, cholinergic, and more specifically mAChR-signaling underlies fast temporally precise cortical state transitions *in vivo* (Pinto et al., 2013). Our findings demonstrate that even brief activation of cholinergic afferents is sufficient to engage mAChRs reliably and at short latencies. How can such spatiotemporally precise signaling be achieved without the benefit of ultrastructurally defined synapses? There are two possibilities: either (i) ultrastructurally defined cholinergic synapses do exist, but lack some of the markers exhibited by classical synapses of other neurotransmitters (Smiley et al., 1997) and have thus evaded detection in most studies, or (ii) cholinergic afferents employ specialized forms of transmission that allow rapid and precise signaling without classical synapses (Bennett et al., 2012, Arroyo et al., 2014). It remains unclear which, or if both, of these is true.

Irrespective of the nature of fast cholinergic signaling, slower and spatially imprecise forms of cholinergic neuromodulation in the neocortex certainly exist (Figure 3.7). Prior studies have identified presynaptically expressed nAChRs and mAChRs that influence release probability (Kimura and Baughman, 1997, Disney et al., 2007, Amar et al., 2010, Urban-Ciecko et al., 2018). Although we did not find convincing evidence of such effects under our conditions (Figure 3.22), this could simply be because our brief 5 ms optical activation paradigm (which is unlikely to evoke >2 spikes in cholinergic afferents) did not allow for spillover of acetylcholine beyond the immediate vicinity of the release site and precluded subsequent engagement of presynaptic receptors. Indeed, at least some functional mAChRs could not be activated by optical stimulation (Figure 3.14). The presence of spatially and functionally distinct classes of cholinergic receptors raises the intriguing possibility that cortical cholinergic signaling may act via at least two distinct modes (Sarter and Kim, 2015): (i) a spatiotemporally precise form described here that is necessary for the rapid changes in cortical states observed *in vivo*, and (ii) a slower less specific form that affects cortical processing via volume transmission.

4.4 Cholinergic control of cortical circuit activity

Our findings are broadly consistent with previous reports of cholinergic-mediated inhibition of evoked Up-states in slices (Favero et al., 2012, Wester and Contreras, 2013). However, since these studies employed exogenous application of acetylcholine or cholinergic agonists, they failed to reveal the underlying spatiotemporal dynamics. Here, we provide evidence that cholinergic control of cortical recurrent activity occurs reliably within 100 ms and involves the

participation of both nAChRs and mAChRs. It is important to note here that although recurrent activity in our experiments was evoked by means of extracellular electrical stimulation within layer 4, it may not necessarily have been initiated there. The spontaneous generation of internal cortical rhythms is critically reliant upon pyramidal cells in layer 5 (Beltramo et al., 2013) and it is possible that evoked recurrent activity in our experiments was initiated via similar mechanisms. In any case, suppression of synchronous cortical activity appears to be a robust feature of cholinergic signaling, as it has now been demonstrated under a host of different experimental conditions, both *in vitro* and *in vivo*.

Acetylcholine has been suggested to alter the balance of excitation and inhibition in cortical circuits, either in favor of inhibition (Lucas-Meunier et al., 2009) or disinhibition of excitatory cells (Kuchibhotla et al., 2017). We examined whether suppression of recurrent activity by synaptic acetylcholine involved similar mechanisms by monitoring the inhibitory and excitatory activity in the local network simultaneously using dual voltage-clamp. We found that optical activation suppressed EPSCs and IPSCs by the same ratio overall, suggesting that cholinergic transmission did not significantly change the balance of excitation and inhibition in the cortical circuit (Figure 3.5). There are three possible ways for achieving this:

(i) Synaptic acetylcholine acts primarily by directly inhibiting excitatory cells. Since local inhibitory interneurons derive most of their excitatory drive from neighboring cells, direct inhibition of excitatory cells will lead to a proportionate decrease in the activity of local inhibitory interneurons, thus leaving the excitation/inhibition ratio unchanged. We provide

strong evidence that this may be a major mechanism: optical stimulation produced mIPSCs in the vast majority of layer 4 excitatory cells (Figure 3.13).

(ii) Synaptic acetylcholine activates inhibitory cells which, in turn, equally inhibit local glutamatergic and GABAergic neurons. SOM cells in the auditory and visual cortices fulfill this criterion (Kato et al., 2015, Adesnik, 2017), and could therefore be a good candidate for mediating such balanced inhibition. Indeed, a sub-group of layer 4 non-FS cells showed robust mEPSCs in our recordings (Figure 3.13). However, in the somatosensory cortex, SOM cells are primarily disinhibitory (Xu et al., 2013) and so this is unlikely to be a major mechanism.

(iii) Cholinergic suppression transiently increases inhibitory drive during the initiation of recurrent activity. Because short-lived increases in the ratio of excitation to inhibition are thought to be important in the generation of cortical recurrent activity (Shu et al., 2003), a cholinergic-mediated blockade of this process could lead to a large suppression of overall levels of activity. Such transient dynamics would not be apparent in measures of charge transferred over the entire duration of activity. As a potential mechanism, we observed nAChR-mediated activation of GABAergic interneurons in the superficial layers.

A combination of these circuit mechanisms probably underlies cholinergic signaling, thereby allowing synaptic acetylcholine to control cortical gain levels while leaving basic properties of the network intact.

4.5 Implications for sensory processing *in vivo*

Efficient encoding of sensory stimuli during high arousal states requires reliable gain modulation of cortical responses. As a means to achieve this, cholinergic signaling may

mediate a powerful gate on the horizontal corticocortical propagation of sensory activation. For instance, application of acetylcholine or the cholinesterase inhibitor donepezil limits the spread of excitation in visual cortex (Kimura et al., 1999, Silver et al., 2008). Furthermore, passive whisker deflections during attentive periods produce cortical responses that are far more spatially restricted than those evoked during quiet wakefulness (Ferezou et al., 2006), suggesting that this maybe a general feature of attentional modulation of cortical activity. Here, we show that layer 2/3 pyramidal neurons are rapidly and transiently inhibited by brief cholinergic activation, providing a circuit mechanism for temporally precise cholinergic control over corticocortical communication.

Synaptically released acetylcholine evoked postsynaptic responses that were highly cell-type specific and varied both qualitatively and quantitatively. Combined with the distinct circuit functions of each cell type, this could provide cholinergic signaling the spatiotemporally precise control over cortical circuit dynamics necessary for the rapid modulation of cortical states observed *in vivo* (Gentet et al., 2010). In addition to cell-type specificity, cholinergic-mediated suppression also showed remarkable layer-specificity (Figure 4.1): while recurrent activity in the superficial layers is controlled over a few hundred milliseconds, in layer 4, inhibition persists for several seconds. The exact computational purpose of this temporal dichotomy remains mysterious. One may speculate that this paradigm enables a long-lasting suppression of noise correlations in layer 4 (Goard and Dan, 2009), while simultaneously allowing for more rapid computations involving horizontal interactions in layer 2/3 (Pluta et al., 2017).

4.6 Conclusions and future directions

Wakefulness features rapid transitions to high arousal states that are characterized by the abolition of slow synchronous cortical activity. Although a plethora of *in vivo* evidence recognizes cholinergic signaling as a crucial mediator of state transitions, the underlying mechanisms remain unclear. Here, we propose a circuit model for fast cholinergic control of cortical network activity (Figure 4.1). We show that brief cholinergic activation is sufficient to robustly suppress cortical recurrent activity. Furthermore, both nAChRs and mAChRs contribute to this suppression, and importantly, they do so via mechanisms that are spatiotemporally distinct. While nAChRs mediate a transient form of suppression by activating GABAergic cells in the superficial layers, mAChRs mediate prolonged suppression by inhibiting layer 4 excitatory cells. One of our principal findings is the identification of thalamorecipient layer 4 as a major target of rapid and reliable mAChR-mediated inhibition. Contrary to the prevalent view that mAChR-signaling is slow and diffuse, we show that they can be rapidly activated and mediate long-lasting inhibition. Thus, cholinergic signaling is able to effectively suppress recurrent activity, thereby reducing the influence of cortically generated firing on neuronal output and potentially improving the efficacy of sensory processing.

While our findings are an important contribution to the understanding of cholinergic function in the neocortex, a number of pertinent questions remain unanswered. For example:
(i) How do our results relate to *in vivo* situations? Employing an *in vitro* model of cortical activity in acute brain slices enabled us to make precise manipulations of recurrent network dynamics and cholinergic signaling. However, *in vivo*, there are dynamic interactions

involving several other signals, such as long-range glutamatergic and other neuromodulatory inputs to the neocortex. How the circuit mechanisms we identified here relate to cortical functions and behavior *in vivo* remains to be explored.

(ii) How do trains of cholinergic input influence evoked recurrent activity? For this study, we focused on brief cholinergic activation and the fast point-to-point signaling that it is likely to mediate. However, numerous examples of cortical cholinergic receptors, such as presynaptic receptors, require more sustained cholinergic input in order to be recruited. Further work is required to assess their specific contributions.

(iii) What is the advantage of layer-specific cholinergic control to cortical processing? Our results identified important distinctions in the circuit mechanisms of cholinergic signaling in layers 2/3 and 4. It remains unclear what computational purpose is served by such layer-specificity, especially in the context of the unique cortical functions served by each layer.

(iv) How does synaptic acetylcholine influence dendritic computations in layer 4 RS cells? We show that glutamatergic EPSPs avoid being shunted by concurrent mIPSPs, suggesting that optical activation preferentially recruits mAChRs located on distal dendritic regions. The structural features of cholinergic afferentation that give rise to this curious circumstance and its functional consequences for dendritic computation are unknown.

Answering these and other questions will be crucial towards arriving at a comprehensive network model of cholinergic function in the neocortex, and also help establish acetylcholine as a potent neurotransmitter in its own right. The development of powerful new tools for cell-type specific manipulation and monitoring (Mardinly et al., 2018) offers quite a few exciting possibilities.

References

Adesnik H (2017) Synaptic Mechanisms of Feature Coding in the Visual Cortex of Awake Mice. Neuron 95:1147-1159.

Agmon A, Connors BW (1991) Thalamocortical responses of mouse somatosensory (barrel) cortex in vitro. Neuroscience 41:365-379.

Alitto HJ, Dan Y (2012) Cell-type-specific modulation of neocortical activity by basal forebrain input. Frontiers in systems neuroscience 6:79.

Amar M, Lucas-Meunier E, Baux G, Fossier P (2010) Blockade of different muscarinic receptor subtypes changes the equilibrium between excitation and inhibition in rat visual cortex. Neuroscience 169:1610-1620.

Andrä J, Lachmann I, Luppa H (1988) A comparison of the localization of acetylcholinesterase in the rat brain as demonstrated by enzyme histochemistry and immunohistochemistry. Histochemistry 88:595-601.

Arroyo S, Bennett C, Aziz D, Brown SP, Hestrin S (2012) Prolonged disynaptic inhibition in the cortex mediated by slow, non-alpha7 nicotinic excitation of a specific subset of cortical interneurons. J Neurosci 32:3859-3864.

Arroyo S, Bennett C, Hestrin S (2014) Nicotinic modulation of cortical circuits. Front Neural Circuits 8:30.

Aston-Jones G, Cohen JD (2005) An integrative theory of locus coeruleus-norepinephrine function: adaptive gain and optimal performance. Annu Rev Neurosci 28:403-450.

Aston-Jones G, Rajkowski J, Cohen J (1999) Role of locus coeruleus in attention and behavioral flexibility. Biol Psychiatry 46:1309-1320.

Ballinger EC, Ananth M, Talmage DA, Role LW (2016) Basal forebrain cholinergic circuits and signaling in cognition and cognitive decline. Neuron 91:1199-1218.

Barth AL, Burkhalter A, Callaway EM, Connors BW, Cauli B, DeFelipe J, Feldmeyer D, Freund T, Kawaguchi Y, Kisvarday Z, Kubota Y, McBain C, Oberlaender M, Rossier J, Rudy B, Staiger JF, Somogyi P, Tamas G, Yuste R (2016) Comment on "Principles of connectivity among morphologically defined cell types in adult neocortex". Science 353:1108.

Beierlein M (2014) Synaptic mechanisms underlying cholinergic control of thalamic reticular nucleus neurons. J Physiol 592:4137-4145.

Beierlein M, Connors BW (2002) Short-term dynamics of thalamocortical and intracortical synapses onto layer 6 neurons in neocortex. J Neurophysiol 88:1924-1932.

Beierlein M, Fall CP, Rinzel J, Yuste R (2002) Thalamocortical bursts trigger recurrent activity in neocortical networks: layer 4 as a frequency-dependent gate. J Neurosci 22:9885–9894.

Beierlein M, Gibson JR, Connors BW (2003) Two dynamically distinct inhibitory networks in layer 4 of the neocortex. J Neurophysiol 90:2987-3000.

Beltramo R, D'Urso G, Dal Maschio M, Farisello P, Bovetti S, Clovis Y, Lassi G, Tucci V, De Pietri Tonelli D, Fellin T (2013) Layer-specific excitatory circuits differentially control recurrent network dynamics in the neocortex. Nat Neurosci 16:227-234.

Bennett C, Arroyo S, Berns D, Hestrin S (2012) Mechanisms generating dual-component nicotinic EPSCs in cortical interneurons. J Neurosci 32:17287-17296.

Bennett C, Arroyo S, Hestrin S (2013) Subthreshold mechanisms underlying state-dependent modulation of visual responses. Neuron 80:350-357.

Berger H (1969) On the electroencephalogram of man. Electroencephalogr Clin Neurophysiol 28:37.

Berridge CW, Page ME, Valentino RJ, Foote SL (1993) Effects of locus coeruleus inactivation on electroencephalographic activity in neocortex and hippocampus. Neuroscience 55:381-393.

Berridge CW, Schmeichel BE, A. ER (2012) Noradrenergic modulation of wakefulness/arousal. Sleep Med Rev 16:187-197.

Bloem B, Schoppink L, Rotaru DC, Faiz A, Hendriks P, Mansvelder HD, van de Berg WD, Wouterlood FG (2014) Topographic mapping between basal forebrain cholinergic neurons and the medial prefrontal cortex in mice. J Neurosci 34:16234-16246.

Brombas A, Fletcher LN, Williams SR (2014) Activity-dependent modulation of layer 1 inhibitory neocortical circuits by acetylcholine. J Neurosci 34:1932-1941.

Bruno RM, Sakmann B (2006) Cortex is driven by weak but synchronously active thalamocortical synapses. Science 302:1622-1627.

Cantrell AR, Ma JY, Scheuer T, Catterall WA (1996) Muscarinic modulation of sodium current by activation of protein kinase C in rat hippocampal neurons. Neuron 16:1019-1026.

Carr DB, Surmeier DJ (2007) M1 muscarinic receptor modulation of Kir2 channels enhances temporal summation of excitatory synaptic potentials in prefrontal cortex pyramidal neurons. J Neurophysiol 97:3432-3438.

Chen JL, Carta S, Soldado-Magraner J, Schneider BL, Helmchen F (2013) Behaviour-dependent recruitment of long-range projection neurons in somatosensory cortex. Nature 499:336-340.

Chen N, Sugihara H, Sur M (2015) An acetylcholine-activated microcircuit drives temporal dynamics of cortical activity. Nat Neurosci 18:892-902.

Chubykin AA, Roach EB, Bear MF, Shuler MG (2013) A cholinergic mechanism for reward timing within primary visual cortex. Neuron 77:723-735.

Connors BW, Gutnick MJ (1990) Intrinsic firing patterns of diverse neocortical neurons. Trends in neurosciences 13:99-104.

Constantinople CM, Bruno RM (2011) Effects and mechanisms of wakefulness on local cortical networks. Neuron 69:1061-1068.

Constantinople CM, Bruno RM (2013) Deep cortical layers are activated directly by thalamus. Science 340:1591-1594.

Coppola JJ, Disney AA (2018) Is There a Canonical Cortical Circuit for the Cholinergic System? Anatomical Differences Across Common Model Systems. Front Neural Circuits 12:8.

Crandall SR, Patrick SL, Cruikshank SJ, Connors BW (2017) Infrabarrels Are Layer 6 Circuit Modules in the Barrel Cortex that Link Long-Range Inputs and Outputs. Cell Rep 21:3065-3078.

Cruikshank SJ, Lewis TJ, Connors BW (2007) Synaptic basis for intense thalamocortical activation of feedforward inhibitory cells in neocortex. Nat Neurosci 10:462-468.

Dasgupta R, Seibt F, Beierlein M (2018) Synaptic release of acetylcholine rapidly suppresses cortical activity by recruiting muscarinic receptors in layer 4. J Neurosci 38:5338-5350.

Descarries L, Gisiger V, Steriade M (1997) Diffuse transmission by acetylcholine in the CNS. Prog Neurobiol 53:603-625.

Descarries L, Mechawar N (2000) Ultrastructural evidence for diffuse transmission by monoamine and acetylcholine neurons of the central nervous system. Prog Brain Res 125:27-47.

Desikan S, Koser DE, Neitz A, Monyer H (2018) Target selectivity of septal cholinergic neurons in the medial and lateral entorhinal cortex. Proc Natl Acad Sci U S A.

Disney AA, Aoki C, Hawken MJ (2007) Gain modulation by nicotine in macaque v1. Neuron 56:701-713.

Duque A, Balatoni B, Detari L, Zaborszky L (2000) EEG correlation of the discharge properties of identified neurons in the basal forebrain. J Neurophysiol 84:1627-1635.

Eggermann E, Feldmeyer D (2009) Cholinergic filtering in the recurrent excitatory microcircuit of cortical layer 4. Proc Natl Acad Sci U S A 106:11753–11758.

Eggermann E, Kremer Y, Crochet S, Petersen CC (2014) Cholinergic signals in mouse barrel cortex during active whisker sensing. Cell Rep 9:1654-1660.

Engel TA, Steinmetz NA, Gieselmann MA, Thiele A, Moore T, Boahen K (2016) Selective modulation of cortical state during spatial attention. Science 354:1140-1144.

Fanselow EE, Richardson KA, Connors BW (2008) Selective, state-dependent activation of somatostatin-expressing inhibitory interneurons in mouse neocortex. J Neurophysiol 100:2640-2652.

Favero M, Varghese G, Castro-Alamancos MA (2012) The state of somatosensory cortex during neuromodulation. J Neurophysiol 4:1010-1024.

Feldmeyer D (2012) Excitatory neuronal connectivity in the barrel cortex. Frontiers in neuroanatomy 6:24.

Feldmeyer D, Brecht M, Helmchen F, Petersen CC, Poulet JF, Staiger JF, Luhmann HJ, Schwarz C (2013) Barrel cortex function. Prog Neurobiol 103:3-27.

Ferezou I, Bolea S, Petersen CC (2006) Visualizing the cortical representation of whisker touch: voltage-sensitive dye imaging in freely moving mice. Neuron 50:617-629.

Fishell G, Heintz N (2013) The neuron identity problem: form meets function. Neuron 80:602-612.

Fournier GN, Semba K, Rasmusson DD (2004) Modality- and region-specific acetylcholine release in the rat neocortex. Neuroscience 126:257-262.

Fu Y, Tucciarone JM, Espinosa JS, Sheng N, Darcy DP, Nicoll RA, Huang ZJ, Stryker MP (2014) A cortical circuit for gain control by behavioral state. Cell 156:1139-1152.

Gabernet L, Jadhav SP, Feldman DE, Carandini M, Scanziani M (2005) Somatosensory integration controlled by dynamic thalamocortical feed-forward inhibition. Neuron 48:315-327.

Garcia-Junco-Clemente P, Ikrar T, Tring E, Xu X, Ringach DL, Trachtenberg JT (2017) An inhibitory pull-push circuit in frontal cortex. Nat Neurosci 20:389-392.

Gavornik JP, Shuler MG, Loewenstein Y, Bear MF, Shouval HZ (2009) Learning reward timing in cortex through reward dependent expression of synaptic plasticity. Proc Natl Acad Sci U S A 106:6826-6831.

Gentet LJ, Avermann M, Matyas F, Staiger JF, Petersen CC (2010) Membrane potential dynamics of GABAergic neurons in the barrel cortex of behaving mice. Neuron 65:422-435.

Gervasoni D, Lin SC, Ribeiro S, Soares ES, Pantoja J, Nicolelis MA (2004) Global forebrain dynamics predict rat behavioral states and their transitions. J Neurosci 24:11137-11147.

Gidon A, Segev I (2012) Principles governing the operation of synaptic inhibition in dendrites. Neuron 75:330-341.

Goard M, Dan Y (2009) Basal forebrain activation enhances cortical coding of natural scenes. Nat Neurosci 12:1444-1449.

Gritti I, Henny P, Galloni F, Mainville L, Mariotti M, Jones BE (2006) Stereological estimates of the basal forebrain cell population in the rat, including neurons containing choline acetyltransferase, glutamic acid decarboxylase or phosphate-activated glutaminase and colocalizing vesicular glutamate transporters. Neuroscience 143:1051-1064.

Gritton HJ, Howe WM, Mallory CS, Hetrick VL, Berke JD, Sarter M (2016) Cortical cholinergic signaling controls the detection of cues. Proc Natl Acad Sci U S A 113:E1089-1097.

Groleau M, Kang JI, Huppé-Gourgues F, Vaucher E (2015) Distribution and effects of the muscarinic receptor subtypes in the primary visual cortex. Front Synaptic Neurosci 7:10.

Guan ZZ, Zhang X, Blennow K, Nordberg A (1999) Decreased protein level of nicotinic receptor alpha7 subunit in the frontal cortex from schizophrenic brain. Neuroreport 10:1779-1782.

Guillem K, Bloem B, Poorthuis RB, Loos M, Smit AB, Maskos U, Spijker S, Mansvelder HD (2011) Nicotinic acetylcholine receptor β2 subunits in the medial prefrontal cortex control attention. Science 333:888-891.

Guillery RW (1967) Patterns of fiber degeneration in the dorsal lateral geniculate nucleus of the cat following lesions in the visual cortex. J Comp Neurol 130:197-221.

Gulledge AT, Bucci DJ, Zhang SS, Matsui M, Yeh HH (2009) M1 receptors mediate cholinergic modulation of excitability in neocortical pyramidal neurons. J Neurosci 29:9888-9902.

Gulledge AT, Park SB, Kawaguchi Y, Stuart GJ (2007) Heterogeneity of phasic cholinergic signaling in neocortical neurons. J Neurophysiol 97:2215-2229.

Gulledge AT, Stuart GJ (2005) Cholinergic inhibition of neocortical pyramidal neurons. J Neurosci 25:10308-10320.

Guo ZV, Li N, Huber D, Ophir E, Gutnisky D, Ting JT, Feng G, Svoboda K (2014) Flow of cortical activity underlying a tactile decision in mice. Neuron 81:179-194.

Halassa MM, Chen Z, Wimmer RD, Brunetti PM, Zhao S, Zikopoulos B, Wang F, Brown EN, Wilson MA (2014) State-dependent architecture of thalamic reticular subnetworks. Cell 158:808-821.

Han Y, Shi YF, Xi W, Zhou R, Tan ZB, Wang H, Li XM, Chen Z, Feng G, Luo M, Huang ZL, Duan S, Yu YQ (2014) Selective activation of cholinergic basal forebrain neurons induces immediate sleep-wake transitions. Curr Biol 24:693-698.

Hangya B, Ranade SP, Lorenc M, Kepecs A (2015) Central cholinergic neurons are rapidly recruited by reinforcement feedback. Cell 162:1155-1168.

Haring JH, Wang RY (1986) The identification of some sources of afferent input to the rat nucleus basalis magnocellularis by retrograde transport of horseradish peroxidase. Brain research 366:152-158.

Harris KD, Thiele A (2011) Cortical state and attention. Nat Rev Neurosci 12:509-523.

Hasselmo ME (2006) The role of acetylcholine in learning and memory. Curr Opin Neurobiol 16:710-715.

Hay YA, Lambolez B, Tricoire L (2016) Nicotinic Transmission onto Layer 6 Cortical Neurons Relies on Synaptic Activation of Non-α7 Receptors. Cereb Cortex 26:2549-2562.

Hedrick T, Danskin B, Larsen RS, Ollerenshaw D, Groblewski P, Valley M, Olsen S, Waters J (2016) Characterization of Channelrhodopsin and Archaerhodopsin in Cholinergic Neurons of Cre-Lox Transgenic Mice. PLoS One 11:e0156596.

Hedrick T, Waters J (2015) Acetylcholine excites neocortical pyramidal neurons via nicotinic receptors. J Neurophysiol 113:2195-2209.

Helmstaedter M, Staiger JF, Sakmann B, Feldmeyer D (2008) Efficient recruitment of layer 2/3 interneurons by layer 4 input in single columns of rat somatosensory cortex. J Neurosci 28:8273-8284.

Herman AM, Ortiz-Guzman J, Kochukov M, Herman I, Quast KB, Patel JM, Tepe B, Carlson JC, Ung K, Selever J, Tong Q, Arenkiel BR (2016) A cholinergic basal forebrain feeding circuit modulates appetite suppression. Nature 538:253-256.

Herreras O (2016) Local Field Potentials: Myths and Misunderstandings. Front Neural Circuits 10:101.

Herrero JL, Roberts MJ, Delicato LS, Gieselmann MA, Dayan P, Thiele A (2008) Acetylcholine contributes through muscarinic receptors to attentional modulation in V1. Nature 454:1110-1114.

Hirabayashi T, Miyashita Y (2014) Computational principles of microcircuits for visual object processing in the macaque temporal cortex. Trends in neurosciences 37:178-187.

Hobson JA (2005) Sleep is of the brain, by the brain and for the brain. Nature 437:1254-1256.

Hubel DH, Wiesel TN (1962) Receptive fields, binocular interaction and functional architecture in the cat's visual cortex. J Physiol 160:106-154.

Jensen JB, Lyssand JS, Hague C, Hille B (2009) Fluorescence changes reveal kinetic steps of muscarinic receptor-mediated modulation of phosphoinositides and Kv7.2/7.3 K+ channels. The Journal of general physiology 133:347-359.

Jiang X, Sheng S, Cadwell CR, Berens P, Sinz F, Ecker AS, Patel S, Tolias AS (2015) Principles of connectivity among morphologically defined cell types in adult neocortex. Science 350:aac9462.

Jones BE (2004) Activity, modulation and role of basal forebrain cholinergic neurons innervating the cerebral cortex. Prog Brain Res 145:157-169.

Jones BE, Cuello AC (1989) Afferents to the basal forebrain cholinergic cell area from pontomesencephalic--catecholamine, serotonin, and acetylcholine--neurons. Neuroscience 31:37-61.

Jones EG, Powell TP (1968) The projection of the somatic sensory cortex upon the thalamus in te cat. Brain research 10:369-391.

Kajikawa Y, Schroeder CE (2011) How local is the local field potential? Neuron 72:847-858.

Kalmbach A, Waters J (2014) Modulation of high- and low-frequency components of the cortical local field potential via nicotinic and muscarinic acetylcholine receptors in anesthetized mice. J Neurophysiol 111:258-272.

Kato HK, Asinof SK, Isaacson JS (2017) Network-Level Control of Frequency Tuning in Auditory Cortex. Neuron 95:412-423.

Kato HK, Gillet SN, Isaacson JS (2015) Flexible Sensory Representations in Auditory Cortex Driven by Behavioral Relevance. Neuron 88:1027-1039.

Kawaguchi Y (1997) Selective cholinergic modulation of cortical GABAergic cell subtypes. J Neurophysiol 78:1743-1747.

Kawaguchi Y, Kubota Y (1997) GABAergic cell subtypes and their synaptic connections in rat frontal cortex. Cereb Cortex 7:476-486.

Kimura F, Baughman RW (1997) Distinct muscarinic receptor subtypes suppress excitatory and inhibitory synaptic responses in cortical neurons. J Neurophysiol 77:709-716.

Kimura F, Fukuda M, Tsumoto T (1999) Acetylcholine suppresses the spread of excitation in the visual cortex revealed by optical recording: possible differential effect depending on the source of input. Eur J Neurosci 11:3597-3609.

Koch C (1999) Biophysics of computation : information processing in single neurons. New York: Oxford University Press.

Kolisnyk B, Guzman MS, Raulic S, Fan J, Magalhaes AC, Feng G, Gros R, Prado VF, Prado MA (2013) ChAT-ChR2-EYFP mice have enhanced motor endurance but show deficits in attention and several additional cognitive domains. J Neurosci 33:10427-10438.

Kuchibhotla KV, Gill JV, Lindsay GW, Papadoyannis ES, Field RE, Sten TA, Miller KD, Froemke RC (2017) Parallel processing by cortical inhibition enables context-dependent behavior. Nat Neurosci 20:62-71.

Leblond L, Beaufort C, Delerue F, Durkin TP (2002) Differential roles for nicotinic and muscarinic cholinergic receptors in sustained visuo-spatial attention? A study using a 5-arm maze protocol in mice. Behavioural brain research 128:91-102.

Lee MG, Hassani OK, Alonso A, Jones BE (2005) Cholinergic basal forebrain neurons burst with theta during waking and paradoxical sleep. J Neurosci 25:4365-4369.

Lee S, Hjerling-Leffler J, Zagha E, Fishell G, Rudy B (2010) The largest group of superficial neocortical GABAergic interneurons expresses ionotropic serotonin receptors. J Neurosci 30:16796-16808.

Lee S, Kruglikov I, Huang ZJ, Fishell G, Rudy B (2013) A disinhibitory circuit mediates motor integration in the somatosensory cortex. Nat Neurosci 16:1662-1670.

Lee SH, Dan Y (2012) Neuromodulation of brain states. Neuron 76:209-222.

Lendvai B, Vizi ES (2008) Nonsynaptic chemical transmission through nicotinic acetylcholine receptors. Physiol Rev 88:333-349.

Letzkus JJ, Wolff SB, A. L (2015) Disinhibition, a circuit mechanism for associative learning and memory. Neuron 88:264-276.

Letzkus JJ, Wolff SB, Meyer EM, Tovote P, Courtin J, Herry C, Lüthi A (2011) A disinhibitory microcircuit for associative fear learning in the auditory cortex. Nature 480:331-335.

Li LY, Li YT, Zhou M, Tao HW, Zhang LI (2013) Intracortical multiplication of thalamocortical signals in mouse auditory cortex. Nat Neurosci 16:1179-1181.

Lien AD, Scanziani M (2013) Tuned thalamic excitation is amplified by visual cortical circuits. Nat Neurosci 16:1315-1323.

Lovett-Barron M, Andalman AS, Allen WE, Vesuna S, Kauvar I, Burns VM, Deisseroth K (2017) Ancestral Circuits for the Coordinated Modulation of Brain State. Cell 171:1411-1423.

Lucas-Meunier E, Fossier P, Baux G, Amar M (2003) Cholinergic modulation of the cortical neuronal network. Pflugers Arch 446:17-29.

Lucas-Meunier E, Monier C, Amar M, Baux G, Frégnac Y, Fossier P (2009) Involvement of nicotinic and muscarinic receptors in the endogenous cholinergic modulation of the balance between excitation and inhibition in the young rat visual cortex. Cereb Cortex 19:2411-2427.

Ma Y, Hu H, Berrebi AS, Mathers PH, Agmon A (2006) Distinct subtypes of somatostatin-containing neocortical interneurons revealed in transgenic mice. J Neurosci 26:5069-5082.

Madison DV, Lancaster B, Nicoll RA (1987) Voltage clamp analysis of cholinergic action in the hippocampus. J Neurosci 7:733-741.

Mardinly AR, Oldenburg IA, Pégard NC, Sridharan S, Lyall EH, Chesnov K, Brohawn SG, Waller L, Adesnik H (2018) Precise multimodal optical control of neural ensemble activity. Nat Neurosci 21:881-893.

Marguet SL, Harris KD (2011) State-dependent representation of amplitude-modulated noise stimuli in rat auditory cortex. J Neurosci 31:6414-6420.

McCormick DA (1992) Neurotransmitter actions in the thalamus and cerebral cortex and their role in neuromodulation of thalamocortical activity. Prog Neurobiol 39:337-388.

McGinley MJ, David SV, McCormick DA (2015a) Cortical Membrane Potential Signature of Optimal States for Sensory Signal Detection. Neuron 87:179-192.

McGinley MJ, Vinck M, Reimer J, Batista-Brito R, Zagha E, Cadwell CR, Tolias AS, Cardin JA, McCormick DA (2015b) Waking state: rapid variations modulate neural and behavioral responses. Neuron 87:1143-1161.

Mesulam MM, Mufson EJ, Levey AI, Wainer BH (1983) Cholinergic innervation of cortex by the basal forebrain: cytochemistry and cortical connections of the septal area, diagonal band nuclei, nucleus basalis (substantia innominata), and hypothalamus in the rhesus monkey. J Comp Neurol 214:170-197.

Mesulam MM, Mufson EJ, Levey AI, Wainer BH (1984) Atlas of cholinergic neurons in the forebrain and upper brainstem of the macaque based on monoclonal choline acetyltransferase immunohistochemistry and acetylcholinesterase histochemistry. Neuroscience 12:669-686.

Metherate R (2004) Nicotinic acetylcholine receptors in sensory cortex. Learn Mem 11:50-59.

Metherate R, Cox CL, Ashe JH (1992) Cellular bases of neocortical activation: modulation of neural oscillations by the nucleus basalis and endogenous acetylcholine. J Neurosci 12:4701-4711.

Meyer HS, Wimmer VC, Oberlaender M, De Kock CP, Saalmann YB, Helmstaedter M (2010) Number and laminar distribution of neurons in a thalamocortical projection column of rat vibrissal cortex. Cereb Cortex 20:2277-2286.

Mountcastle VB (1997) The columnar organization of the neocortex. Brain 120 (Pt 4):701-722.

Mufson EJ, Counts SE, Perez SE, Ginsberg SD (2008) Cholinergic system during the progression of Alzheimer's disease: therapeutic implications. Expert Rev Neurother 8:1703-1718.

Müller C, Remy S (2017) Septo-hippocampal interaction. Cell Tissue Res doi: 10.1007/s00441-00017-02745-00442.

Muñoz W, Rudy B (2014) Spatiotemporal specificity in cholinergic control of neocortical function. Curr Opin Neurobiol 26:149-160.

Muñoz W, Tremblay R, Levenstein D, Rudy B (2017) Layer-specific modulation of neocortical dendritic inhibition during active wakefulness. Science 355:954-959.

Nagasaka K, Watanabe Y, Takashima I (2017) Topographical projections from the nucleus basalis magnocellularis (Meynert) to the frontal cortex: A voltage-sensitive dye imaging study in rats. Brain Stimul 10:977-980.

Nelson A, Mooney R (2016) The Basal Forebrain and Motor Cortex Provide Convergent yet Distinct Movement-Related Inputs to the Auditory Cortex. Neuron 90:635-648.

Neske GT, Patrick SL, Connors BW (2015) Contributions of diverse excitatory and inhibitory neurons to recurrent network activity in cerebral cortex. J Neurosci 35:1089-1105.

Niell CM, Stryker MP (2010) Modulation of visual responses by behavioral state in mouse visual cortex. Neuron 65:472-479.

O'Connor DH, Peron SP, Huber D, Svoboda K (2010) Neural activity in barrel cortex underlying vibrissa-based object localization in mice. Neuron 67:1048-1061.

Obermayer J, Verhoog MB, Luchicchi A, Mansvelder HD (2017) Cholinergic Modulation of Cortical Microcircuits Is Layer-Specific: Evidence from Rodent, Monkey and Human Brain. Front Neural Circuits 11:100.

Origlia N, Kuczewski N, Aztiria E, Gautam D, Wess J, Domenici L (2006) Muscarinic acetylcholine receptor knockout mice show distinct synaptic plasticity impairments in the visual cortex. J Physiol 577:829-840.

Parikh V, Kozak R, Martinez V, M. S (2007) Prefrontal acetylcholine release controls cue detection on multiple timescales. Neuron 56:141-154.

Peters A (1990) The axon terminals of vasoactive intestinal polypeptide (VIP)-containing bipolar cells in rat visual cortex. J Neurocytol 19:672-685.

Petersen CC (2007) The functional organization of the barrel cortex. Neuron 56:339-355.

Petersen CC, Crochet S (2013) Synaptic computation and sensory processing in neocortical layer 2/3. Neuron 78:28-48.

Pfeffer CK, Xue M, He M, Huang ZJ, Scanziani M (2013) Inhibition of inhibition in visual cortex: the logic of connections between molecularly distinct interneurons. Nat Neurosci 16:1068-1076.

Pi HJ, Hangya B, Kvitsiani D, Sanders JI, Huang ZJ, Kepecs A (2013) Cortical interneurons that specialize in disinhibitory control. Nature 503:521-524.

Pinto DJ, Hartings JA, Brumberg JC, Simons DJ (2003) Cortical damping: analysis of thalamocortical response transformations in rodent barrel cortex. Cereb Cortex 13:33-44.

Pinto L, Goard MJ, Estandian D, Xu M, Kwan AC, Lee SH, Harrison TC, Feng G, Dan Y (2013) Fast modulation of visual perception by basal forebrain cholinergic neurons. Nat Neurosci 16:1857-1863.

Pluta SR, Lyall EH, Telian GI, Ryapolova-Webb E, Adesnik H (2017) Surround Integration Organizes a Spatial Map during Active Sensation. Neuron 94:1220-1233.

Polack PO, Friedman J, Golshani P (2013) Cellular mechanisms of brain state-dependent gain modulation in visual cortex. Nat Neurosci 16:1331-1339.

Poorthuis RB, Bloem B, Schak B, Wester J, P. dKC, Mansvelder HD (2013) Layer-specific modulation of the prefrontal cortex by nicotinic acetylcholine receptors. Cereb Cortex 23:148-161.

Poorthuis RB, Enke L, Letzkus JJ (2014) Cholinergic circuit modulation through differential recruitment of neocortical interneuron types during behaviour. J Physiol 592:4155-4164.

Poorthuis RB, Muhammad K, Wang M, Verhoog MB, Junek S, Wrana A, Mansvelder HD, Letzkus JJ (2018) Rapid Neuromodulation of Layer 1 Interneurons in Human Neocortex. Cell Rep 23:951-958.

Poulet JF, Petersen CC (2008) Internal brain state regulates membrane potential synchrony in barrel cortex of behaving mice. Nature 454:881-885.

Raghanti MA, Simic G, Watson S, Stimpson CD, Hof PR, Sherwood CC (2011) Comparative analysis of the nucleus basalis of Meynert among primates. Neuroscience 184:1-15.

Ramon y Cajal S (1899) Histology of the Nervous System, Swanson, N, and Swanson, LW (trans) (Wien, New York: Springer).

Reimer J, Froudarakis E, Cadwell CR, Yatsenko D, Denfield GH, Tolias AS (2014) Pupil fluctuations track fast switching of cortical states during quiet wakefulness. Neuron 84:355-362.

Reimer J, McGinley MJ, Liu Y, Rodenkirch C, Wang Q, McCormick DA, Tolias AS (2016) Pupil fluctuations track rapid changes in adrenergic and cholinergic activity in cortex. Nat Commun 7:13289.

Roberts MJ, Zinke W, Guo K, Robertson R, McDonald JS, Thiele A (2005) Acetylcholine dynamically controls spatial integration in marmoset primary visual cortex. J Neurophysiol 93:2062-2072.

Rudy B, Fishell G, Lee S, Hjerling-Leffler J (2011) Three groups of interneurons account for nearly 100% of neocortical GABAergic neurons. Developmental neurobiology 71:45-61.

Rye DB, Wainer BH, Mesulam MM, Mufson EJ, Saper CB (1984) Cortical projections arising from the basal forebrain: a study of cholinergic and noncholinergic components employing combined retrograde tracing and immunohistochemical localization of choline acetyltransferase. Neuroscience 13:627-643.

Sarid L, Feldmeyer D, Gidon A, Sakmann B, Segev I (2015) Contribution of intracolumnar layer 2/3-to-layer 2/3 excitatory connections in shaping the response to whisker deflection in rat barrel cortex. Cereb Cortex 25:849-858.

Sarter M, Kim Y (2015) Interpreting chemical neurotransmission in vivo: techniques, time scales, and theories. ACS Chem Neurosci 6:8-10.

Satoh K, Armstrong DM, Fibiger HC (1983) A comparison of the distribution of central cholinergic neurons as demonstrated by acetylcholinesterase pharmacohistochemistry and choline acetyltransferase immunohistochemistry. Brain Res Bull 11:693-720.

Saunders A, Granger AJ, Sabatini BL (2015) Corelease of acetylcholine and GABA from cholinergic forebrain neurons. Elife 4:e06412.

Schneider DM, Nelson A, Mooney R (2014) A synaptic and circuit basis for corollary discharge in the auditory cortex. Nature 513:189-194.

Schoonover CE, Tapia JC, Schilling VC, Wimmer V, Blazeski R, Zhang W, Mason CA, Bruno RM (2014) Comparative strength and dendritic organization of thalamocortical and corticocortical synapses onto excitatory layer 4 neurons. J Neurosci 34:6746-6758.

Shai AS, Anastassiou CA, Larkum ME, Koch C (2015) Physiology of layer 5 pyramidal neurons in mouse primary visual cortex: coincidence detection through bursting. PLoS Comput Biol 11:e1004090.

Shimaoka D, Harris KD, Carandini M (2018) Effects of Arousal on Mouse Sensory Cortex Depend on Modality. Cell Rep 22:3160-3167.

Shiromani PJ, Gillin JC, Henriksen SJ (1987) Acetylcholine and the regulation of REM sleep: basic mechanisms and clinical implications for affective illness and narcolepsy. Annu Rev Pharmacol Toxicol 27:137-156.

Shu Y, Hasenstaub A, McCormick DA (2003) Turning on and off recurrent balanced cortical activity. Nature 423:288-293.

Silver MA, Shenhav A, D'Esposito M (2008) Cholinergic enhancement reduces spatial spread of visual responses in human early visual cortex. Neuron 60:904-914.

Simons DJ, Carvell GE (1989) Thalamocortical response transformation in the rat vibrissa/barrel system. J Neurophysiol 61:311-330.

Smiley JF, Morrell F, Mesulam MM (1997) Cholinergic synapses in human cerebral cortex: an ultrastructural study in serial sections. Exp Neurol 144:361-368.

Staiger JF, Flagmeyer I, Schubert D, Zilles K, Kötter R, Luhmann HJ (2004) Functional diversity of layer IV spiny neurons in rat somatosensory cortex: quantitative morphology of electrophysiologically characterized and biocytin labeled cells. Cereb Cortex 14:690-701.

Steriade M, McCormick DA, Sejnowski TJ (1993) Thalamocortical oscillations in the sleeping and aroused brain. Science 262:679-685.

Steriade M, Timofeev I, Grenier F (2001) Natural waking and sleep states: a view from inside neocortical neurons. J Neurophysiol 85:1969-1985.

Sun YG, Pita-Almenar JD, Wu CS, Renger JJ, Uebele VN, Lu HC, Beierlein M (2013) Biphasic cholinergic synaptic transmission controls action potential activity in thalamic reticular nucleus neurons. J Neurosci 33:2048-2059.

Taniguchi H, He M, Wu P, Kim S, Paik R, Sugino K, Kvitsiani D, Fu Y, Lu J, Lin Y, Miyoshi G, Shima Y, Fishell G, Nelson SB, Huang ZJ (2011) A resource of Cre driver lines for genetic targeting of GABAergic neurons in cerebral cortex. Neuron 71:995-1013.

Terry AVJ (2008) Role of the central cholinergic system in the therapeutics of schizophrenia. Curr Neuropharmacol 6:286-292.

Thiele A (2013) Muscarinic signaling in the brain. Annu Rev Neurosci 36:271-294.

Turrini P, Casu MA, Wong TP, De Koninck Y, Ribeiro-da-Silva A, Cuello AC (2001) Cholinergic nerve terminals establish classical synapses in the rat cerebral cortex: synaptic pattern and age-related atrophy. Neuroscience 105:277-285.

Unal CT, Pare D, Zaborszky L (2015) Impact of basal forebrain cholinergic inputs on basolateral amygdala neurons. J Neurosci 35:853-863.

Urban-Ciecko J, Jouhanneau JS, Myal SE, Poulet JFA, Barth AL (2018) Precisely Timed Nicotinic Activation Drives SST Inhibition in Neocortical Circuits. Neuron 97:611-625.

Verhoog MB, Obermayer J, Kortleven CA, Wilbers R, Wester J, Baayen JC, De Kock CP, Meredith RM, Mansvelder HD (2016) Layer-specific cholinergic control of human and mouse cortical synaptic plasticity. Nat Commun 7:12826.

Vinck M, Batista-Brito R, Knoblich U, Cardin JA (2015) Arousal and locomotion make distinct contributions to cortical activity patterns and visual encoding. Neuron 86:740-754.

Volpicelli LA, Levey AI (2004) Muscarinic acetylcholine receptor subtypes in cerebral cortex and hippocampus. Prog Brain Res 145:59-66.

von Engelhardt J, Eliava M, Meyer AH, Rozov A, Monyer H (2007) Functional characterization of intrinsic cholinergic interneurons in the cortex. J Neurosci 27:5633-5642.

Wamsley B, Fishell G (2017) Genetic and activity-dependent mechanisms underlying interneuron diversity. Nat Rev Neurosci 18:299-309.

Wester J, Contreras D (2013) Differential modulation of spontaneous and evoked thalamocortical network activity by acetylcholine level in vitro. J Neurosci 33:17951-17966.

Woolf NJ, Butcher LL (2011) Cholinergic systems mediate action from movement to higher consciousness. Behavioural brain research 221:488-498.

Wu H, Williams J, Nathans J (2014) Complete morphologies of basal forebrain cholinergic neurons in the mouse. Elife 3:e02444.

Xu H, Jeong HY, Tremblay R, Rudy B (2013) Neocortical somatostatin-expressing GABAergic interneurons disinhibit the thalamorecipient layer 4. Neuron 77:155-167.

Xu M, Chung S, Zhang S, Zhong P, Ma C, Chang WC, Weissbourd B, Sakai N, Luo L, Nishino S, Dan Y (2015) Basal forebrain circuit for sleep-wake control. Nat Neurosci 18:1641-1647.

Xue M, Atallah BV, Scanziani M (2014) Equalizing excitation-inhibition ratios across visual cortical neurons. Nature 511:596-600.

Yamasaki M, Matsui M, Watanabe M (2010) Preferential localization of muscarinic M1 receptor on dendritic shaft and spine of cortical pyramidal cells and its anatomical evidence for volume transmission. J Neurosci 30:4408-4418.

Yang C, McKenna JT, Zant JC, Winston S, Basheer R, Brown RE (2014) Cholinergic neurons excite cortically projecting basal forebrain GABAergic neurons. J Neurosci 34:2832-2844.

Yang H, Kwon SE, Severson KS, O'Connor DH (2016) Origins of choice-related activity in mouse somatosensory cortex. Nat Neurosci 19:127-134.

Yerkes RM, Dodson JD (1908) The relation of strength of stimulus to rapidity of habit-formation. J Comp Neurol Psychol 18:459-482.

Zagha E, McCormick DA (2014) Neural control of brain state. Curr Opin Neurobiol 29:178-186.

Zavitsanou K, Katsifis A, Mattner F, Huang XF (2004) Investigation of m1/m4 muscarinic receptors in the anterior cingulate cortex in schizophrenia, bipolar disorder, and major depression disorder. Neuropsychopharmacology : official publication of the American College of Neuropsychopharmacology 29:619-625.

Zhao S, Ting JT, Atallah HE, Qiu L, Tan J, Gloss B, Augustine GJ, Deisseroth K, Luo M, Graybiel AM, Feng G (2011) Cell type–specific channelrhodopsin-2 transgenic mice for optogenetic dissection of neural circuitry function. Nature Methods 8:745-752.

Zoli M, Jansson A, Syková E, Agnati LF, Fuxe K (1999) Volume transmission in the CNS and its relevance for neuropsychopharmacology. Trends Pharmacol Sci 20:142-150.

Vita

Rajan Dasgupta was born in 1990 in Kolkata, India, the only son of Tamali Dasgupta and Malay Kishore Dasgupta. After passing the Indian School Certificate board examinations from The Future Foundation School, Kolkata in 2007, he joined an integrated Master's program at the University of Pune, Pune, India. In 2012, he graduated with a Master of Science degree in Biotechnology. In August the following year, he entered the Ph.D. program at the University of Texas MD Anderson Cancer Center UTHealth McGovern Graduate School of Biomedical Sciences.